EXPERIMENTAL AND THEORETICAL STUDIES OF OXYCARBENES: THEIR REARRANGEMENTS, HOMOLYSIS AND INTERMOLECULAR REACTIONS WITH CARBON DISULFIDE.

By

DARREN L. REID, B.Sc.

A Thesis

Submitted to the School of Graduate Studies

In Partial Fulfillment of the Requirements

for the Degree

Doctor of Philosophy

McMaster University

EXPERIMENTAL AND THEORETICAL STUDIES OF OXYCARBENES

DOCTOR OF PHILOSOPHY (2000)
(Chemistry)

McMaster University
Hamilton, Ontario

TITLE: Experimental and Theoretical Studies of Oxycarbenes: Their Rearrangements, Homolysis and Intermolecular Reactions with Carbon Disulfide.

AUTHOR: Darren L. Reid, B. Sc. (Mount Allison University)

SUPERVISOR: Professor John Warkentin

NUMBER OF PAGES: xv, 175

Abstract

The first portion of this research focuses on some of the intramolecular chemistry of oxy- and dioxycarbenes. Carbenes belonging to this group are known to fragment to radicals, both in gas and in solution phases. The computational work presented here identifies the homolysis from the singlet ground state as a viable pathway for this fragmentation. The study then concentrates on the mechanism for the homolysis of these singlet carbenes and the possibility that this apparently-simple fragmentation could involve a transition state. In accordance with models, such as Valence Bond Configuration Mixing (VBCM), transition states involving changes in bonding are said to result from destabilization due to the change from one stable ground state electronic configuration to another. The results indicated that the homolysis has an unusual conformational dependence that cannot be explained by a first approximation of the VBCM model, and is in fact attributable to a mismatch in the electronic structures of the states involved.

The second portion of this work focuses on expanding the chemistry of dioxycarbenes with thiocarbonyl compounds. To this end the reaction of dimethoxycarbene with carbon disulfide (CS_2) is examined both experimentally and computationally. The reaction gave a surprisingly complicated product, which suggested the participation of zwitterionic, dipolar and neutral intermediates. The neutral thiocarbonyl intermediates are apparently quite reactive and undergo subsequent

nucleophilic attacks by dimethoxycarbene. Initial results for the reaction of diphenoxycarbene with carbon disulfide showed diphenyl thionocarbonate as the only CS_2-derived product, emphasizing the influence that exchangeable carbene substituents have on the chemistry of the zwitterionic intermediates.

Dihydroxycarbene was used to model the interactions of dioxycarbenes with CS_2. The theoretical results indicate that dioxycarbenes do not undergo concerted cycloadditions to a carbon-sulfur double bond, but instead prefer nucleophilic attack at carbon to form zwitterionic intermediates, or electrophilic attack at sulfur to form ylides with an unexpected twisted geometry. Direct nucleophilic attack at carbon has also been observed computationally by previous workers for the reaction of dihydroxycarbene with carbon dioxide. These results emphasize the differences between cumulated systems and simple carbonyl systems studied in the past. Both the zwitterionic and ylide intermediates have available reaction pathways to thionocarboxylic acid (HOCSOH) and carbon monosulfide, however it was not possible to distinguish a preferred route from these results.

Acknowledgments

I would like to thank my supervisor Dr. J. Warkentin for his constant support and encouragement. He has always provided a stimulating environment for research and discussion. I also thank the other members of my supervisory committee, Dr. N. H. Werstiuk and Dr. M. J. McGlinchey for the many useful insights they have provided during our meetings.

A number of other people have been instrumental in assisting me with my efforts to produce this thesis. In particular I thank Dr. J. Hernández-Trujillo who collaborated with me on the hydroxycarbene study presented here. The time we spent working together was the most enjoyable and exciting of my career. I thank Dr. J. R. Kramer and P. V. Collins for supplying computational support and facilities, funded by NSERC. Computational resources and support were also supplied by the Department of Chemistry, McMaster University, and M. G. Malott. I am indebted to Drs. N. H. Werstiuk, D. L. Pole, H. M. Muchall, and N. W. H. Adams for many helpful discussions with regard to molecular modelling. Dr. D. Hughes, B. G. Sayer and G. Timmins deserve thanks for technical assistance, particularly for their help in obtaining NMR spectra.

My coworkers in Dr. Warkentin's group have helped make my experience here a positive one. In particular I have to acknowledge, Dr. David L. Pole, Dr. Karim Kassam, Hui-Teng Er, Dr. Philippe Couture, Joe Ross, Dr. John P. Pezacki, Dr. Paul C. Venneri, Nadine A. Merkley, Xiaosong Lu, and Dr. M. El-Saidi. Special thanks go to the many

friends I have made here over the years, especially Dr. Rodica Himmeldirk, Dr. Klaus Himmeldirk, Dr. Jesús Hernández-Trujillo, Adrienne Boden, Helen Manolopoulos, and Susanne Ackloo.

I must also thank my family, especially my parents, Austin and Elizabeth Reid, who have been an endless source of support and encouragement from the earliest days of my education. Finally, I thank Candace Webb for everything that she has done, and the way that it has all felt to me.

Table of Contents

List of Figures

List of Tables

Glossary of General Abbreviations

AIM	Atoms in Molecules
DMAD	Dimethyl Acetylenedicarboxylate
FMO	Frontier Molecular Orbital
GC	Gas Chromatography
HFIP	1,1,1,3,3,3-Hexafluoro-2-propanol
HMBC	Heteronuclear Multiple-Bond Correlation
HOMO	Highest Occupied Molecular Orbital
IR	Infrared Spectroscopy
ISC	Intersystem Crossing
KIE	Kinetic Isotope Effect
LFP	Laser Flash Photolysis
LUMO	Lowest Unoccupied Molecular Orbital
MS (CI)	Mass Spectrum (Chemical Ionization)
MS (EI)	Mass spectrum (Electron Impact)
NMR	Nuclear Magnetic Resonance
NRMS	Neutralization-Reionization Mass Spectrometry
SET	Single Electron Transfer
TEMPO	2,2,6,6-Tetramethyl-1-Piperidinyloxy, Free Radical
VBCM	Valence-Bond Configuration Mixing
VLVP	Very Low Vapour Pressure
VSEPR	Valence-Shell Electron-Pair Replusion

Glossary of Molecular Modeling Abbreviations*

B3LYP	Becke's 3-Parameter Hybrid Method Using the Lee-Yang-Parr Correlation Functional
CAS	Complete Active Space
cc-pVDZ	Dunning's Correlation-Consistent Polarized-Valence, Double-Zeta
CC	Coupled Cluster
CI	Configuration Interaction
DFT	Density Functional Theory
DZP	Double-Zeta plus Polarization Functions
FC	Frozen Core
GAMESS	General Atomic and Molecular Electronic Structure System
HF	Hartree-Fock
INDO/S	Intermediate Neglect of Differential Overlap/Spectra
MINDO/3	Modified Intermediate Neglect of Differential Overlap, Version 3
MP(#)	Møller-Plesset Truncated at 2^{nd} or 4^{th} Order
MR	Multireference
P	Projected
R	Restricted
S	Single Substitutions
SCF	Self-Consistent Field
SD	Single and Double Substitutions
SDT	Single, Double and Triple Substitutions
SDTQ	Single, Double, Triple and Quadruple Substitutions
STO-3G	Slater-Type Orbitals with 3 Gaussian Primitives per Basis Function
U	Unrestricted
ZPE	Zero Point Vibrational Energy

* Abbreviations may appear in various combinations.

Chapter 1

Introduction

Carbon atoms prefer a tetravalent electronic structure in which four pairs of electrons are shared with the atoms covalently bonded to them. However, a number of di- or trivalent carbon-centered species are also well known and they exist as four distinct types: (1) carbocations, (2) carbanions, (3) free radicals, and (4) carbenes (Figure 1).[1] Although some stable, low-valent carbon species are known, they are usually short-lived species, known as *reactive intermediates*, formed in the course of chemical reactions. Carbenes are particularly interesting as they can take on characteristics of the three other carbon-centred reactive intermediates, making them extremely versatile. It is this versatility that explains the intense interest they have generated in a wide range of chemistry sub-disciplines, including the synthetic, physical organic and theoretical fields.[2-4] This chapter gives an overview of the basic principles and models used to understand carbenic behaviour, especially that of nucleophilic carbenes with an emphasis on the chemistry of oxy and dioxycarbenes.

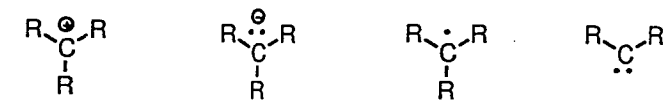

Figure 1. Low-valent carbon species.

1.1. Electronic Structure of Carbenes

Carbenes are among the few simple molecules (O_2 is another) that have more than one accessible low-energy electronic state.[5] They are neutral species in which a divalent carbon possesses a total of four valence electrons, of which two are bonding and two are non-bonding. Four valence atomic orbitals, the 2s and the three 2p-orbitals, contribute to bonding in carbenes. This combination allows for a low energy singlet or triplet electronic configuration. One could consider an extreme linear geometry of the parent carbene, methylene, corresponding to sp hybridization at the carbon, with two degenerate unhybridized p-orbitals each occupied by a single electron (Figure 2).

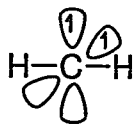

Figure 2. Hypothetical linear triplet carbene.

Electron spin resonance measurements made on triplet methylene show that it is actually a bent molecule with an angle of 136°.[6-8] This result suggests that methylene is approximately sp^2-hybridized, with two non-degenerate, non-bonding orbitals: an in-plane sp^2-orbital (σ), and an unhybridized p-orbital (Figure 3). In fact singlet methylene has a H-C-H angle of 102° and carbenes can generally be thought of as being sp^2 roughly hybridized (Figure 3).[8,9] The distribution of the two non-bonding electrons in the non-bonding molecular orbitals, and hence the multiplicity of the ground state, is determined by the relative orbital energies and the electron-electron repulsion. If the difference in energy between the nonbonding orbitals is greater than the energy required to bring the

electrons together in a single orbital, then the carbene will have two electrons paired in an sp^2 type orbital. This hybridization is in keeping with the Pauli exclusion principle and gives a ground state singlet. On the other hand, if the energy difference between the nonbonding orbitals is less than the energy required to pair the electrons in the same orbital, then the two nonbonding electrons will occupy two different orbitals. According to Hund's rule these electrons should be unpaired in order to achieve the minimum energy, resulting in a ground state triplet.

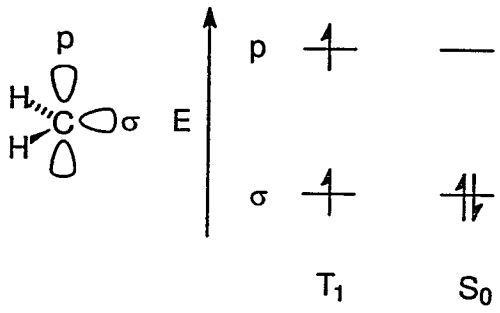

Figure 3. The sp^2 hybridization and geometry of triplet and singlet methylene.

Methylene is a ground state triplet for which experimental and theoretical estimates of the singlet-triplet energy gap (ΔH_{st}) now converge at 9 ± 1 kcal mol^{-1}.[8,9] Many alkyl-substituted carbenes have small ΔH_{st} gaps with singlet dimethylcarbene (Me_2C:) only 1.4 to 1.6 kcal mol^{-1} more stable than the triplet.[10,11] The factors that influence the spacing between the singlet and triplet states can be analyzed in terms of electronic and steric effects.[12]

The most influential electronic effect is the interaction of the carbenic p-orbital with p- or π-orbitals of the substituent(s). Fleming has classified substituents that interact with a π system into three classes: X (π-electron donors such as -NR_2, -OR, -SR, -F, -Cl,

-Br and –I), Z (π-electron acceptors such as -COR, -SOR, -SO_2R, -NO and -NO_2), and C (conjugating groups such as vinyl, alkynyl or aryl groups).[13]

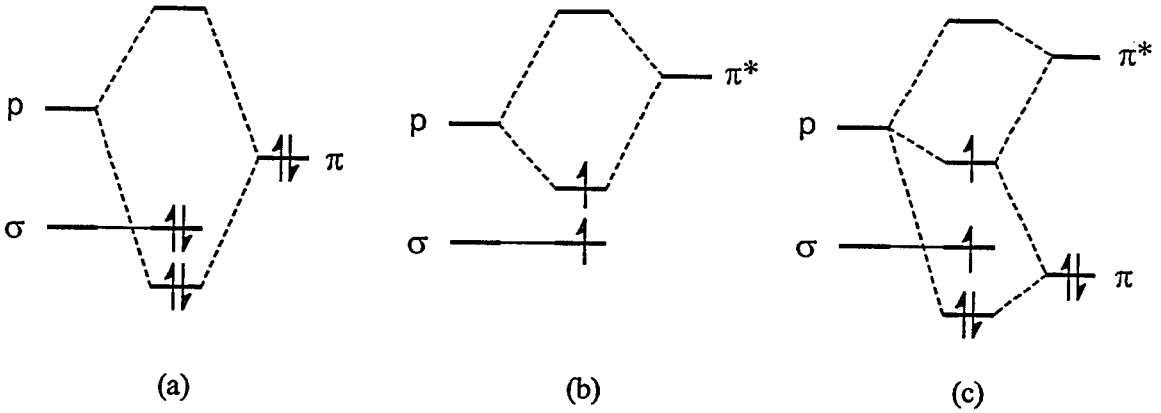

Figure 4. MO diagrams of the interaction of the nonbonded orbitals of a carbene with (a) an X substituent, (b) a Z substituent, and (c) a C substituent.

Figure 4(a) shows how a π-electron donor of type X interacts with the carbene p-orbital to raise its energy. This increases the separation between the carbene σ- and p-orbitals resulting in a ground state singlet. For example in fluorocarbene (HCF) the singlet has been calculated to be 14.7 kcal mol^{-1} lower in energy than the triplet.[14] The addition of a second fluoro group to give difluorocarbene (CF_2) increases the singlet triplet gap to -56.6 kcal mol^{-1}.[15] In the case of dimethoxycarbene† (1) the singlet has been calculated to lie 76.3 kcal mol^{-1} below the triplet.[16] A valence bond analysis of these types of carbenes indicates that the singlet ground state is stabilized by donation from the X type substituent to the carbene p-orbital as illustrated for dimethoxycarbene (1) in

† The generic nomenclature, e.g. dialkoxycarbene, is used throughout this thesis rather than the more specific nomenclature, e.g. dioxacarbene, which requires locant numbers for positions of the atoms. Warkentin, J. In *Advances in Carbene Chemistry*; Brinker, U. H., Ed.; JAI Press Inc.: London, 1998; Vol. 2, pp 245-295.

Figure 5. This electron donation results in considerable double bond character in the carbene donor bond. For dihydroxycarbene (**2**) it has been calculated that breaking this double bond character by rotating the C-O bond costs ~13 kcal mol^{-1}.[17] A second, less important effect, is also active here. Inductive withdrawal by these electronegative substituents through the σ framework stabilizes the nonbonding electrons that occupy the carbene σ-orbital.[18] Since this orbital is doubly occupied in the singlet, but only singly occupied in the triplet, this effect is thought to stabilize the singlet relative to the triplet state.

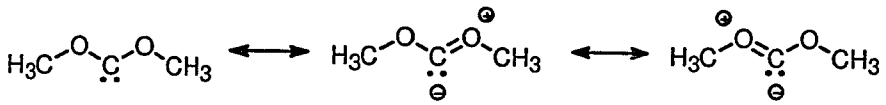

1

Figure 5. Stablization of singlet dimethoxycarbene (**1**) by back donation from oxygen.

Z and C substituents, on the other hand, have low lying π*-orbitals which either lower the energy of the carbene p-orbital or leave it relatively unaffected as demonstrated in Figure 4(b and c). A triplet ground state is therefore expected for these carbenes. Simple aryl and vinyl derivatives of methylene do indeed have triplet ground states, as do carbenes with directly attached electron withdrawing substituents such as -CN, C(O)Ph, and -C(O)OR.[6,19,20]

The magnitude of the singlet-triplet gap is also sensitive to the bond angle at the carbene carbon and *vice versa*. At a bond angle of 180°, methylene has two degenerate p-orbitals on the carbene carbon. Decreasing this bond angle from 180° increases the s character of one of the orbitals creating a σ-orbital, thereby removing the degeneracy.

Calculations show that smaller bond angles favour singlet ground states. Continuing to decrease the bond angle eventually separates the σ- and p-orbital energies enough to give a singlet ground state.[21,22] However, it is not always clear how much stabilization can be expected from forcing small carbene bond angles. For example, calculations on cyclobutylidene (**3**) suggest that the singlet is 5.9 kcal mol^{-1} more stable than the triplet state, as compared to dimethylcarbene in which the difference is 1.4 to 1.6 kcal mol^{-1}.[10,23] The 5.9 kcal mol^{-1} of stablization is less than expected, which is thought to be due to the loss of hyperconjugative stabilization from the adjacent C-H bonds at small carbene centre angles.

3

1.2. Singlet vs. Triplet Carbene Reactivity

The state in which a carbene is produced depends on the method of generation.[24] Singlets are normally formed in thermal reactions and photochemical reactions without triplet sensitizers while triplet carbenes are formed from photochemical reactions in the presence of a sensitizer. If a carbene is produced in an excited electronic state it will normally undergo fast decay to its ground state.[25] As a result, carbenes will react from their excited state only if they are trapped very quickly.

Generally, carbene reactivity is determined by the spin-state and they react by spin-state-specific mechanisms.[26] Triplet carbenes normally behave as free radicals, and participate in stepwise reactions involving biradicals or radical pairs. For singlet

carbenes concerted reactions are possible and stereochemistry is often conserved. The reactions of carbenes with olefins have been well studied and they illustrate the differences between singlet and triplet reactivity.

Skell and Woodworth proposed that the spin-state of a carbene can be determined from the stereochemistry of cyclopropane formation.[5,27,28] The addition of a singlet carbene to an olefin generally proceeds in a single step so that the geometry of the alkene is preserved in the cyclopropane (Figure 6(a)).[29] However, concerted cycloadditions are not possible for triplet carbenes due to spin conservation requirements, and isomerization can occur in the diradical intermediate depending on the rate of spin inversion (Figure 6(b)).[29]

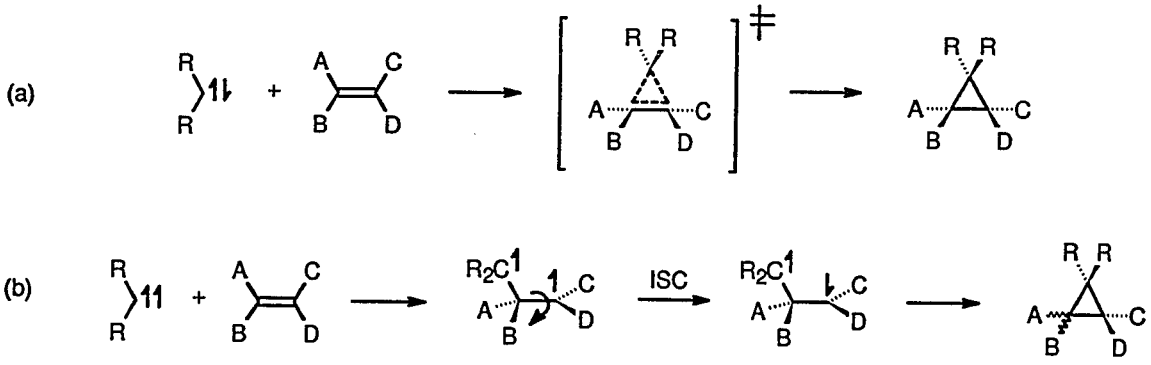

Figure 6. Typical mechanisms for the addition of carbenes to olefins: (a) concerted mechanism for singlet carbenes; (b) stepwise mechanism for triplet carbenes with loss of stereochemistry.

Singlet carbenes also insert into C-H bonds with retention of configuration and a single step process is likely (Figure 7(a)).[30] Triplet carbenes, on the other hand, are thought to react by a hydrogen abstraction mechanism similar to that of free radicals (Figure 7(b)).[31]

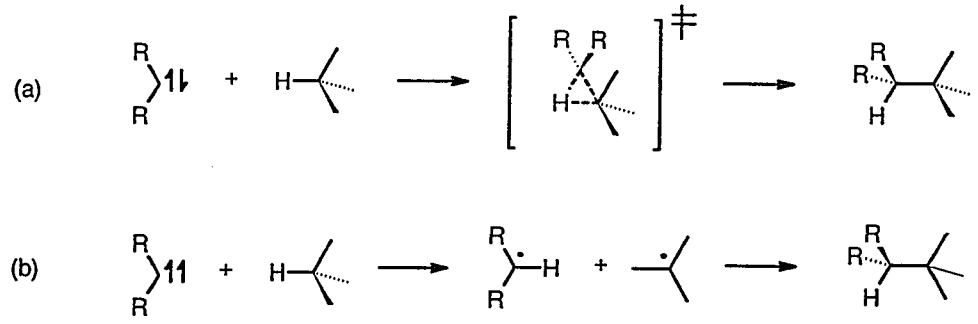

Figure 7. Typical mechanisms for the insertion of carbenes into C-H bonds: (a) concerted mechanism for singlet carbenes; (b) stepwise mechanism for triplet carbenes.

Of course adherence to these mechanistic types to distinguish between singlet and triplet carbenes can be complicated by a number of factors. For example, the small S-T gaps of arylcarbenes can result in misleading results.[30] Section 1.5.2 will also show that there is no requirement for singlet carbenes to react by a concerted mechanism and there are circumstances where triplet carbenes react with retention of stereochemistry.[32,33]

1.3. Electrophilic vs. Nucleophilic Reactivity of Singlet Carbenes

Carbenes lack a complete valence octet, and completing the valence shell is an important driving force in carbene chemistry. Skell[34] and Doering[35] carried out early reactivity measurements in which two alkenes were allowed to react with an insufficiency of dibromocarbene[34] (CBr_2) and dichlorocarbene[35] (CCl_2). CBr_2 and CCl_2 were found to be electrophilic, reacting most rapidly with simple, alkyl substituted alkenes. Since this early work the selection of available carbenes has grown considerably and the "philicity"

of carbenes now extends from the conventional electrophiles to ambiphiles and nucleophiles.

Work by Moss has been instrumental in developing an understanding of the philicity of carbenes.[36,37] He has developed a selectivity index, m_{CXY}, in which the olefinic selectivity of carbenes is quantified with a free energy relationship. The relative rates of addition of a given carbene (CXY) to a standard series of electron rich alkenes are plotted against the same measurements for CCl_2 (by definition $m_{CXY} = 1.00$ for CCl_2) to give m_{CXY} as the slope of a log-log correlation. Multiple linear regression analysis of the dependence of m_{CXY}(obsd) on σ_R^+ and σ_I afforded the substituent parameter correlation, eq. 1, which allows for the determination of m_{CXY} for unknown carbenes or carbenes which are unreactive with the chosen set of alkenes.

$$m_{CXY} = -1.10\Sigma_{X,Y}\sigma_R^+ + 0.53\Sigma_{X,Y}\sigma_I - 0.31 \qquad (1)$$

Although there are no absolute "borders" between the m_{CXY} values of electrophilic, ambiphilic and nucleophilic carbenes, it is useful to examine some of these values. The border between electrophilicity and ambiphilicity appears to be experimentally located at $m_{CXY} \cong 1.5$, while carbenes with $m_{CXY} > 2.2$ are nucleophilic. For example, the electrophile, chloro(methyl)carbene (MeCCl) has an experimental m_{CXY} value of 0.58, while the ambiphile, fluoro(methoxy)carbene (MeOCF) has a value of 1.85. The nucleophilic carbenes, dimethoxycarbene (**1**) and methoxy(dimethylamino)carbene ($MeOCNMe_2$) (**4**), have calculated m_{CXY} values of 2.22 and 2.91 respectively.

Frontier molecular orbital (FMO) theory[13] can be used to account for Moss's selectivity index.[37-39] The addition of a singlet carbene to an alkene involves simultaneous interactions of the virtual carbenic p-orbital (Lowest Unoccupied Molecular Orbital) with the filled alkene π-orbital (Highest Occupied Molecular Orbital) (Figure 8(a)) and of the filled carbenic σ-orbital (HOMO) with the virtual π*-orbital (LUMO) of the alkene (Figure 8(b)).

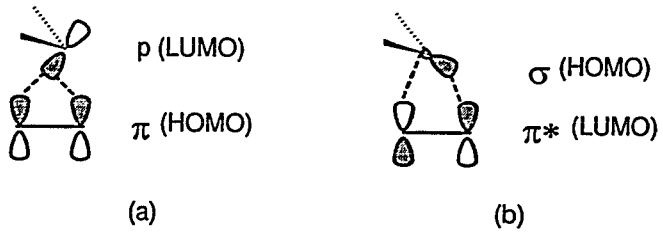

Figure 8. HOMO-LUMO interactions for cycloadditions of singlet carbenes to alkenes.

The dominant orbital interaction can be determined by examining the differential HOMO/LUMO energies. The orbital energies are usually calculated for carbenes and are known from spectroscopy for alkenes.[37,38] For electrophilic carbenes such as CCl_2 the dominant interaction is $LUMO_{CXY}$-$HOMO_{alkene}$ (Figure 9(a)), while for nucleophilic carbenes such as dimethoxycarbene (1) the dominant interaction is $LUMO_{alkene}$-$HOMO_{CXY}$ (Figure 9(b)). It was also found that for ambiphilic carbenes the differential HOMO and LUMO energies are comparable (Figure 9(c)). Therefore substitution of electron-donating or electron-withdrawing substituents on the alkene should convert Figure 9(c) to Figure 9(a) or (b) respectively.

It is interesting to analyze the consequences of this model for nucleophilic carbenes such as dimethoxycarbene (**1**). A glance at Figure 4(a) indicates that X substituents, such as methoxy groups, actually result in a higher energy virtual p-orbital rather than a higher energy σ-orbital, lowering the preferred $LUMO_{CXY}$-$HOMO_{alkene}$ interaction. The electron donating groups help to complete the carbenic centre's octet. The combined result is that nucleophilic carbenes do not react with simple alkenes.[36] In order for a nucleophilic carbene such as **1** to react with an alkene, the alkene's π* LUMO must in fact be lowered in energy by adding electron withdrawing substituents.

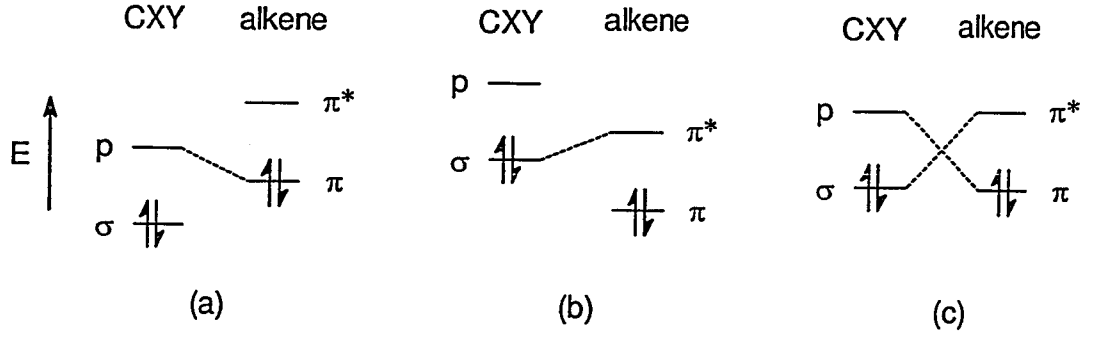

Figure 9. Relative FMO energies and dominant interactions for the reaction of an alkene with: (a) an electrophilic carbene; (b) a nucleophilic carbene; and (c) an ambiphilic carbene.

These trends also appear to be reflected in the calculated tilt angle, α, for the carbene CXY plane with respect to the original ethylene plane at the addition transition state (Figure 10).[38] For a pure electrophilic approach α would be 0°, while α would be 90° for a pure nucleophilic approach. The theoretical results using the STO-3G basis set indicated that α increased smoothly from 36° for CCl_2 to 58° for $C(OH)_2$, suggesting that

α increases with increasing $HOMO_{CXY}$-$LUMO_{alkene}$ interaction. Naively, α may be taken as an indicator of carbene philicity: for electrophiles $\alpha < 45°$, whereas for nucleophiles $\alpha > 50°$.

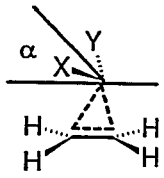

Figure 10. Transition state geometry for cycloadditions of singlet carbenes to alkenes.

1.4. Generation of Oxy- and Dioxycarbenes

A wide variety of techniques have been developed for the generation of oxy- and dioxycarbenes. Each method has advantages depending on whether the resultant carbene is to be used for synthetic, spectroscopic or kinetic applications. A number of these techniques have recently been reviewed.[40]

1.4.1. α-Elimination

Dialkoxy-*p*-chlorophenoxymethanes (**5**) have been investigated by Scheeren as possible dioxycarbene sources when treated with strong base.[41] Formation of dioxycarbenes in this system is complicated by a number of competing pathways that yield the apparent carbene products, tetraalkoxyethylenes (**6**) (Scheme 1). Due to the alternative pathways, the formation of a carbene intermediate is ambiguous in these

systems and α-elimination is not a suitable technique for mechanistic studies where the identity of the reactive intermediate must be clearly established.

Scheme 1

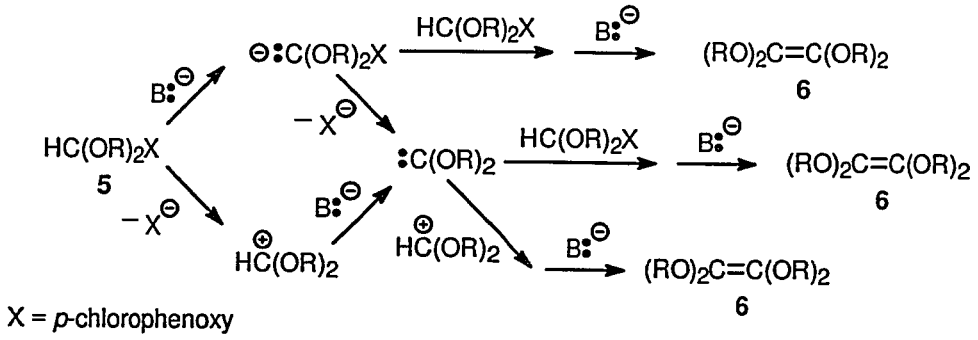

In a similar reaction, cyclic and acyclic dioxycarbenes have been generated by the treatment of dialkoxymethyl fluoroborate with base as shown in equation 2 for a cyclic system.[42]

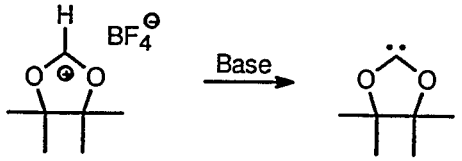

(2)

Thermal α-elimination of acetic acid from methylacetate derivatives has also been used to generate a handful of oxy- and dioxycarbenes (Scheme 2).[43] The elimination was suggested to proceed through a five-membered ring transition state (Scheme 2). Due to the high temperatures involved, the carbenes generated in this manner follow possible rearrangement and fragmentation pathways (See Section 1.5.1.1).

Scheme 2

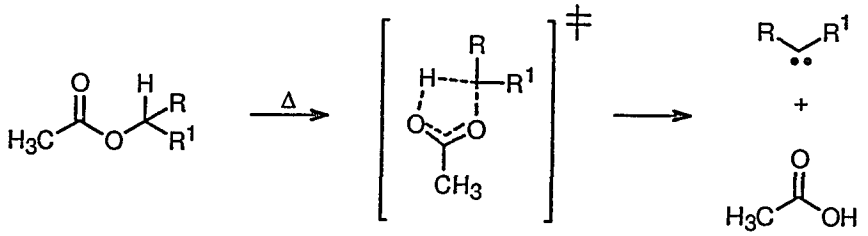

Hoffmann has shown that trimethylorthoformate (**7**) can be used to generate dimethoxycarbene (**1**) when heated (~150 °C) with arylisocyanates (**8**) (Scheme 3).[44] The mechanism involves a stepwise α-elimination (Scheme 3). While this approach has been useful for the studying the reaction of dimethoxycarbene (**1**) with arylisocyanates (**8**) the presence of these isocyanates limits this method's utility in other synthetic or mechanistic applications.

Scheme 3

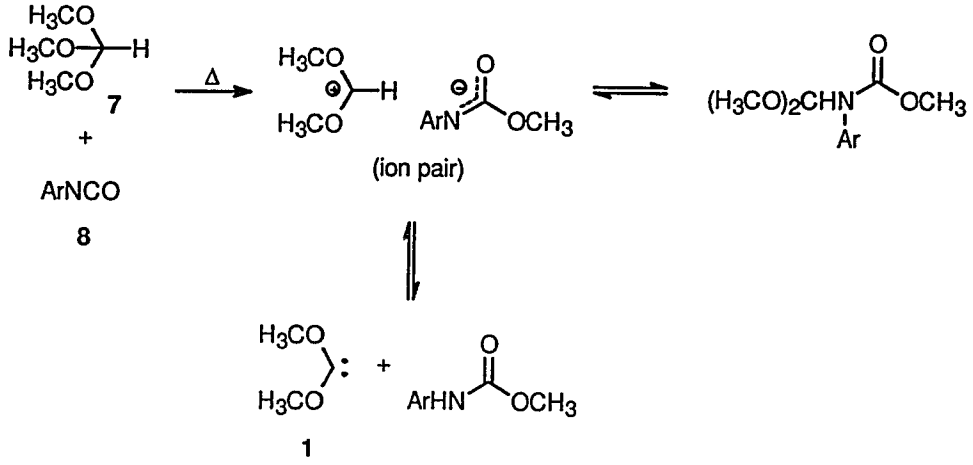

1.4.2. Fragmentation of *p*-Tosylhydrazone Salts

The salts of *p*-tosylhydrazones (**9**) decompose thermally and photochemically to diazo-compounds (Scheme 4).[45] Under protic conditions the diazo-compounds (**10**) generated by this route decompose by a cationoid mechanism, however under aprotic conditions a carbenoid mechanism prevails.

Scheme 4

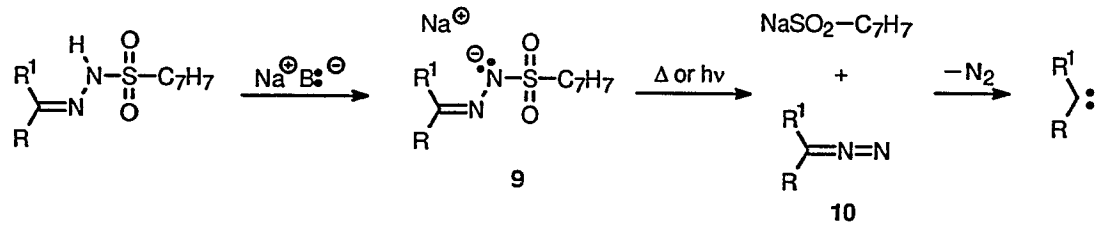

A variety of oxy- and dioxycarbenes have been generated by this method.[45-48] However, the high temperatures (~160 to 310 °C) required usually result in homolytic fragmentation (See Section 1.5.1.1) of the carbene and this has limited use of *p*-tosylhydrazone salts as a synthetic source of oxy- and dioxycarbenes.

1.4.3. Photolysis and Thermolysis of Oxalic and Pyruvic Acid

The parent dioxycarbene, dihydroxycarbene (**2**) has been suggested as an intermediate in the gas phase photolysis[49] and thermolysis[50] of oxalic acid (Scheme 5) while hydroxy(methyl)carbene has also been generated by the photolysis[51] and pyrolysis of pyruvic acid[52].

Scheme 5

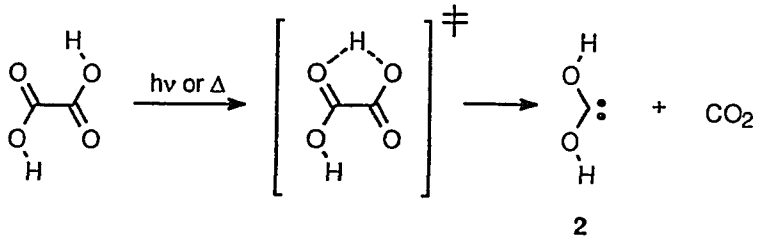

2

1.4.4. Photochemical Fragmentation of Cyclic Ketones

Cyclic ketones can be photochemically converted to cyclic oxycarbenes by ring expansion.[53,54] It is now generally accepted that the reaction proceeds by a stepwise mechanism with α-cleavage to a biradical followed by rebonding on oxygen (Scheme 6). Despite the stepwise mechanism, it is interesting to note that retention of stereochemistry is observed when the cyclic ketone possesses a stereogenic centre.[53,55] A wide variety of cyclic oxycarbenes have been generated in this manner and the reaction does have some synthetic utility.[53,55]

Scheme 6

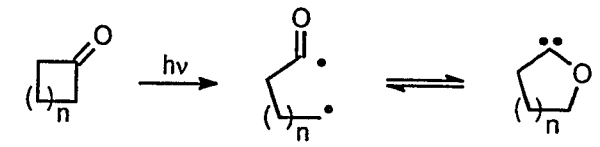

n = 1 or 2

1.4.5. Cycloreversion

Cycloreversion or cycloelimination is the cleavage of a carbocycle or heterocycle into two or more independent fragments.[56] Cycloreversion may also be defined as the

reverse of cycloaddition and as such is subject to the same selection rules.[57] Cycloreversion from a ring having an even number of members (atoms) generally leads to fragments that have an even number of former ring atoms. These even fragments have saturated valences and are therefore of relatively low energy. However, cycloreversion from rings with odd numbers of ring atoms must yield odd fragments with unsaturated valences and high energy. Cycloreversions may be thermally or photochemically initiated and do not require the presence of other reagents. For these reasons, cycloreversion forms the basis of a number of important procedures for the generation of carbenes.

In 1964 Hoffmann and Lemal both independently developed the thermolysis of 1,2,3,4-tetrachloro-7,7-dialkoxy-5-phenylnorbornadienes (**11**) as a route to dialkoxycarbenes.[58,59] This carbene precursor could be easily synthesized by the Diels-Alder addition of the tetrachlorocyclopentadienone ketal (**12**) to phenylacetylene (Scheme 7). Unfortunately the synthesis of tetrachlorocyclopentadienone ketals (**12**) is not general and only a limited number of symmetric carbenes can be generated by this route.[56,60] Scheme 7(a) illustrates the fragmentation of **11** to give the dialkoxycarbene which is driven by the formation of the aromatic tetrachlorobiphenyl (**13**). There is also an additional competing pathway (Scheme 7(b)) and it is necessary to remove the byproducts from both pathways in order to isolate the carbenic products.

Scheme 7

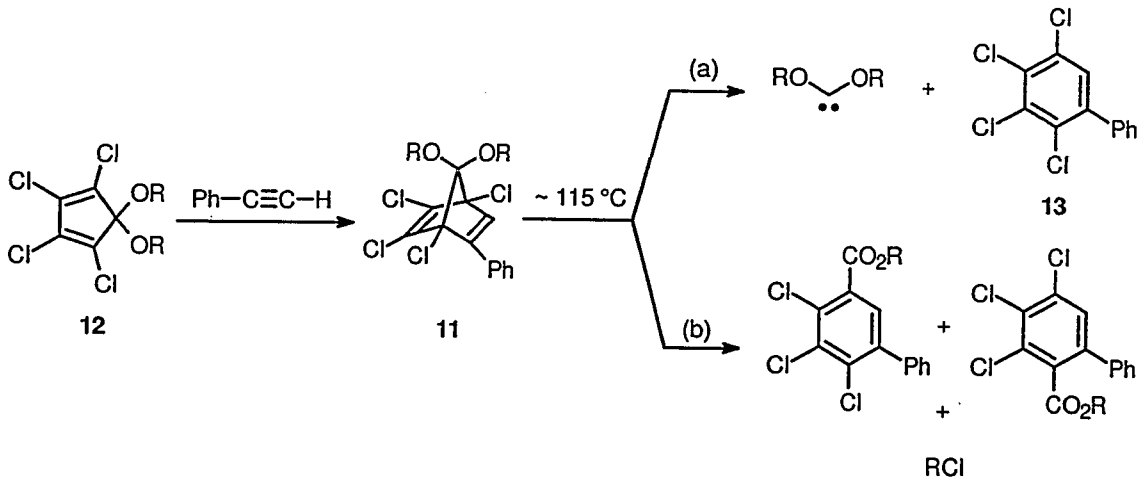

While **11** proved to be the most useful of the norbornadiene carbene precursors, a variety of other derivatives have been examined including the parent 7,7-dialkoxynorbornadienes (**14**).[56,61-63] It is interesting to note that attempts to generate methoxycarbene (H_3COCH) (**15**) from the appropriate nornbornadiene precursor, **16**, have been unsuccessful.[64] It has been suggested that two alkoxy groups are required to stabilize the heterolytic component of the fragmentation pathway which leads to a singlet carbene.[65]

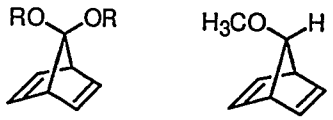

14 **16**

Quadricyclane derivatives (**17**) have also been used as sources of dioxycarbenes. It is thought that the fragmentation probably proceeds through norbornadienone ketal intermediates (Scheme 8).[56,61,66]

Scheme 8

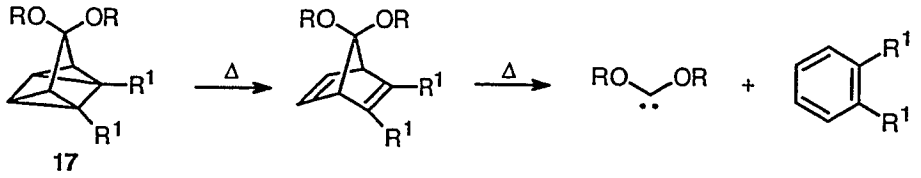

17

$R^1 = CO_2CH_3$ or H

In addition, Hoffmann has used 7,7-dimethoxycycloheptatriene (**18**) to generate dimethoxycarbene (**1**) at high tempetatures (Scheme 9).[67]

Scheme 9

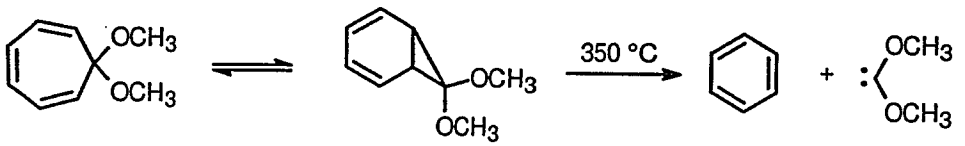

18 **1**

Hexamethoxycyclopropane is also a thermal source of dimethoxycarbene (**1**) (eq. 2).[68] However, the high temperature required has prevented its use in synthetic applications.

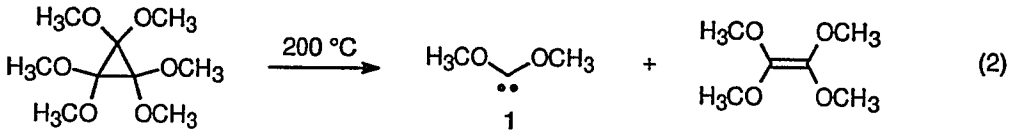

(2)

It has been suggested that tetramethoxyoxirane (**19**), could be formed in the ozonolysis of tetramethoxyethylene (**20**), and fragment to dimethoxycarbene (**1**) at 100 °C (Scheme 10).[69] However, there is very little evidence for formation of **1** from **19** or even for **19** itself.[69,70]

Scheme 10

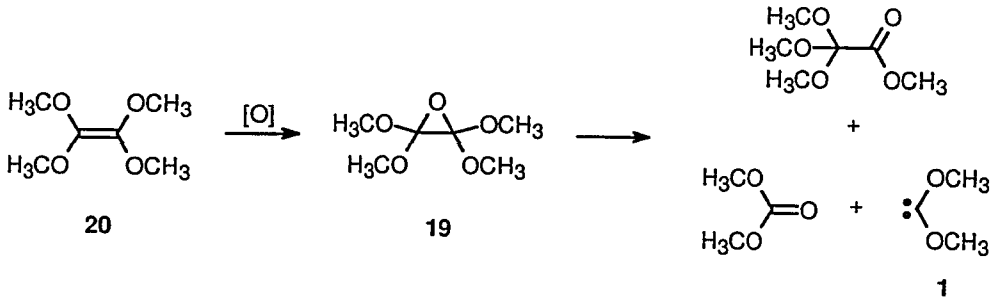

In 1982 Moss made a significant advance with the introduction of methoxy(phenyl)diazirine (**21**) as a photochemical and thermal source of methoxy(phenyl)carbene (**22**) (eq. 3).[71,72]

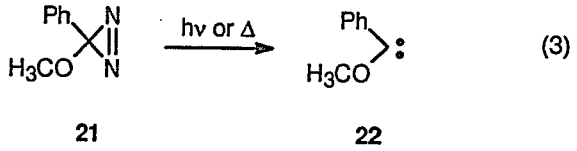

(3)

The general sequence for the synthesis of **21** is illustrated in Scheme 11 where R^1 is phenyl and R^2 is methyl. In 1988 the methoxy(methyl)carbene (**23**) precursor, methoxy(methyl)diazirine (**24**), was produced by a simple modification of this procedure with R^1 equal to methyl.[73] This synthesis has been shown to be quite versatile and a number of alkyl(methoxy)diazirines have been generated.[74]

Scheme 11

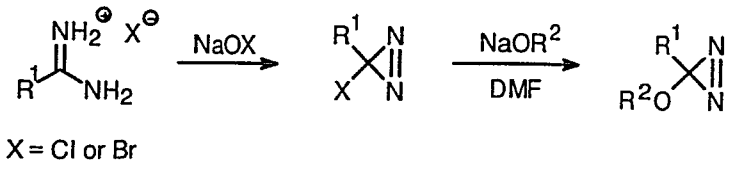

In 1987 Moss produced the methoxy(phenoxy)carbene precusor, **25**, by this procedure.[75] Since this initial success with dioxycarbene synthesis, Moss has also undertaken work to generalize the reaction by producing dimethoxydiazirine[16] (**26**), trifluoroethoxy(methoxy)diazirine[76] (**27**), and bis-trifluoroethoxydiazirine[76] (**28**).

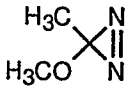

24

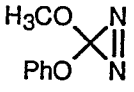

25

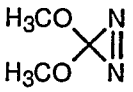

26

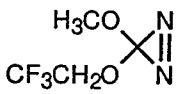

27

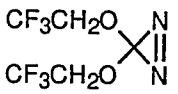

28

The diazirine methodology has allowed for significant advances in the direct observation of oxy and dioxycarbenes, providing the means for careful examination of their kinetics with laser flash photolysis (LFP) methods. Diazirines also remain the only photochemical source of dioxycarbenes. However, they do have a couple of drawbacks. Diazirines have short lifetimes, with half-lives ranging from only 5 to 60 minutes in pentane at 25 °C.[37,77] They are also hazardous materials that can be explosive in their pure form. Due to these difficulties, diazirines have limited applications as synthetic reagents.

In 1981, Békhazi and Warkentin introduced 2-methoxy-2,5,5-trimethyl-Δ^3-1,3,4-oxadiazoline (29) as a thermal (~80 °C) source of methoxy(methyl)carbene (**23**) and dimethylcarbene (Me_2C:).[78] The oxadiazoline undergoes cycloreversion to a carbonyl ylide which can then fragment by path (a) or (b) to yield the carbenes (Scheme 12). In subsequent papers, these carbenes, as well as a number of other derivatives, were explored using oxadiazoline precursors of this type.[79-82]

Scheme 12

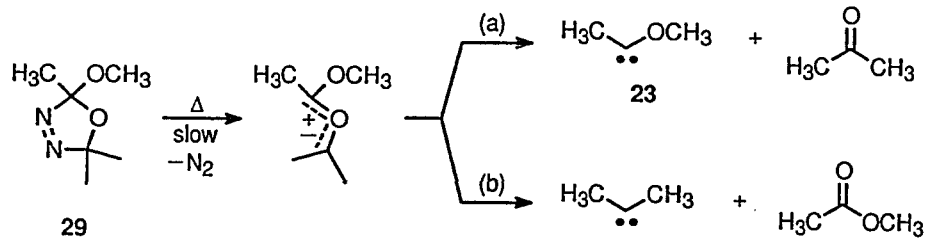

2,2-Dialkoxy-Δ^3-1,3,4-oxadiazolines **30** were introduced by Warkentin's group in 1992 as readily accessible, shelf-stable liquids that serve as convenient thermal sources (~100 to 110 °C) of dialkoxycarbenes.[83] Unlike the monoalkoxy analogues, these oxadiazolines undergo cycloreversion and fragmentation of the ylide to yield dialkoxycarbenes almost exclusively. Their introduction has considerably increased the range of dialkoxycarbenes that can be generated (Scheme 13).

Scheme 13

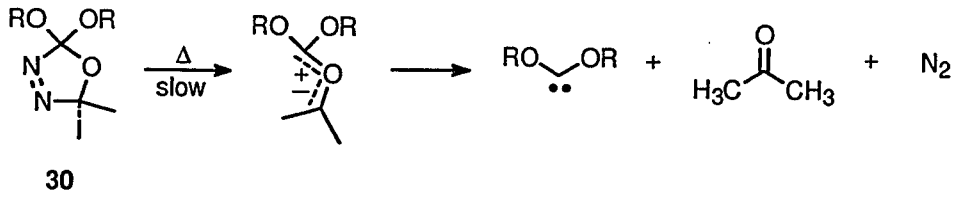

30

Two general approaches are available for the production of these oxadiazolines.[78,83-86] In the first approach, oxidation of (alkylcarbonyl)hydrazones (**31**, R^1 = alkyl) or (alkoxycarbonyl)hydrazones (**32**, R^1 = alkoxy) of acetone by lead tetraacetate (LTA)[83], iodobenzene diacetate[85], or by electrochemical means[86] can yield oxadiazolines, as pure compounds (Scheme 14).

Scheme 14

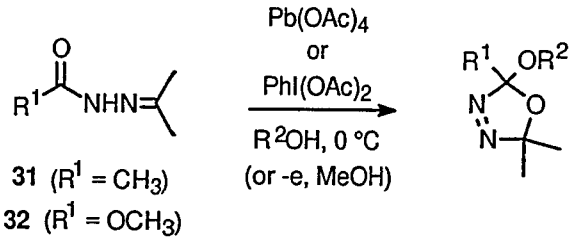

The second method is an extremely versatile approach to 2,2-dialkoxy-Δ^3-1,3,4-oxadiazolines (**30**) from 2-acetoxy-2-alkoxy-5,5-dimethyl-Δ^3-1,3,4-oxadiazolines (**33**). This method allows for the introduction of alkoxy groups into the carbene that would have been oxidized by the first method.[84] Treatment of **33** with an alcohol or phenol in CH_2Cl_2 containing acetic acid results in acetoxy exchange to give dialkoxyoxadiazolines **30** (Scheme 15).

Scheme 15

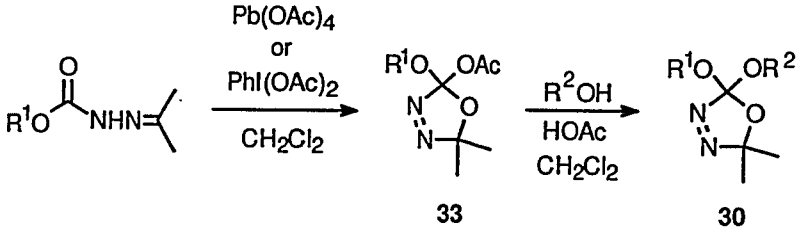

Oxadiazolines have many advantages over other thermal sources of oxycarbenes for synthetic applications. They are shelf stable for extended periods and a wide variety of symmetric and asymmetric carbenes can be generated at reasonable temperatures. For the dialkoxyoxadiazolines (**30**) in particular, the byproducts of thermolysis (N_2 and acetone) do not interfere with the isolation of the carbene derived products.

1.4.6. Neutralization-Reionization Mass Spectrometry

Neutralization-Reionization Mass Spectrometry (NRMS) has been used to study a number of carbenes in the gas phase. The technique involves ionization of a carbene precursor, which then undergoes fragmentation to a radical cation corresponding to the carbene of interest. This radical cation is neutralized by electron capture to give the carbene. For example, various dioxycarbenes have been generated by NRMS using an oxadiazoline as the precursor (Scheme 16).[87,88]

Scheme 16

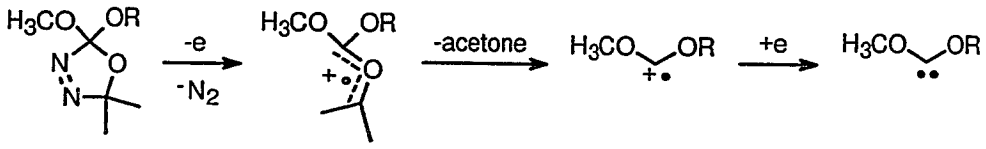

R = CH_3, CH_2CH_3, CH_2CF_3 or $CH(CH_3)_2$

By the same technique dihydroxycarbene (**2**) has been generated using fumaric acid[89] or oxalic acid[90] as the precursor, as well as hydroxy(methyl)carbene (CH_3COH) from pyruvic acid[91], hydroxycarbene from methanol[92,93] or methyl glyoxylate[94] and ethoxycarbene from ethyl glyoxylate.[95]

1.5. Chemistry of Oxy- and Dioxycarbenes

In this section, emphasis is placed on the chemistry of oxy- and dioxycarbenes, which is the focus of this thesis. Where it is instructive, the chemistry of other carbenes is included.

1.5.1. **Intramolecular Reactions**

1.5.1.1. *Fragmentations to Radicals*

Oxy and dioxycarbenes can undergo fragmentation to radicals either photochemically or thermally. Homolysis of cyclic oxycarbenes, generated by the photolysis of cycloalkanones, to acyl alkyl biradicals has been suggested[54,96] and established[97] (Scheme 6, Section 1.4.4). Ring opening of cyclic oxy[48,98-100] and dioxycarbenes[47] has also been proposed in a number of cases where the carbenes were generated by the pyrolysis of tosylhydrazone salts **9** at temperatures ranging from 190 to 210 °C (Scheme 17 and Scheme 18).

Scheme 17

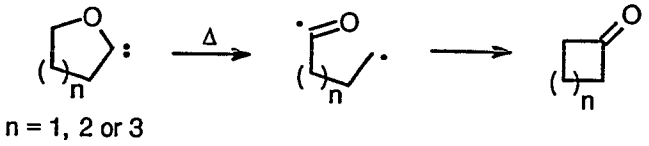

Scheme 18

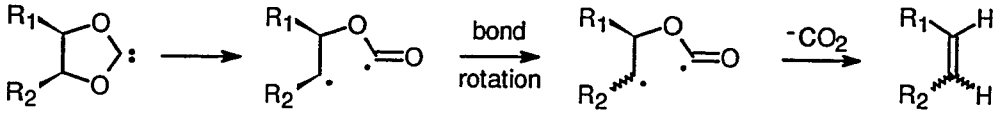

The fragmentation of cyclic dioxycarbenes (Scheme 18) is related to the well known Corey-Winter alkene synthesis.[101,102] In this case the carbene, which is usually generated by refluxing a cyclic thionocarbonate **34** in trimethyl phosphite (~112 °C), undergoes cycloreversion with retention of stereochemistry at the C-C bond (Scheme 19).[103]

Scheme 19

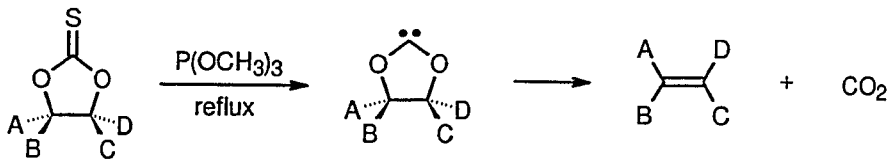

34

The lower temperature required for the Corey-Winter reaction is a likely reason for the retention of stereochemistry in these reactions, as opposed to the loss of stereochemistry that occurs when cyclic dioxycarbenes are generated by the tosylhydrazone route.[47] Theoretical calculations by Sauers have identified a transition state for this concerted cycloreversion.[104] The Corey-Winter synthesis has also been modified, replacing trimethyl phosphite with a diazaphospholidine, allowing for the generation of olefins at room temperature.[103]

Acyclic oxy and dioxycarbenes also appear to decompose to radical pairs when generated thermally by the tosylhydrazone route at 158 and 175 °C in solution (Scheme 20).[45,46]

Scheme 20

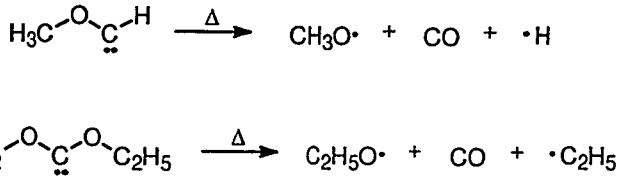

A number of authors have suggested that dioxycarbenes fragment thermally to yield alkyl and oxycarbonyl radicals (eq. 4). Lemal *et al.* proposed that dimethoxycarbene, generated by the vapour phase pyrolysis of norbornadienone ketals at

200 °C, fragments to methyl and methoxycarbonyl radicals.[60,61] Vibrationally excited dimethoxycarbene[87] (**1**) and 2,2,2-trifluoroethoxy(methoxy)carbene[88] ($CH_3COCOCH_2CF_3$) (**35**), generated by neutralization-reionization mass spectrometry from oxadiazoline precursors, are also believed to fragment to radicals. Hoffmann *et al.* performed labelling studies to show that the esters derived from the gas phase pyrolysis of 7-methoxy-7-allyloxy-bicyclo[2.2.1]heptadiene and 7,7-diallyloxy-bicyclo[2.2.1]heptadiene at 250 °C come from a radical mechanism, likely through the allyloxy substituted carbenes.[62]

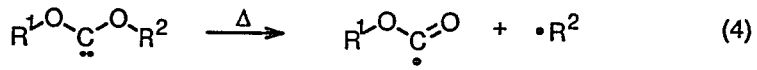

(4)

Recent carbene and radical trapping studies by Venneri and Warkentin provided strong evidence for the thermal fragmentation of allyloxy(methoxy)carbenes (**36**) to radicals in solution at 110 °C to give products of apparent [1,2]- and [2,3]-sigmatropic rearrangements **37** (Scheme 21).[105]

Scheme 21

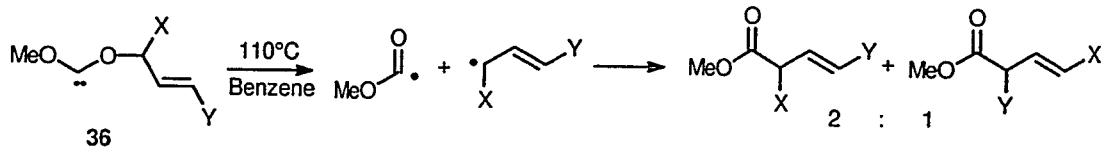

36

(X = Ph, Y = H) or
(X = H, Y = Ph)

37

The Warkentin group has also shown that benzyloxy(methoxy)carbene ($MeOCOCH_2Ph$) (**38**) and benzyloxy(4-substituted benzyloxy)carbenes

($PhCH_2OCOCH_2Ar$) (**39**) fragment to radicals.[106,107] They were able to estimate that the rate constant for fragmentation of **38** to methoxycarbonyl (MeOCO) and benzyl radicals ($PhCH_2$) was $\leq 10^7$ s^{-1} at 100 °C.[106] In addition, by using an oxadiazoline to generate **39**, they found that the homolytic fragmentation favoured formation of the benzyl radical with an electron-withdrawing group in the para position.

Surprisingly, there has been very little theoretical consideration given to the mechanism for homolysis of oxy- and dioxycarbenes. Computational work on the photochemical rearrangement of cyclic carbonyl compounds to oxycarbenes indirectly explored a triplet mechanism for the homolysis of oxycarbenes.[108,109] The triplet (T_1) state (n-π^*) of the oxycarbene would be reached either photochemically or thermally by intersystem crossing, followed by β-scission to give the biradical. Borden *et al.* studied the homolysis of the w-conformer of dihydroxycarbene (**2**) from its singlet ground state (S_0) and found the H and COOH radicals to be 48 kcal mol^{-1} (CISD/STO-3G) above the carbene (43 kcal mol^{-1} at the CISD/DZP level).[110] These authors also found an additional barrier of ~3 kcal mol^{-1} corresponding to a transition state for fragmentation to the radicals, but they were not able to conclude from their results if such a barrier was real. They suggested that the fragmentation should be similar to the homolysis of formaldehyde to the same radicals, which was previously reported to occur without a transition state.[111] The same view was expressed by Saito *et al.* when they suggested homolysis as a pathway for dihydroxycarbene (**2**).[112] They pointed out that for simple scission reactions, the threshold energies can be nearly equal to the heats of reaction.

1.5.1.2. *Concerted [1,2]-Migrations*

[1,2]-Hydrogen shifts and, to a lesser extent, [1,2]-carbon migrations are the most common carbenic rearrangements.[74] For simple carbenes the mechanism is generally thought to involve migration of a group with its pair of electrons to a formally vacant carbenic p-orbital. Therefore this process is favoured if the orbitals involved in the transition state are coplanar, as demonstrated in Figure 11 for a hydride shift. Like [1,2]-migrations of carbocations, this is an allowed 2-electron transition state, and as a result, the activation energy can be very low. For example the rate constant for the [1,2]-hydrogen shift of dimethylcarbene has been estimated to be greater than 10^8 s^{-1} at ambient temperatures.[74,113] The qualitative ranking of migratory aptitudes, H > aryl > alkyl for carbocations, also holds for carbenes.[114]

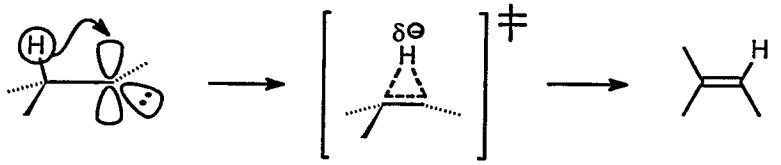

Figure 11. Preferred geometry for the [1,2]-hydrogen migration of a generalized singlet carbene.

Electron-donating substituents on the carbene centre raise the activation energy and slow down the rearrangement. High level Møller-Plesset *ab initio* calculations predict activation energy barriers for the [1,2]-H shifts of carbenes (Me-C-X), of 0.5, 11.5, 19, and 27 kcal mol^{-1} for X = H, Cl, F and OMe (*trans*-Me-C-OMe), respectively.[74] Better electron donors decrease the electrophilicity of the carbenic p-orbital (the migration terminus), raising the activation energy of the [1,2]-H shift, and slowing down the rearrangement. Experimental results support these theoretical expectations and the

order of effectiveness of the spectator substituents in slowing [1,2]-H or [1,2]-C migrations is MeO >> F > Cl. For example, in the carbene system **40** the rate constant for the [1,2]-C shift (eq. 5) decreases from 9.0×10^5 s^{-1} to 3×10^3 s^{-1} on changing X from Cl to MeO.[115,116]

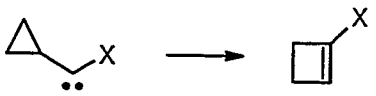

40 (5)

The picture is very different for migration of a group from an electron donor to the carbenic centre. Concerted, solution-phase [1,2]-rearrangements of dialkoxycarbenes have not been observed. The barriers for [1,2]-alkyl shifts are quite high and the rate of dimerization of the carbene is usually faster then the rate of migration. As a result of interest in the gas phase chemistry of formic acid, reports of *ab initio* studies of the [1,2]-hydrogen migration of formic acid to dihydroxycarbene (**2**) have appeared in the literature.[110,117-119] It was found that hydrogen migrates in the plane of the carbenic lone pair (Figure 12). This in-plane migration is analogous to a [1,2]-shift in a carbanion and would be destabilized by the antiaromatic nature of a four-electron transition state.[110]

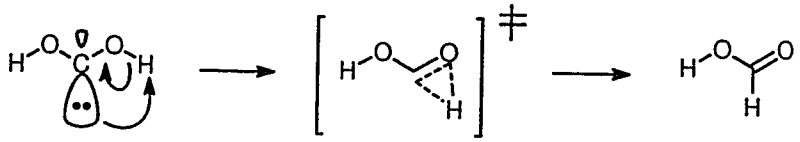

2

Figure 12. TS geometry for the [1,2]-hydrogen migration of dihydroxycarbene.

Borden *et al.* calculated the barrier for the [1,2]-H shift from s-dihydroxycarbene to formic acid to be 52.6 kcal mol^{-1} at the CISD/DZP level of theory.[110] They were able to predict that the barrier should be reduced to 40 kcal mol^{-1} if they moved to a higher basis set. Redington *et al.* reduced this barrier to 38.0 kcal mol^{-1} for w-dihydroxycarbene at the MP4(SDTQ)/6-31G**//6-31G** level.[119] The barrier was calculated by Francisco to be only 33.0 kcal mol^{-1} at the PMP4/6-311++G**//UMP2/6-311G** level with zero point energy corrections.[118] Goddard *et al.* reported the barrier for the transformation from formic acid to dihydroxycarbene (**2**).[117] Their value of 79.8 kcal mol^{-1} calculated at the DZ+P CCSDT-1//DZ+P CCSD level is in agreement with the work by the Borden, Redington and Francisco groups.

There have been a couple of theoretical investigations of [1,2]-alkyl rearrangements for oxycarbenes.[120,121] The reaction coordinate for the [1,2]-allyl migration of allyloxycarbene **41** has been analyzed by Iwamura *et al.* (eq. 6).[121] Although they made no attempt to optimize a transition state, the barrier for the migration was estimated at 42.5 kcal mol^{-1} at the MINDO/3 level of theory.

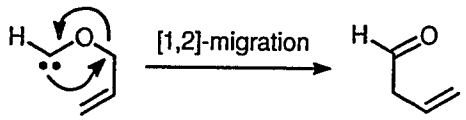

(6)

41

Francisco found that the [1,2]-trifluoromethyl migration of trifluoromethoxy(hydroxy)carbene ($HOCOCF_3$) (**42**) to trifluoroacetic acid had a barrier of 60.2 kcal mol^{-1} at the PMP4/6-31G*//UHF/6-31G* level of theory.[120] It is important to note that unlike the [1,2]-H migrations which proceed in the plane of the carbenic lone

pair according to all the calculations,[110,117-119] the [1,2]-trifluoromethyl migration was 57.6° out-of-plane. From very low vapour phase (VLVP) pyrolysis experiments, 2,2,2-trifluoroethoxymethoxycarbene (**35**), generated from its oxadiazoline precursor, was found to isomerize completely via a [1,2]-trifluoroethyl shift into methyl-3,3-trifluoropropanoate with no apparent methyl shift (eq. 7).[88]

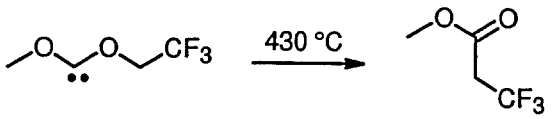

35 (7)

These results suggested a transition state model (Figure 13) similar to the out-of-plane [1,2]-H migrations of alkyl substituted carbenes where the migrating hydrogen is suggested to rearrange with a pair of electrons.[74] The negative charge buildup in the trifluoroethyl migrating group is stabilized by the electronegative trifluoroethyl group.

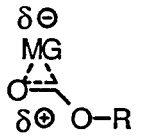

Figure 13 . Transition state model for the [1,2]-alkyl migration of dioxycarbenes.

1.5.1.3. *Concerted [2,3]-Sigmatropic Rearrangements*

The first [2,3]-sigmatropic rearrangement of a heterocarbene was discovered by Baldwin and Walker in 1972.[122] They found that the allylthio(methylthio)carbenes (**43a**) generated by the tosylhydrazone route at 65 °C, rearranged almost quantitatively into the

dithioester (**44a**). This procedure was later expanded by Nakai and Mikami, who found a high degree of stereoselectivity (~100%) favouring the *trans* geometry of the newly formed double bond as shown in equation 8 for **43b** and **43c**.[123,124]

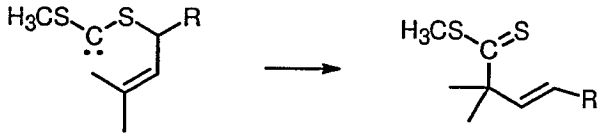

43 **44** (8)

a (R = H), **b** (R = CH_3), **c** (R = $Si(CH_3)_3$)

The high *trans* selectivity was explained in terms of a "folded envelope" transition state in which Figure 14(a) is favoured over Figure 14(b), since the R group should prefer the pseudoequatorial orientation, resulting in the *trans* product.

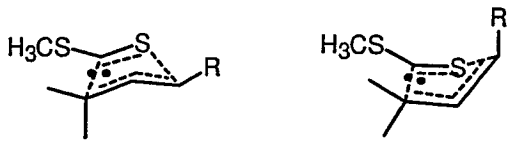

(a) (b)

Figure 14. "Folded envelope" transition states for the [2,3]-sigmatropic rearrangement of dithiocarbenes showing: (a) the preferred pseudoequatorial conformer and (b) the disfavoured pseudoaxial conformer.

High stereoselectivities, as well as good chiral transmission (96-100%), have also been observed for allyloxy(dimethylamino)carbenes in refluxing toluene (111 °C) (eq. 9).[125] These results strongly favour the concerted mechanism. However, poorer stereoselectivities[124,126] and chiral transmission[126] have been observed at higher

temperatures (160 °C). A competing dissociation-recombination mechanism has been suggested to explain the poor chiral transfer.[126]

(9)

One computational study has appeared, in which the reaction coordinate for the [2,3]-sigmatropic rearrangement of allyloxycarbene (**41**) was analyzed at the MINDO/3 level of theory (eq. 10).[121] Although a transition state was not optimized, the barrier to rearrangement was estimated to be 31.5 kcal mol^{-1}. This barrier can be compared to that for the corresponding [1,2]-allyl migration, which was estimated to be 42.5 kcal mol^{-1} at the same level of theory (Section 1.5.1.2). This result is consistent with orbital symmetry rules which suggest that the [2,3]-sigmatropic rearrangement should be allowed while the [1,2]-migration should be forbidden.[57,110] The [2,3]-sigmatropic transition state was also found to be early, which is reasonable for an exothermic reaction requiring a relatively small activation energy.[121,127]

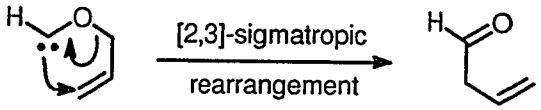

41

(10)

1.5.2. **Intermolecular Reactions**

1.5.2.1. *Dimerization*

Dimerization is a common reaction of nucleophilic carbenes that was reported by Lemal in 1964 for coupling of dimethoxycarbene (**1**) to give tetramethoxyethylene (**20**) (eq. 11).[59] It is often observed with other reactions as a competing process.

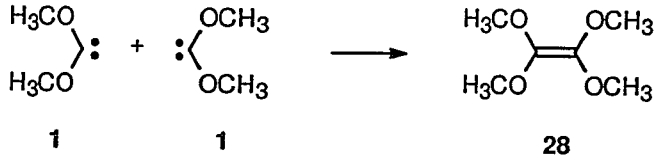

1 **1** **28** (11)

1.5.2.2. *Reactions with O-H Bonds*

Nucleophilic carbenes do not generally insert into C-H bonds in the normal sense.[128] Insertion into O-H bonds on the other hand, is a characteristic reaction of nucleophilic carbenes.[26] The insertion of singlet carbenes into C-H bonds is usually thought of as a single step process, as discussed in Section 1.2. For insertion into polar O-H bonds three mechanisms are normally considered: (a) electrophilic attack by the carbene on the oxygen atom, followed by proton transfer (ylide mechanism), (b) protonation of the carbene to give an ion pair which collapses to an ether (carbocation mechanism), and (c) concerted O-H insertion (Scheme 22). While the concerted process for O-H insertion cannot be excluded *a priori*, it has not received definitive experimental support.

Scheme 22

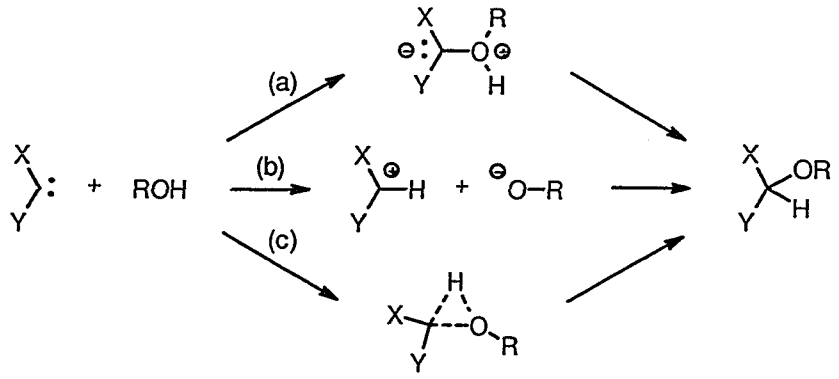

Laser flash photolysis has been used extensively to study the reaction of oxy- and dioxycarbenes with alcohols. Dimethoxycarbene (**1**), generated by the diazirine route, has been directly observed (λ_{max} = 255 nm) in a 3-methylpentane matrix and in a pentane solution.[16] The reactivity of **1** covered four orders of magnitude with the rate constant for carbene decay in 1M ROH/MeCN at 20 °C ranging from 3.2×10^4 s^{-1} for ethanol to 6.7×10^8 s^{-1} for HFIP (1,1,1,3,3,3-hexafluoro-2-propanol).[129] The Brønsted catalysis coefficient, α, was found to be -0.66 for this series of alcohols suggesting a substantial degree of proton transfer in the transition state. Photolysis of dimethoxydiazirine (**26**) in methanol afforded the product of trapping by the alcohol in 90% yield. The reaction was first order in the range of concentrations, $0.08 \leq [MeOH] \leq 1.54$ with $k = 6.4 \times 10^6$ $M^{-1}s^{-1}$.[130] Trapping of **1** with MeOD instead of MeOH revealed a large kinetic isotope effect (KIE), $k_H/k_D = 3.3 \pm 0.5$.[130] More acidic quenchers, AcOH ($k = 2.91 \times 10^9$ $M^{-1}s^{-1}$) and AcOD ($k = 2.84 \times 10^9$ $M^{-1}s^{-1}$), had no significant KIE, where k approaches the diffusion controlled limit.[130] Similarly, no significant KIE was observed for

methoxy(methyl)carbene (23) trapping with oligomeric MeOH ($k = 5.3 \times 10^9$ $M^{-1}s^{-1}$) and MeOD ($k = 4.8 \times 10^9$ $M^{-1}s^{-1}$).[130]

The sizable primary KIE observed in the dimethoxycarbene/MeOH(D) reaction is consistent with a carbene protonation mechanism, Scheme 22(b), or a concerted O-H insertion mechanism, Scheme 22(c).[130] In a linear transition state the magnitude of the primary KIE is largest for the most symmetrical TS and decreases as the TS more closely resembles the product or reactant states.[24] Therefore, the diffusion controlled dimethoxycarbene/AcOH(D) or methoxy(methyl)carbene/MeOH(D) reactions may each traverse a very reactant-like (or non-linear) transition state.

The reactions of alkyoxy(halo)carbenes with alcohols provide important information about O-H insertion. The reaction of the "invisible" chloro(methoxy)carbene (ClCOMe) with methanol, monitored by time resolved photoacoustic calorimetry, was found to have a bimolecular rate constant (k) of 6.8×10^4 $M^{-1}s^{-1}$.[131-133] Fluoro(methoxy)carbene (FCOMe) was found to be surprisingly unreactive with alcohols and methanol did not quench the carbene at 1 M in acetonitrile.[129] Only HFIP ($k = 9 \times 10^3$ s^{-1}) and AcOH ($k = 2.0 \times 10^7$ s^{-1}) at 1 M quenched fluoro(methoxy)carbene competitively with its dimerization and other decay pathways. A substantial KIE ($k_H/k_D = 1.95$) was also obtained for trapping by AcOH(D). The sequence of carbene stabilization energies, $(MeO)_2C:$ > F(MeO)C: > Cl(MeO)C:, is not reflected by the reaction rates with O-H bonds.[26] The most stable carbene, dimethoxycarbene **1** is in fact the most reactive. These results suggest a carbocation mechanism, (Scheme 22(b)), instead of the concerted O-H insertion (Scheme 22(c)).

An interesting variation on the reaction of carbenes with O-H groups occurs when dimethoxycarbene (**1**) is trapped by enols to give overall C-H insertion.[128] The reaction is shown in Scheme 23 for 2,4-pentanedione (**45**), and is thought to involve initial proton abstraction by **1** from the enol tautomer (**46**), followed by collapse of the resulting ion pair.

Scheme 23

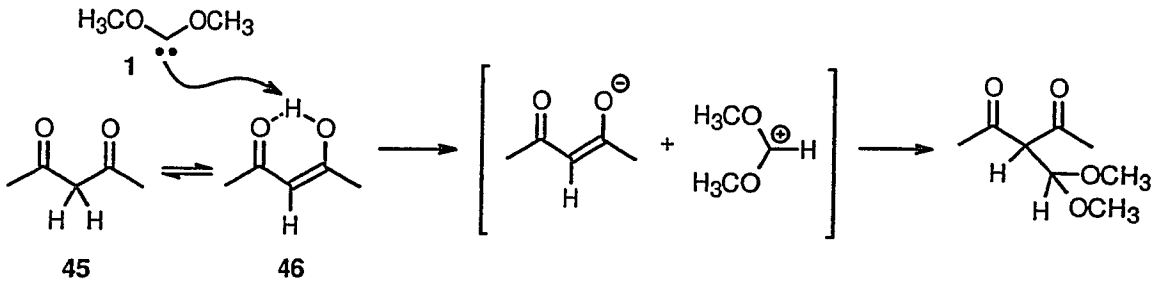

1.5.2.3. *Reactions with Multiple Bonds*

1.5.2.3.1. Alkenes

As discussed in Section 1.3, nucleophilic carbenes do not generally react with simple olefins, and the presence of electrophilic substituents on the alkene is usually required.[36,37] Due to the development of diazirines as photochemical sources of oxy[71-74] and dioxycarbenes[16,75] (Section 1.4.5), Moss has been able to obtain absolute rate constants for reactions of a number of alkenes with oxy and dioxycarbenes (Table 1).[16,134] For a traditional ambiphilic carbene (MeOCCl), the absolute rate constant increases for trapping by both electron-rich and electron-poor alkenes. For nucleophilic carbenes, such

as dimethoxycarbene (**1**), the rate constant increases for the reaction with electron-poor alkenes.

Table 1. Absolute rate constants (25 °C) for carbene-alkene additions.

	Rate Constants ($M^{-1}s^{-1}$)			
	MeO-C-Cl	MeO-C-Ph	MeO-C-Me	$(MeO)_2C$
$Me_2C{=}CMe_2$	4.2×10^3	-	-	$< 10^3$ [a]
$Me_2C{=}CH_2$	1.8×10^3	4.0×10^4	4.8×10^3	-
$H_2C{=}CHCN$	1.8×10^4	1.7×10^6	1.5×10^6	$\sim 10^3$
$H_2C{=}CClCN$	5.6×10^5	3.4×10^7	4.9×10^7	5.0×10^5

[a] $(Me)O_2C$ (**1**) was not quenched by 2.7 M $Me_2C{=}CMe_2$ in pentane.

The reactions of dioxycarbenes with alkenes have been extensively studied due to the availability of a number of a very good dioxycarbene precursors including 1,2,3,4-tetrachloro-7,7-dialkoxy-5-phenylnorbornadienes[58,59] (**11**), dioxydiazirines[16,75,76], and 2,2-dioxy-Δ^3-1,3,4-oxadiazolines[83], as discussed in Section 1.4.5.

Although dioxycarbenes appear to undergo concerted additions to alkenes in a number of cases, dipolar intermediates have often been postulated for reactions with highly electron-deficient alkenes. Hoffmann has studied the addition of dimethoxycarbene (**1**) to diethyl maleate (**47**) and diethyl fumarate (**48**) (Scheme 24).[135] The cyclopropane products were not observed in these reactions and the final product in each case was rationalized in terms of a thermally unstable cyclopropane intermediate which is in equilbrium with the dipolar intermediate, **49**. Proton migration in the dipolar intermediate results in the final product (**50**).

Scheme 24

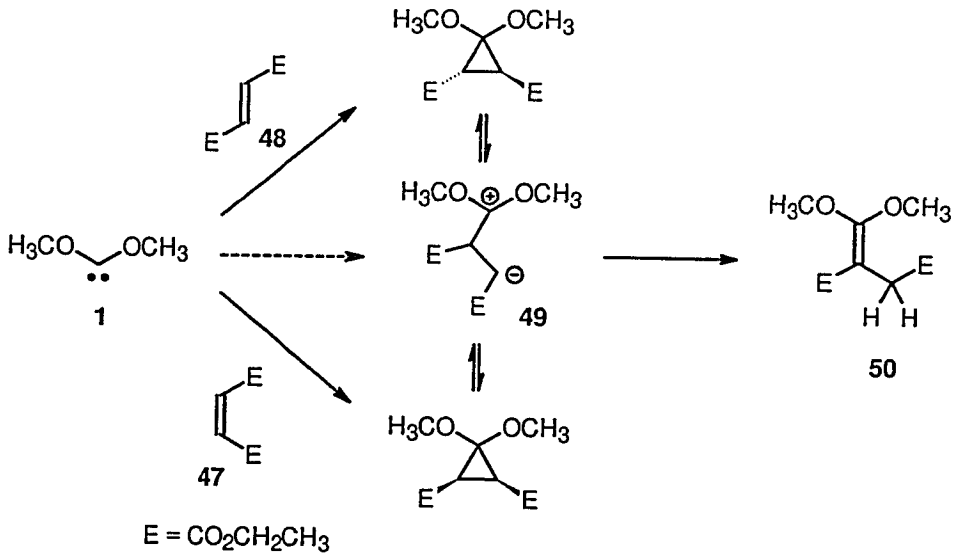

Dipolar intermediates also seem likely in the reaction of dimethoxycarbene (**1**) with the strain and substituent-activated olefin, **51** (Scheme 25).[136] The carbene derived products were rationalized in terms of an addition to form the diastereomeric dipolar adducts, **52a** and **52b**. **52a** and **52b** subsequently undergo ring expansions, methyl transfers, and methoxy transfers to give the products. A product (19%) resulting from initial attack at the carbonyl group was also recovered.

Scheme 25

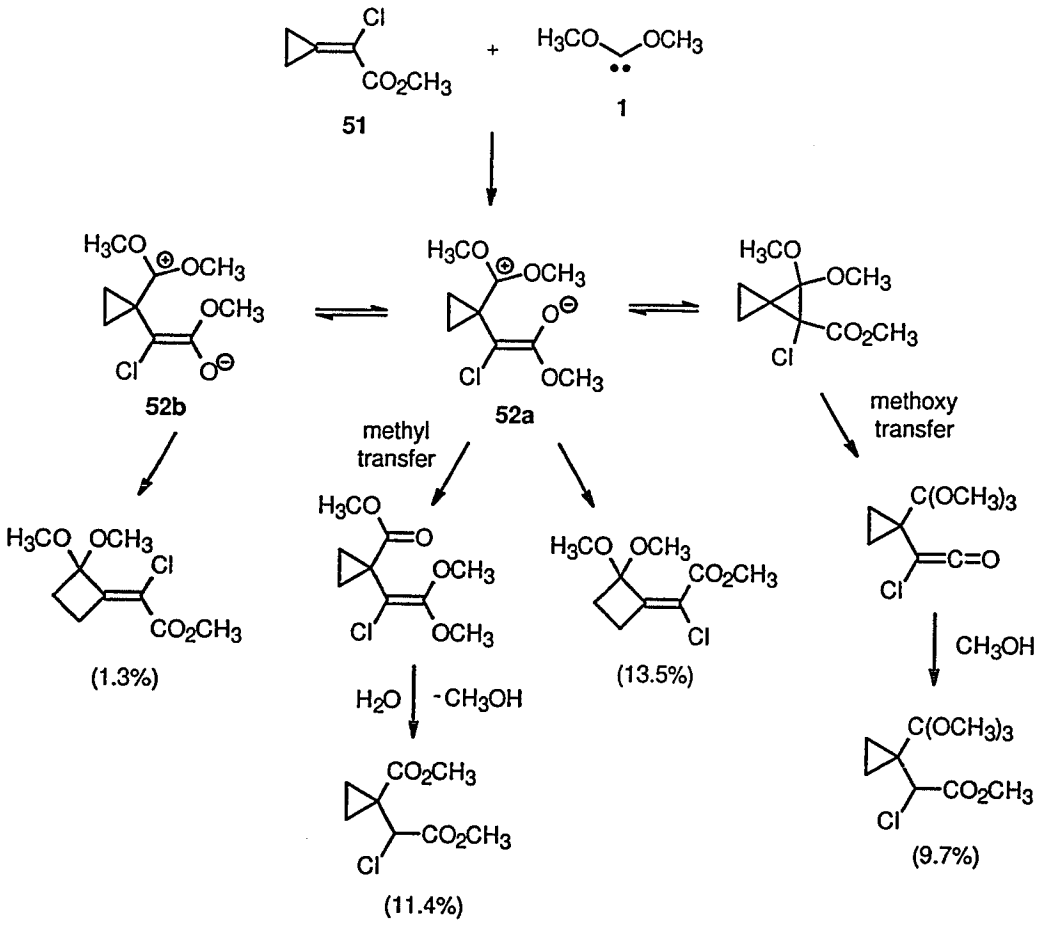

These results can be contrasted with Moss's research on *cis*- and *trans*-β-deuteriostyrene[137] (**53a** and **b**) and Hoffmann's studies with ethyl cinnamate[135] (**54**) and 1,1-diphenylethylene[135] (**55**) (Scheme 26). In the Moss and Hoffmann examples, the products of cycloaddition, cyclopropanes, are the final products. In addition, the reactions of **1** with **53a,b** and **54** indicate that the stereochemistry of the alkenes is conserved in the products, suggesting a concerted mechanism with no intervening dipolar intermediates. Unfortunately, these results do not provide an answer to the question of

whether or not the dipolar intermediates postulated above are the primary products of the carbene addition reactions, or simply fragmentations of initially formed cyclopropanes.

Scheme 26

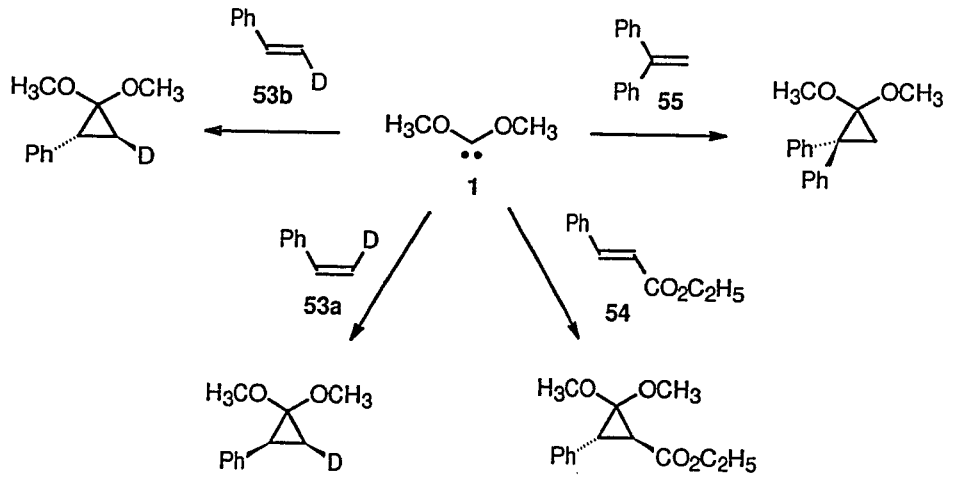

N-Phenylmaleimide **56** also undergoes cyclopropanation reactions with dimethoxycarbene[40] (**1**), while methoxy(trimethylsilylethoxy)carbene[138] (**57**) affords a surprisingly rearranged product through a mechanism apparently involving dipolar intermediates (Scheme 27).

Scheme 27

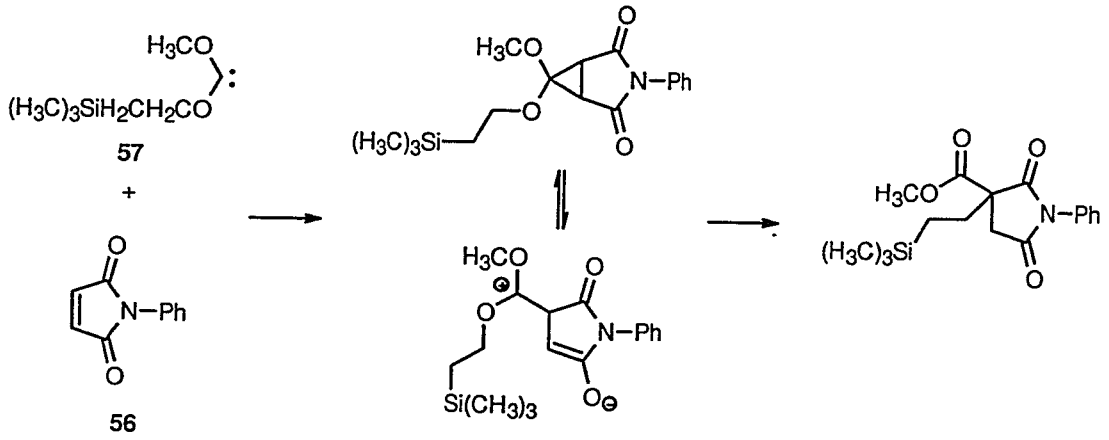

Nucleophilic aromatic substitution by dialkoxycarbenes has been observed with 2,4-dinitrofluorobenzene (**58**) and hexafluorobenzene as shown in Scheme 28 for **58**.[139] The reaction can be explained in terms of a nucleophilic aromatic substitution through an intermediate (**59**), that resembles the classical Meisenheimer intermediate, followed by fast [1,2]-F migration.

Scheme 28

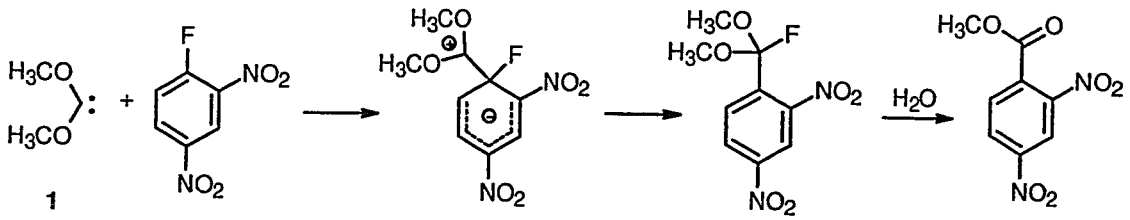

Dimethoxycarbene (**1**) also performs an overall nucleophilic substitution on perchloro-olefins.[140] The mechanism is thought to involve an interesting series of reactions that likely starts with a Michael type addition with loss of chloride ion, followed by a substitution reaction. An example of this reactivity is shown for hexachlorocyclopentadiene (**60**) in Scheme 29.

Scheme 29

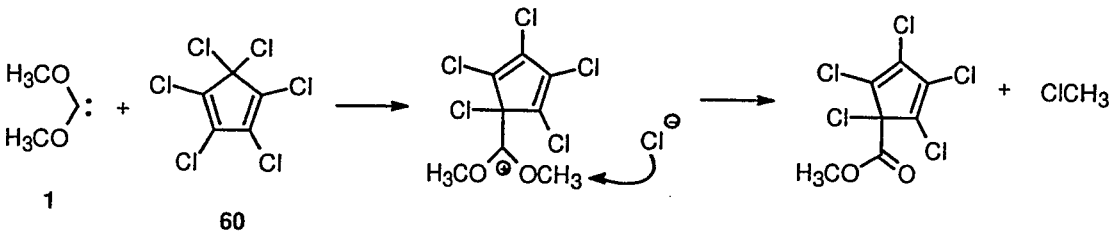

The presence of activating substituents is not the only way to increase the reactivity of an alkene toward dioxycarbenes. Activation can also be provided by the introduction of strain. For example, bicyclopropylidene reacts with a number of dialkoxycarbenes to afford acetals of dispiro[2.0.2.1]heptan-7-one (eq. 12).[136]

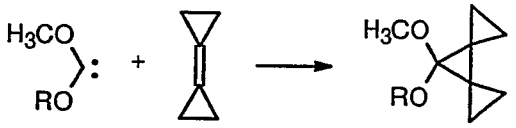

R = CH_3 (71%)
R = t-Bu (37%)
R = $CH_2CH_2Si(CH_3)_3$ (91%)
R = CH_2CH_2Cl (72%)
R = CH_2CH_2Br (56%) (12)

Dioxycarbenes such as dimethoxycarbene (**1**) also cyclopropanate the electrophilic double bonds of buckminsterfullerene (C_{60}) to give a methanofullerene adduct (eq. 13).[141-143] Cyclopropanation only occurs across [6,6] ring junctures since there is higher double bond character at the [6,6] junctures compared to the [5,6] ring junctures.[143]

1 (13)

Another interesting example of regioselectivity occurs in the low yield reactions of dimethoxycarbene (**1**) and chloro(methoxy)carbene (**61**) with 6,6-dimethylfulvene (eq. 14).[144] Electrophilic carbenes react exclusively at the endocyclic π bonds while the more nucleophilic **1** and **61** react with the exocyclic double bond due to the larger LUMO coefficient in this position.

(14)

1 (X = OCH_3)
61 (X = Cl)

X = OCH_3 (8%)
X = Cl (35%)

1,4-Additions can also compete with the 1,2-cycloadditions, as observed by Hoffmann for tetraphenylcyclopentadienone (**62**) and tropone (**63**) (Scheme 30).[145]

Scheme 30

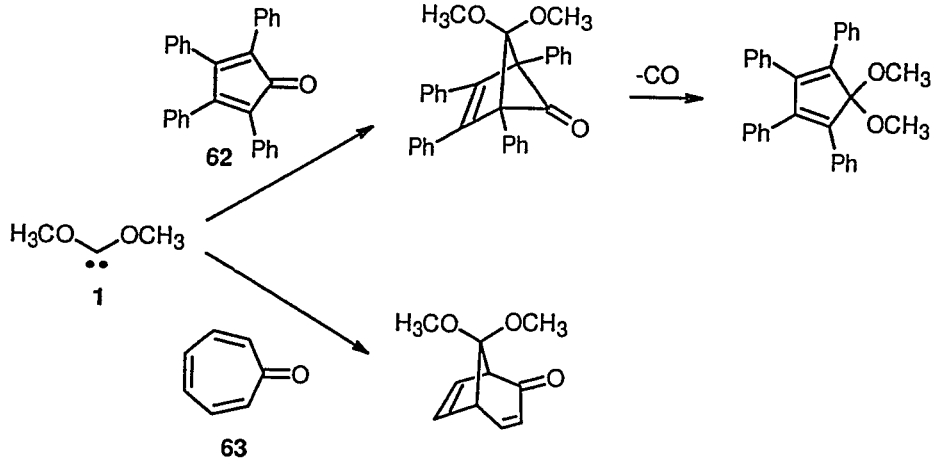

Attempts to trap methoxy(phenoxy)carbene[75] (**64**) and methoxy(phenyl)carbene[77] (**22**) with tetramethylethylene did not result in the expected cyclopropanation products. The olefins that were generated instead may have resulted from an "ene" reaction (eq. 15).

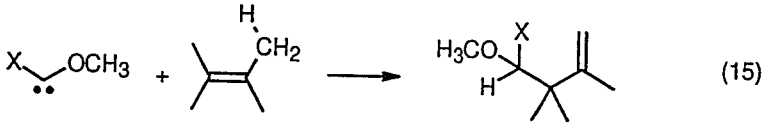

(15)

64 (X = PhO)
20 (X = Ph)

1.5.2.3.2. Alkynes

Dioxycarbenes appear to react readily with alkynes bearing one or more electron-withdrawing substituents. In 1974 Hoffmann studied the reaction of dimethyl acetylenedicarboxylate (DMAD) (**65**) with dimethoxycarbene (**1**).[135] These reactions generally involve dipolar intermediates and often result in 1:2, carbene to trap, products. The reaction of **1** with excess DMAD afforded the dihydrofuran derivative (**66**) in 37% yield (Scheme 31). The proposed mechanism involves a dipolar intermediate (**67**) (which can also be written as a vinyl carbene), produced by nucleophilic carbene attack at the sp carbon, which adds across the carbonyl group of a second molecule of DMAD (Scheme 31).

Scheme 31

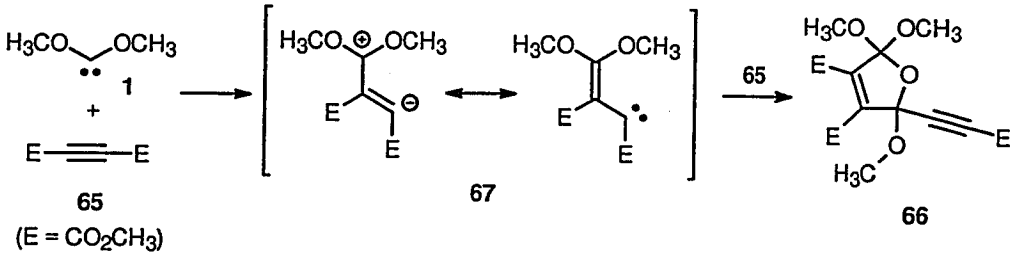

Hoffmann found that dimethoxycarbene (**1**) undergoes a similar reaction with phenyl acetylene (**68**) to give the acetal (**69**), except in this case the dipole is captured by deprotonation of a second equivalent of phenyl acetylene (**68**), followed by collapse of the ion pair (Scheme 32). The hydrolysis product (**70**) of the acetal (**69**) was isolated in 50% yield. Similar reactivity with DMAD and phenyl acetylene (**68**) has been observed by Warkentin for other dioxycarbenes.[138,146,147] Warkentin has also taken advantage of

this chemistry by using tethered alkynes, including some without activating groups.[148-151] The reactions benefited from the increase in the rate expected for intramolecular reactions.[149-151]

Scheme 32

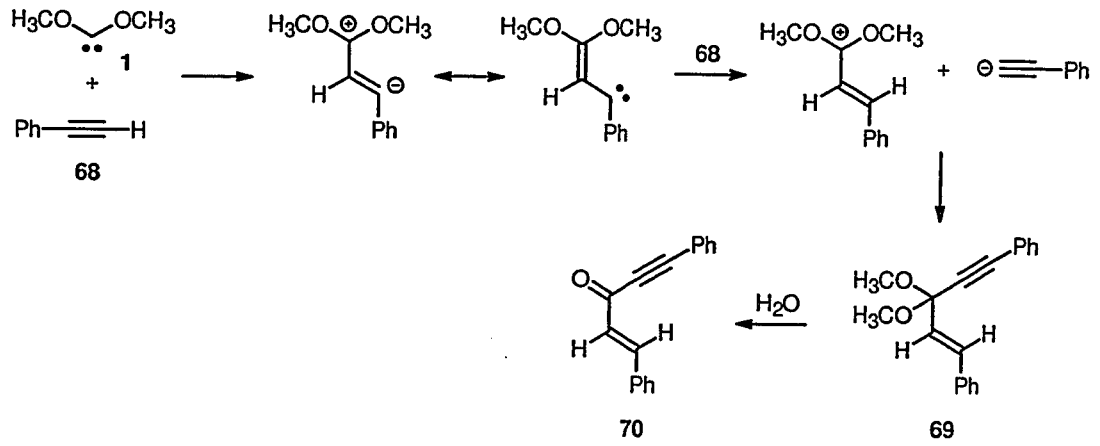

1.5.2.3.3. C=X Bonds

A number of groups have taken advantage of the nucleophilic character of dioxycarbenes by exploring their chemistry with carbonyl compounds. Hoffmann has used 1,2,3,4-tetrachloro-7,7-dimethoxyoxy-5-phenylnorbornadiene (Section 1.4.5) as a source of dimethoxycarbene (1) to study a number of these reactions. Dimethoxycarbene (1) reacts with benzoyl chloride by a mechanism suggested to involve nucleophilic attack at the carbonyl carbon, giving a tetrahedral intermediate (71). This intermediate (71) could lose a chloride ion which then demethylates the counter ion to give the observed pyruvate (72) (Scheme 33).[135]

Scheme 33

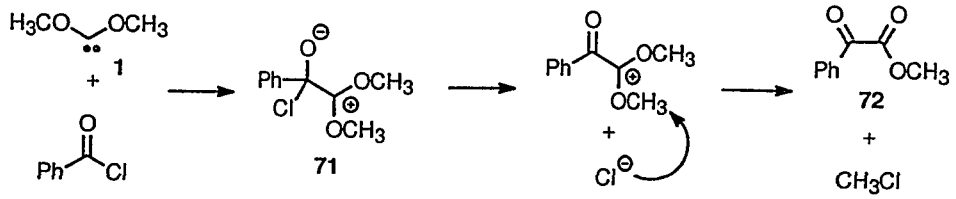

Trapping of **1** with biacetyl resulted in two isomeric products that were 2:1 carbene to trap adducts.[152] The diastereomeric products can be rationalized in terms of a nucleophilic attack by dimethoxycarbene (**1**) to yield a tetrahedral intermediate (**73**) which adds to a second molecule of biacetyl across the carbonyl bond (Scheme 34).

Scheme 34

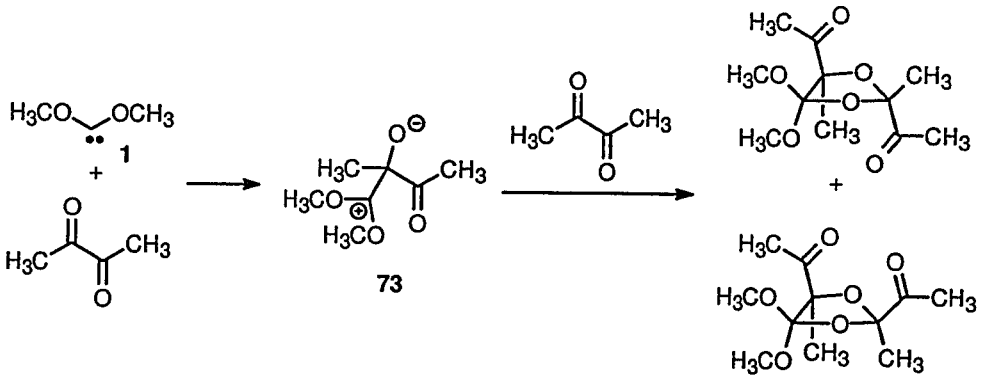

More recently, Pole and Warkentin have used anhydrides as traps for dimethoxycarbene (**1**) and 2,2,2-trifluoroethoxy(methoxy)carbene (**35**) (Scheme 35).[85] They observed the apparent C-O insertion product, and favoured the mechanism presented in (Scheme 35). No products from attack by **1** at the olefinic bond were detected. For asymmetric anhydrides the carbenes attacked the most electrophilic carbonyl carbon, overriding steric effects.

Scheme 35

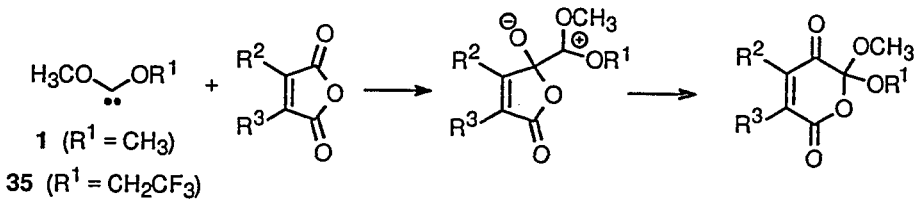

Pole and Warkentin have also obtained some important results from the reaction of **1** with fluorenone (Scheme 36).[153] It was shown that the initial product of the reaction is the oxirane (**74**), which was the first evidence for an oxirane intermediate in the addition of a dialkoxycarbene to a carbonyl group. Isotopic labelling studies were employed to show that the final product (**75**) resulted from a [1,2]-methoxy migration pathway such as the one presented in Scheme 36, instead of an inter- or intramolecular methyl transfer.

Scheme 36

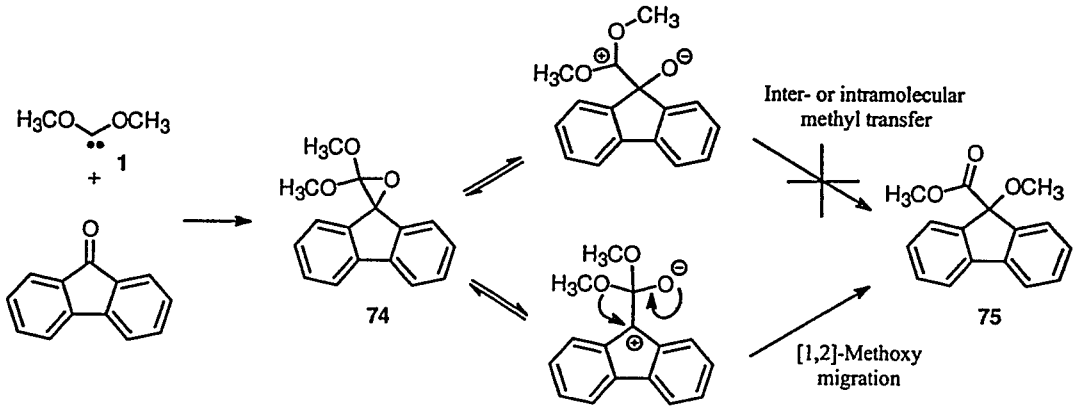

Cyclic unsaturated perchloroketones are also attacked by dimethoxycarbene at the carbonyl carbon atom and can undergo a number of transformations through apparent

dipolar intermediates, including ring expansion as shown in Scheme 37 for the reaction of 1 with hexachlorobicyclo[3.2.0]-6,3-diene-2-one (76).[140] This was the first example of an overall C-C bond insertion for an alkyloxy- or dialkyloxycarbene.

Scheme 37

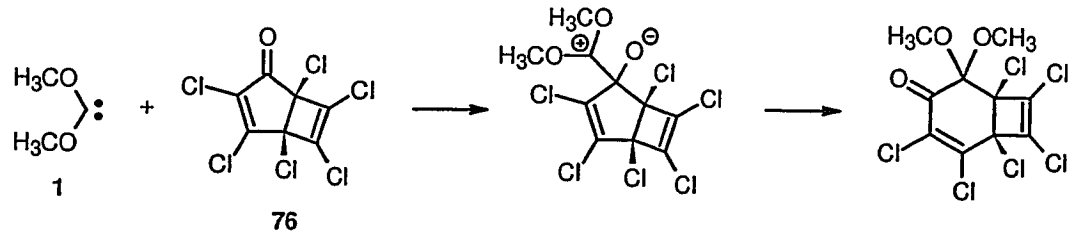

The reaction of 1 with tetrachloro-1,4-benzoquinone does not result in ring expansion.[140] Instead, a pair of the ylide intermediates (77) appear to participate in intermolecular methyl transfers to give the final product (78) in 82% yield (Scheme 38). The ylide (77) probably results from ring opening of the oxirane (79), however direct formation of (77) by attack of 1 at the carbonyl oxygen was not ruled out.

Scheme 38

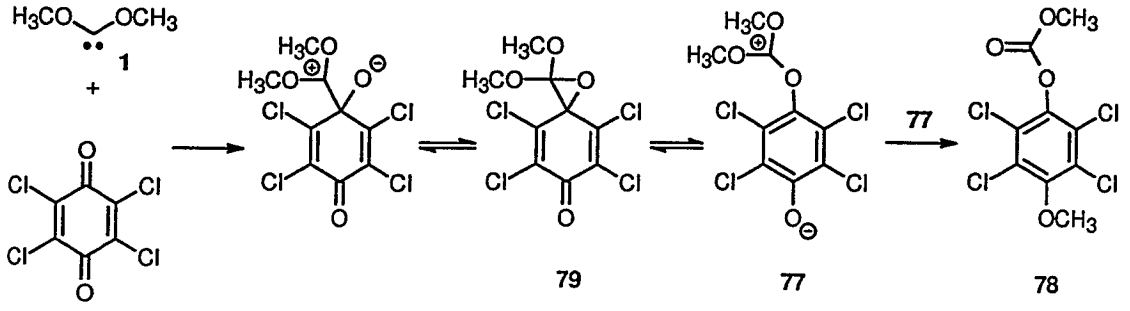

Recent work by Venneri and Warkentin has shown that cyclopropanones, a cyclopropenone, cyclobutanones, a cyclobutane-1,3-dione, and a cyclobutene-1,2-dione all react with dimethoxycarbene (1) to afford acetals of the next larger ring size by formal

insertion of the carbene into a C-C bond alpha to the carbonyl group. The reaction is shown for cyclobutanone in Scheme 39.[154]

Scheme 39

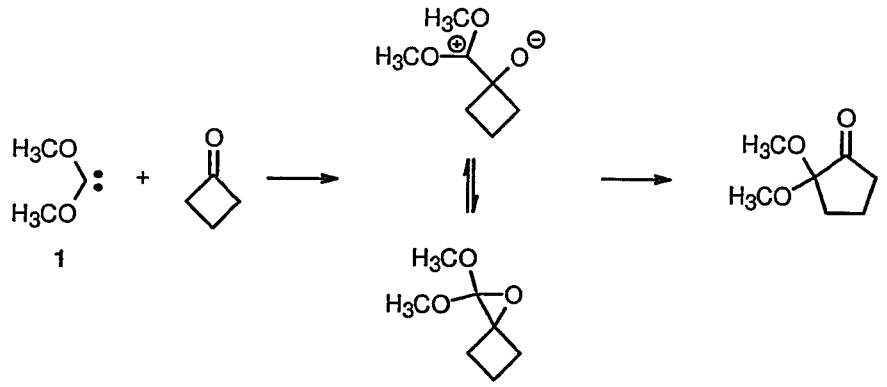

β-Propiolactone also gives a ring expanded product with overall C-O insertion (eq. 16).[154]

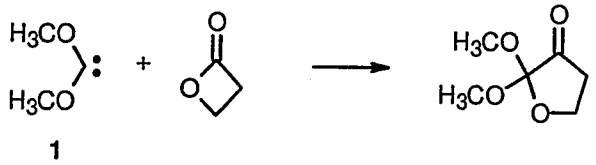

(16)

With the electron deficient conjugated imines a different reaction pathway is observed. For example with **80** and **81**, dimethoxycarbene (**1**) undergoes formal [1 + 4] cycloadditions (Scheme 40).[152]

Scheme 40

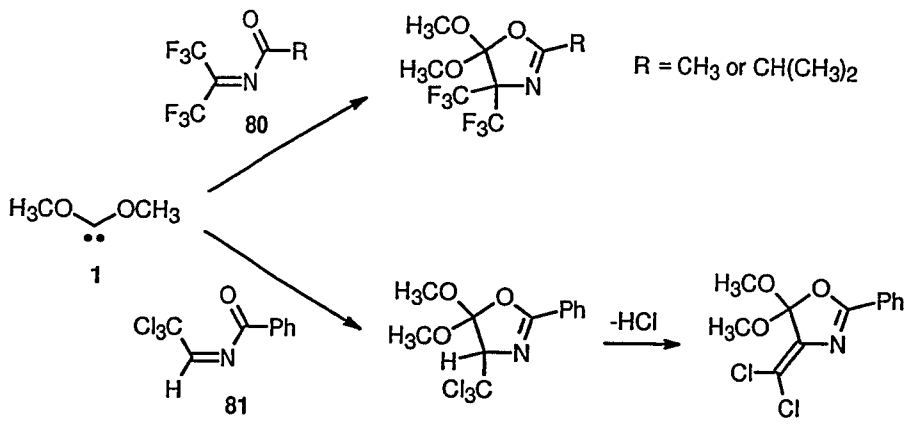

Similarly, 1,2,4,5-tetrazines react with dioxycarbenes to give isopyrazoles (**82**) by a formal [4 + 1] cycloaddition followed by loss of N_2 (Scheme 41).[155]

Scheme 41

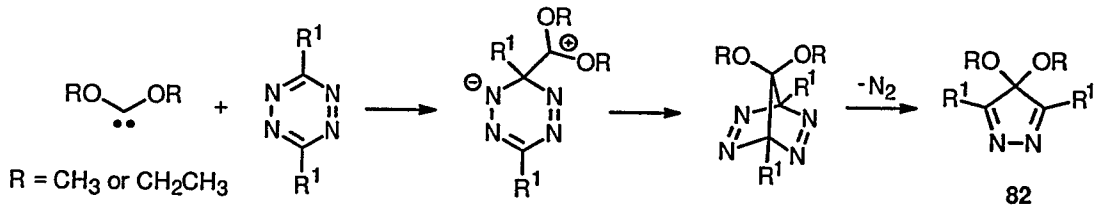

It is interesting to note that despite the apparent importance of dipolar intermediates in the reactions of nucleophilic carbenes with carbonyl compounds, the available theoretical evidence suggests a concerted cycloaddition by the carbene at the carbonyl group (Figure 15).[156-159]

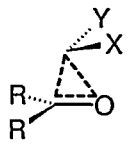

Figure 15. Transition state geometry for cycloadditions of nucleophilic carbenes to alkenes.

Only a handful of examples have been studied. Pole examined the cycloaddition of dihydroxycarbene (**2**) to the carbonyl group of maleic anhydride (**83**) and maleimide (**84**) at the HF/3-21G level of theory.[159] In both cases the nucleophilic attack was found to be an asynchronous, but concerted, cycloaddition in which the C-C bond was formed slightly ahead of the C-O bond. Similar results were obtained by León[156] and by Ahmed *et al.*[158] for the reaction of hydroxycarbene (HCOH) with formaldehyde ($H_2C{=}O$) at the HF/3-21G and MP2/6-31G(d) levels of theory respectively, although the C-O bond was formed slightly ahead of the C-C bond at the lower level of theory. Pliego and Almeida have also examined the cycloaddition of dichlorocarbene (Cl_2C:) to formaldehyde using large basis sets and high level methods to include electron correlation (CASSCF(2,2), MP2, MP4(SDQ), CCSD(T)).[157] Their results mirror León's[156] high level results for hydroxycarbene.

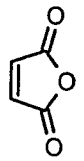

83

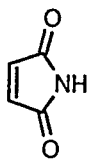

84

1.5.2.3.4. Heterocumulenes

Nucleophilic carbenes react with heterocumulenes by a number of different pathways depending on the nature of both the carbene and the substrate. However the initial step is invariably nucleophilic addition of the carbene to the sp-hybridized carbon to produce a dipolar zwitterionic intermediate. In fact Bock and Redington have shown, computationally, that the zwitterion (**85**) corresponding to nucleophilic attack by dihydroxycarbene (**2**) on carbon dioxide represents a stable intermediate (Scheme 42).[160] They were also able to locate a planar transition state (**86**) for the fragmentation of this zwitterion (**85**) to dihydroxycarbene (**2**) and carbon dioxide. The transition state (**86**) was only 11.0 kcal mol^{-1} higher in energy than the zwitterion and only 0.7 kcal mol^{-1} above the free carbene (**2**) and carbon dioxide at the MP2/6-31G*(5d)//HF/6-31G level. Structure **86** represents a rather unique transition state when compared to the computational results presented above (Section 1.5.2.3.3) for concerted cycloaddition at carbonyl double bonds.[156-159] However, no attempt was made by these authors to find a transition state or intermediate corresponding to the concerted cycloaddition at one of the carbonyl bonds.

Scheme 42

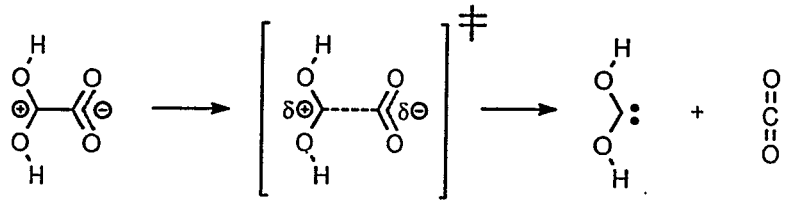

85 86 2

Experimentally, the zwitterionic intermediates have been found to be so stable that in some cases they constitute the final product. For example unsaturated diaminocarbenes[161] (87) (eq. 17), as well as saturated imidazol-2-ylidenes[162-164] (88) (eq. 18) were reported to react with carbon disulfide to yield stable dithioquaternary salts which, in turn, were proven to be good nucleophiles.

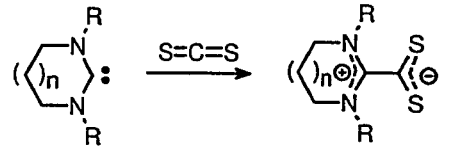

87
n = 0 or 1

(17)

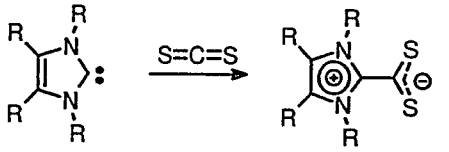

88

(18)

Imidazol-2-ylidenes (88) also yield the analogous 1,3-dipoles when trapped by phenyl isothiocyanate (89) (eq. 19).[165,166]

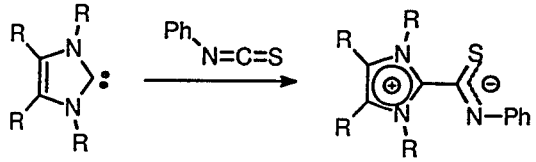

88 89

(19)

Dioxycarbenes are known to react with a variety of heterocumulenes by apparent initial nucleophilic attack at the carbonyl carbon. Using 7,7-dimethoxynorbornadienes as the carbene precursor, Hoffmann and coworkers have trapped dimethoxycarbene (1) with

aryl isocyanates (**90**) and aryl isothiocyanates (**91**) to give 5,5-dimethoxyhydantoins (**92**) and 5,5-dimethoxydithiohydantoins (**93**) respectively (Scheme 43).[167] Reassuringly, trapping of **1**, generated from its oxadiazoline precursor, with phenyl isocyanate **94** also gives the 5,5-dimethoxyhydantoin (**92**).[83] The reaction is suggested to occur in a stepwise manner with **1** performing a nucleophilic attack on the (thio)carbonyl carbon to yield the zwitterions, **95** or **96**, followed by addition of a second molecule of aryl iso(thio)cyanate to give the product, **92** or **93**.[167] In competition experiments Hoffmann reported that *p*-tolyl isocyanate reacted eleven times faster than phenyl isothiocyanate.[167] This is a surprising result in light of studies which suggest that thiocarbonyl groups are much more reactive to nucleophiles than carbonyl groups.[168] The high reactivity of thiocarbonyl groups is generally attributed to the inherent instability of the C=S π-bond, which is due to the poor overlap of the C-2p and S-3p-orbitals.[169]

Scheme 43

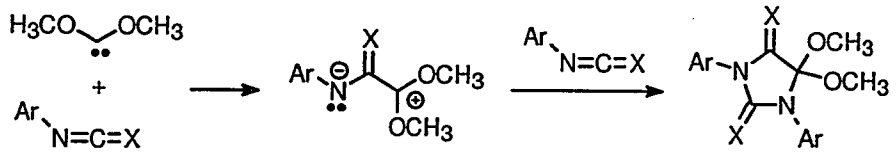

90 (X = O)
91 (X = S)

95 (X = O)
96 (X = S)

92 (X = O)
93 (X = S)

It is instructive here to consider the reaction of methoxy(dimethylamino)carbene (**97**) with aryl isocyanates (**90**) and phenyl isothiocyanates (**89**).[170] Trapping of **97** by aryl isocyanates (**90**) gave the expected cycloadducts, resulting from trapping by two equivalents of **90**. However trapping of **97** by phenyl isothiocyanates (**89**) gave slightly different results depending on the reaction conditions (Scheme 44). The reaction did

yield the expected dithiohydantoins (**98**) resulting from trapping of the carbene (**97**) by two equivalents of phenyl isothiocyanate (**89**). However two additional products were observed. These products resulted from trapping by one equivalent of **97**. Both additional products can be explained by subsequent rearrangements of the zwitterionic intermediate (**99**). The product, **100**, results from an inter- or intramolecular methyl transfer from oxygen to sulfur. It appears that **101** results from the formation of an episulfide from **99**, followed by ring opening in the opposite direction and methoxy migration.

Scheme 44

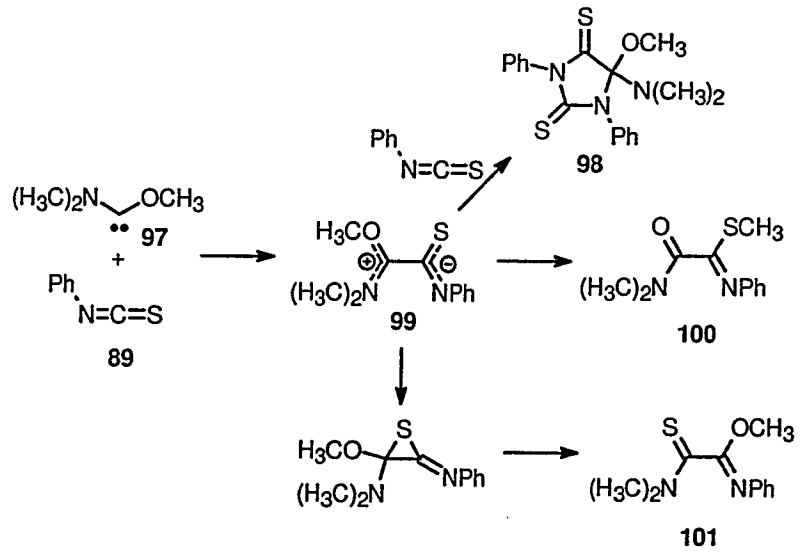

The extraordinary chemistry of methoxy(dimethylamino)carbene (**97**) with the isothiocyanate, **89**, is an exception to the rule. For a variety of carbenes (Figure 16) trapping with aryl isothiocyanates (**91**), in the absence of additional traps, leads to the normal 1:2 products.[162,163,171-174]

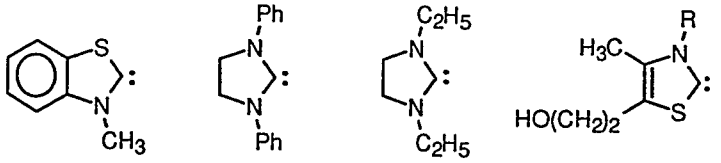

Figure 16. Aminocarbenes that give 1:2 adduct with isothiocyanates.

The aminothiocarbene (**102**) yields both the 1:1 and 1:2 adducts with aryl isothiocyanates (**91**) (Scheme 45).[174] This carbene (**102**) also gave the salts of the 1:1 adducts in the presence of di-*p*-tolylcarbodiimide (**103**) when it was generated from thiazolium halide precursors (Scheme 45).[152]

Scheme 45

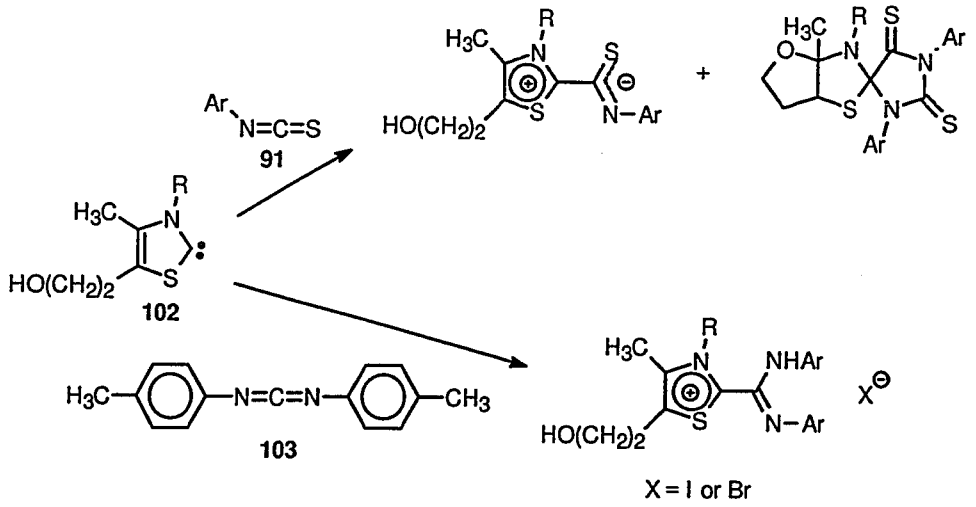

A slightly different reaction path is observed for trapping of oxythiocarbenes (**104**) by phenyl isocyanate (**94**) (Scheme 46). In each case the major products are a pair of diastereomeric 2:2 adducts (**105**) formed along with the diastereomeric 1:2 adduct (**106**).[175] The products result from initial nucleophilic addition to form a dipolar intermediate (**107**) followed by intramolecular ring closure to give **108**. It was suggested

that the differences between the behaviour of the dipolar intermediates **107** and their dioxy analogues, for instance, may be attributed to the lower stability of the former.

Scheme 46

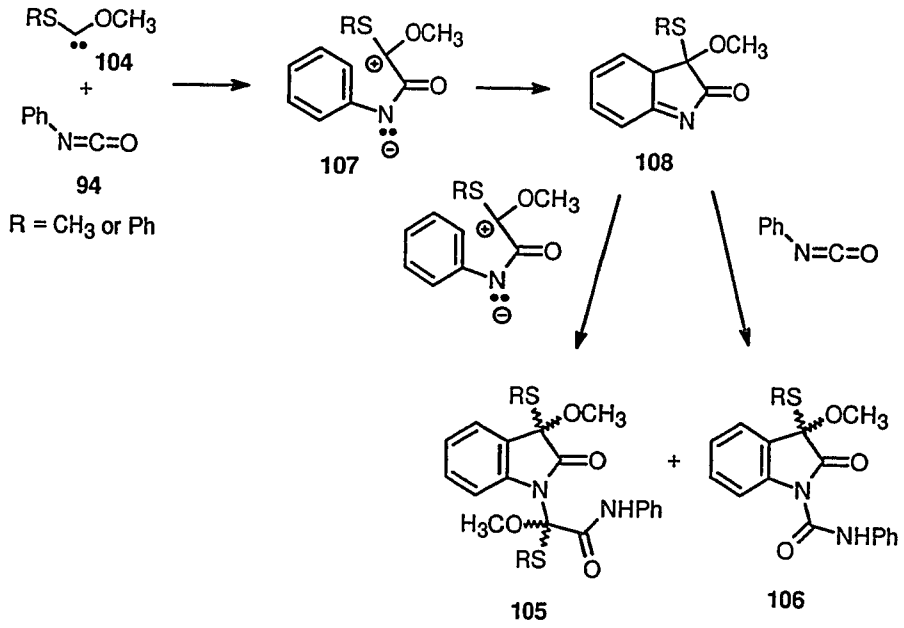

This [1+4] cycloaddition pathway is also active for the reaction of a variety of dithio-, dioxy- and amino(oxy)carbenes with vinyl isocyanates (Scheme 47).[176-179]

Scheme 47

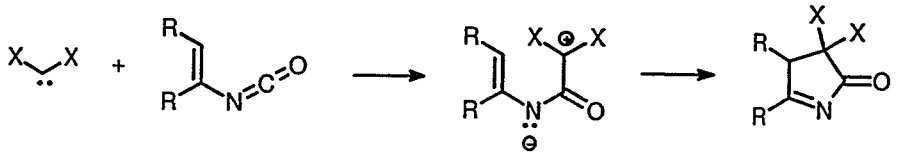

Hoffmann has found that dimethoxycarbene (**1**) undergoes a series of reactions in the presence of diphenylketene to give a 1:2 adduct (Scheme 48).[135] Recently, even a

1,2-bisketene (**109**) has been successfully used to trap dimethoxycarbene (**1**), generated by the oxadiazoline method (Scheme 49).[180]

Scheme 48

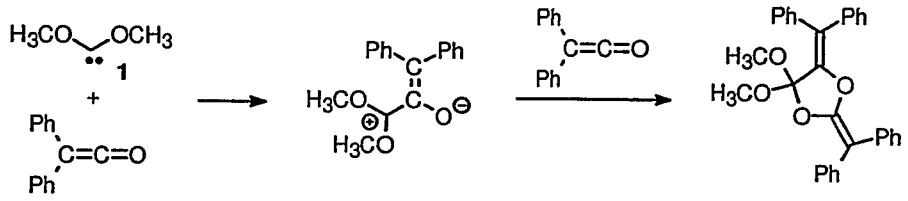

Scheme 49

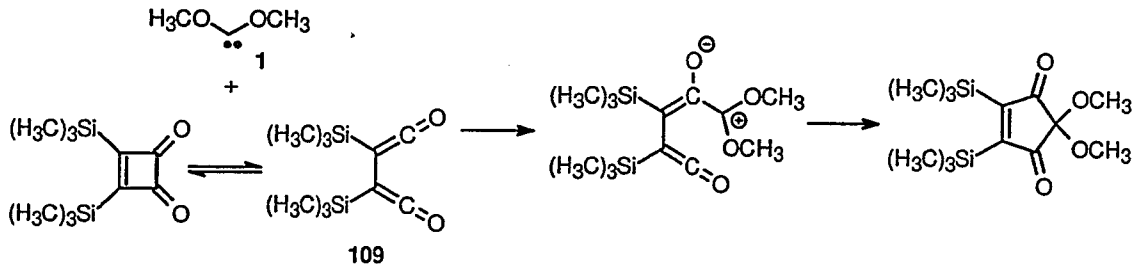

1.6. Objective

The proceeding chapter represents a brief review of the chemistry of oxy- and dioxycarbenes. It is clear that these reactive intermediates have generated intense interest in many chemical fields, challenging synthetic and theoretical chemists alike. The research described in the coming chapter will focus on two aspects of carbene reactivity. The first project was designed to examine the unexpected observation in our group that the [1,2] and [2,3]-sigmatropic rearrangements of allyloxymethoxycarbenes **36** proceed by a stepwise homolytic fragmentation/recoupling mechanism (Section 1.5.1.1).[105] This

primarily theoretical/computational project examined four possible rearrangement mechanisms and the study resulted in a detailed analysis of the homolysis of an oxycarbene from its singlet ground state. The objective of this work was to determine if an apparent transition state in this homolysis could be real, and if so, to define the factors that result in this unusual barrier. The second objective of this work was to expand the intermolecular chemistry of dioxycarbenes with thiocarbonyl compounds (Section 1.5.2.3.4). As a starting point, the chemistry of dioxycarbenes with carbon disulfide was explored both experimentally and computationally.

Chapter 2

Results and Discussion

This chapter is divided into two major sections. The first section comprises a computational study of the homolysis of oxycarbenes. It begins by describing an investigation designed to explain the unexpected observation by Venneri and Warkentin that the formal [1,2] and [2,3]-sigmatropic rearrangements of allyloxy(methoxy)carbenes (**36**) involve a stepwise homolytic fragmentation/recoupling mechanism, instead of the expected concerted rearrangements.[105] This study then focuses on the underlying physical nature of the fragmentation mechanism for oxycarbenes and the possibility that this simple homolysis actually involves a transition state. Analysis of some simple properties, including the atomic charges and the dipole moments provides important information about the nature of this fragmentation. In the second section of this chapter the reactions of dioxycarbenes with carbon disulfide are described and a theoretical investigation of this unique chemistry is presented.

2.1. Homolytic Fragmentations of Oxycarbenes

2.1.1. Homolysis of Allyloxyhydroxycarbene. A Density Functional and *Ab Initio* Study

Venneri and Warkentin recently reported that allyloxy(methoxy)oxadiazolines (**110**) undergo thermolysis in solution (110 °C, sealed tube) to esters (**37**) (SECTION 1.5.1.1) (eq. 20).[105]

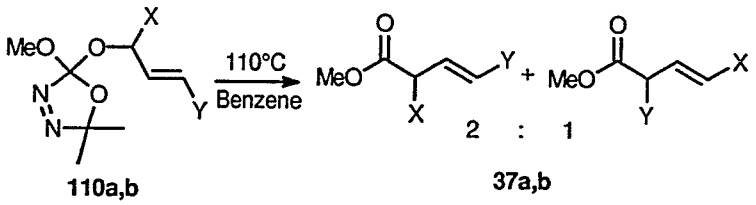

110a,b **37a,b** (20)

a = (X = Ph, Y = H) ; b = (X = H, Y = Ph)

The oxadiazolines (**110**) afforded dioxycarbene intermediates (**36**), trappable by *t*-BuOH, but the esters arose from radicals, trappable by TEMPO, by a mechanism of either type c or d of Scheme 50. That result was surprising in view of the known cases of concerted [2,3]-sigmatropic rearrangements of analogous (bisheteroatom)carbenes.[122-124,181] These thermal fragmentations are reminiscent of the radical mechanism accepted for the [1,2]-Wittig rearrangement of deprotonated ethers.[182] In the case of an allyl ether, the concerted [2,3]-Wittig rearrangement is favoured.[181,183,184] Wittig rearrangements have been the subject of a number of theoretical investigations but such studies are complicated by the uncertain role of the counterion.[185-193]

Scheme 50

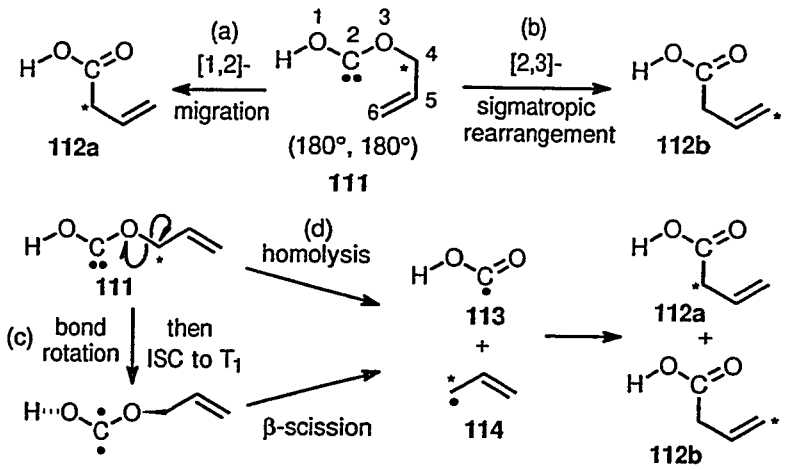

Four mechanisms (Scheme 50) for the formation of the esters (eq. 20) were investigated with the GAUSSIAN94, Revision E.2, system of programs[194], using allyloxy(hydroxy)carbene (AHC) (**111**) as a model for methoxy(allyloxy)carbenes (**36**).[195] Electron correlation was included with the Becke's 3-parameter hybrid method using the Lee-Yang-Parr correlation functional (B3LYP) density functional theory (DFT) method and the Møller-Plesset method with the correlation energy truncated at the second order (MP2). MP2 calculations were run with the frozen core approximation. Zero point energies were corrected using a scaling factor of 0.98 and 0.97 for the B3LYP and MP2 methods, respectively.[196,197] The triplet calculations were unrestricted and the dissociation energies were calculated by optimizing the radicals individually as unrestricted doublets. All other calculations were restricted. For AHC, the HOCO dihedral angle (θ_1) and the OCOC dihedral angle (θ_2) were defined (Scheme 50). Calculations on the conformers of AHC agree with those by Räsänen *et al.* for DHC in that the (180°, 180°) or *trans,trans*-conformer has the lowest energy at higher levels of

theory (Table 2).[17] Energies are therefore expressed relative to the fully optimized *trans,trans*-AHC (179.8°, 179.4° (B3LYP) and 179.6°, 178.5° (MP2)) and the text refers to ΔE_T + ZPE at the B3LYP/6-31+G(d) or MP2(FC)/6-31+G(d) level unless stated otherwise (Table 3). Single point calculations, using the larger B3LYP/6-311++G(3df,2p) basis set on the B3LYP/6-31+G(d) stationary points, had only minor effects on ΔE_T (Table 3). Some key results for singlet AHC are summarized in Figure 17, starting from the lowest energy conformation (*trans,trans*) of allyloxy(hydroxy)carbene and ending with the lowest energy conformation of the acid (*cis*-**112**). For convenience, the allyl substituent is drawn in the OCOC plane, although the lowest energy conformers have twisted COCC and OCCC dihedral angles. Minor differences imposed by the other stable HOCO (θ_1) conformers are presented in Table 3 and discussed below. Structural data for the fully optimized stationary points appear in Appendix I.

Table 2. Relative energies[a,b] (ΔE_T) (kcal mol^{-1}) of constrained[c] S_0 and T_1 AHC conformers.

		B3LYP/6-31+G(d)		MP2(FC)/6-31+G(d)	
θ_1	θ_2	S_0	T_{1v}[d]	S_0	T_{1v}[d]
0	0	11.65	84.03	12.89	87.02
0	90	19.50	71.47	20.91	75.49
0	180	0.54	75.61	0.86	77.81
90 (270)	0	20.62	72.59	22.32	76.79
90	90	40.99	66.52	44.80	70.05
270	90	38.52	64.46	41.96	68.08
90 (270)	180	17.19	68.11	18.25	72.34
180	0	2.47	74.64	2.45	78.13
180	90	17.56	64.70	18.87	69.42
180	180	0	72.02	0	75.53

[a] Total energy of (180°, 180°) conformer is -306.401085 hartrees. [b] Minor errors may be expected here due to the conformational mobility of the allyl group. [c] θ_1 and θ_2 frozen; other parameters optimized. [d] T_{1v}: vertical T_1 surface.

For *trans,trans*-AHC, the lowest energy transition state for the concerted [1,2]-migration (**TS1(a)**) (Figure 18) (Scheme 50a) was 41.90 and 43.90 kcal mol^{-1} above this conformer at the B3LYP and MP2 levels respectively (Table 3, Figure 17). However, the lowest energy transition state, (**TS1(b)**) (Figure 18), for the [1,2]-migration of *cis,trans*-AHC, was located at 40.76 (B3LYP) and 42.46 kcal mol^{-1} (MP2) (Table 3). The *cis,trans*-AHC conformer is certainly accessible, lying only 0.10 (B3LYP) and 0.51 kcal mol^{-1} (MP2) above the *trans,trans* conformer while the rotational barrier (**TS2**) for conversion of *trans,trans*-AHC to *cis,trans*-AHC is 15.59 (B3LYP) and 16.81 kcal mol^{-1} (MP2) (Table 3). As might be expected, the transition state barriers calculated here for the [1,2]-migrations of *trans,trans*- and *cis,trans*-AHC are lower than the 60.2 kcal mol^{-1} (PMP4/6-31G*//UHF/6-31G*) barrier for the [1,2]-CF_3 migration of

trifluoromethoxy(hydroxy)carbene (**42**), although a direct comparison cannot be made.[17] These activation energies are also high compared to the barrier for the [1,2]-hydrogen migration of dihydroxycarbene (**2**) which has been calculated to be as low as 33 kcal mol^{-1} at the PMP4/6-311++G**//UMP2/6-311G** + ZPE level.[110,117,119,198] The [1,2]-allyl migration was found to occur out-of-plane (51.7°(B3LYP) and 53.8°(MP2) for **TS1(a)**; 46.8° (B3LYP) and 52.5° (MP2) for **TS1(b)**) like the CF_3 migration in trifluoromethoxy(hydroxy)carbene (**42**) (57.6°) and unlike the [1,2]-H migrations of dihydroxycarbene (**2**) which proceed in-plane.[110,117,119,198]

Table 3. Energies, relative to *trans,trans*-AHC, in kcal mol^{-1} for the important stationary points.

	B3LYP/X[a]		B3LYP/Z// B3LYP/X[a]	MP2(FC)/X[a]	
Isomer	ΔE_T	ΔE_T + ZPE	ΔE_T	ΔE_T	ΔE_T + ZPE
trans,cis-AHC	2.45	2.39	2.73	2.45	2.45
cis,trans-AHC	0.53	0.10	0.74	0.86	0.51
TS1(a)	43.98	41.90	43.55	45.84	43.90
TS1(b)	42.78	40.76	42.53	44.62	42.46
TS2	17.29	15.59	16.61	18.39	16.81
TS3(a)	21.99	20.89	21.20	25.61	24.76
TS3(b)	22.89	20.89	21.75	26.03	24.92
TS4	15.14	14.30	14.71	16.59	15.70
Trans-**112**	-49.07	-48.98	-50.50	-53.07	-53.04
cis-**112**	-55.20	-54.89	-55.62	-59.78	-59.51
Trans-**113** + **114**	18.55	13.80	16.48	29.81	25.27
cis-**113** + **114**	20.50	15.45	18.44	31.71	27.00

[a] X and Z represent the 6-31+G(d) and 6-311++G(3df,2p) basis sets respectively. For w-AHC in hartrees; ΔE_T = -306.401088, ΔE_T + ZPE = -306.308228 at the B3LYP/X level, ΔE_T = -305.471333, ΔE_T + ZPE = -307.378281 at the MP2(FC)/X level and ΔE_t = -306.507716 at the B3LYP/X//B3LYP/Z level.

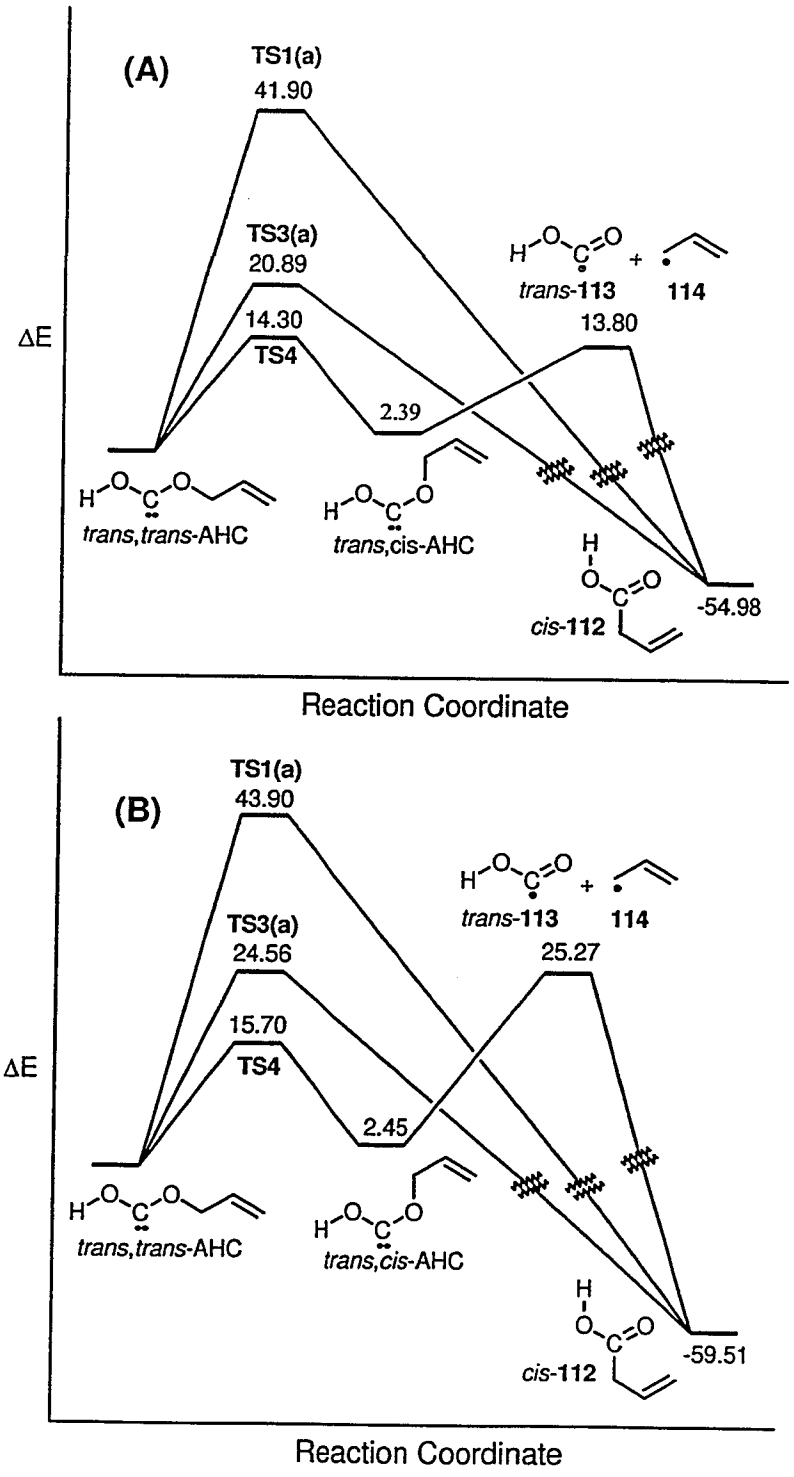

Figure 17. Schematic representation of the reaction coordinate (kcal mol^{-1}) for the rearrangements of AHC at the: (A) B3LYP/6-31+G(d) + ZPE level, (B) MP2(FC)/6-31+G(d) + ZPE level.

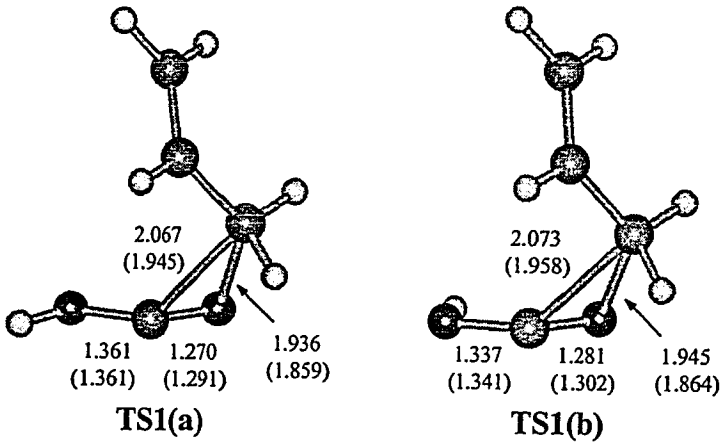

Figure 18. TS geometries for the [1,2]-migration at the B3LYP/6-31+G(d) level with bond lengths (Å). MP2(FC)/6-31+G(d) bond lengths (Å) in brackets.

The different geometries for the transition states of [1,2]-migrations of alkyl substituted carbenes[74] and oxycarbenes are due to the nucleophilicity of the oxy- and dioxycarbenes and the double bond character of the C-O migration centres.[110] However, there appears to be no explanation in the literature for the difference in calculated transition state geometries or the difference in the transition state barriers between hydrogen and alkyl migrating groups of oxy and dioxycarbenes. Although it is not strictly correct to apply a frontier molecular orbital (FMO) analysis to intramolecular reactions,[199] applying this theory to the [1,2]-migrations of oxycarbenes does provide some useful insights. Consider the FMO model for the well known inversion of stereochemistry observed for S_N2 reactions (Figure 19).[13,200] The important FMO interaction is between the HOMO of the nucleophile and the LUMO of the electrophile. When a nucleophile approaches opposite to the leaving group, the orbital interaction is bonding (Figure 19(a)), but when the approach is adjacent to the leaving group the orbital

interaction has both bonding and anti-bonding components (Figure 19(b)). Clearly, attack opposite to the leaving group is favoured. The FMO analysis for the [1,2]-migrations of a nucleophilic carbene should follow a similar model. The important HOMO/LUMO interaction should be between the carbene centred HOMO and the LUMO of the O-H /O-R bond (Figure 19(c-d)). For the O-H and O-R cases, the HOMO/LUMO interaction will be both bonding and anti-bonding. However, for the [1,2]-H migration the orbital overlap between the carbene HOMO and the very symmetrical bonding portion of the LUMO centred on hydrogen should be large (Figure 19(c)). Hence, the overall interaction should be bonding. The situation is different for a [1,2]-alkyl migration (Figure 19(d)). The preferred attack for nucleophilic substitutions, opposite to the leaving group (in this case oxygen), is not available. In addition, the bonding interaction for the front side attack will be less than that for the [1,2]-H migration. This is clear since the O-R LUMO has three nodes while the O-H LUMO has only two nodes and a good portion of the LUMO is on the wrong side of the alkyl group and is not available for overlap with the carbene HOMO. This poor bonding interaction results in a high energy transition state. In order to stabilize the transition state, the migrating group must move out-of-plane to take advantage of a favourable bonding interaction between the carbene centred LUMO and the HOMO of the O-R bond (Figure 19(e)). A similar FMO model has been used to explain the stability of certain carbene conformers in the past.[201]

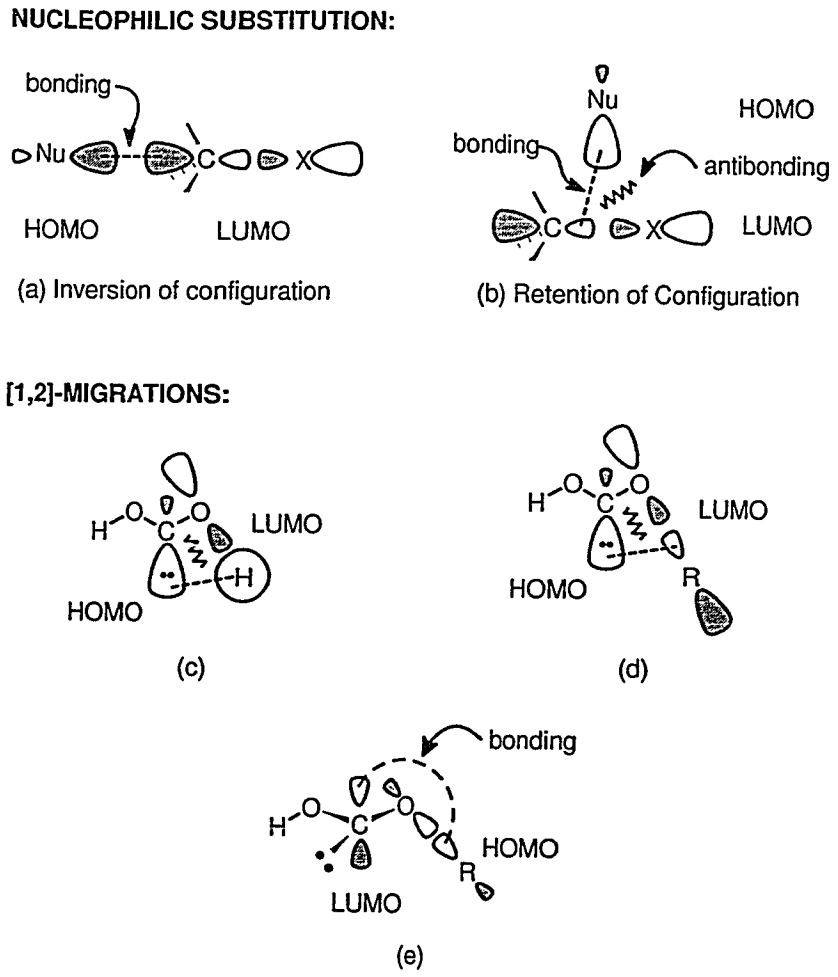

Figure 19. FMO model of the [1,2]-migrations and the S_N2 analogy.

The transition states reported here (**TS3(a)**) and **TS3(b)**) (Figure 20) for the [2,3]-sigmatropic rearrangement (Scheme 50b), resemble the Rautenstrauch model for the [2,3]-Wittig rearrangement in that C5 is out of the plane of the 5-membered transition state.[185,188,189] **TS3(a)** and **TS3(b)** are also early, which could indicate the presence of an intermediate on the reaction coordinates, however none was found with an intrinsic reaction coordinate calculation at the RB3LYP/6-31+G(d) level for the *trans,trans*-AHC

reaction coordinate. These early transition states are consistent with the results of Iwamura *et al.* for allyloxycarbene (**41**) (Section 1.5.1.3), and are reasonable for exothermic reactions requiring relatively small activation energies, in accordance with the Hammond postulate.[121,127]

TS3(a) for the rearrangement of *trans,trans*-AHC was found to lie 20.89 (B3LYP) and 24.76 kcal mol^{-1} (MP2) above the ground state while **TS3(b)** for the migration in *cis,trans*-AHC was found to lie 20.89 (B3LYP) and 24.92 kcal mol^{-1} (MP2) above *trans,trans*-AHC. Coincidentally the B3LYP values for ΔE + ZPE of **TS3(a)** and **TS3(b)** are identical, while **TS3(a)** is slightly lower in energy at the MP2 level of theory. Therefore, the [2,3]-sigmatropic rearrangement has a barrier roughly half that of the [1,2]-allyl migration (Table 3, Figure 17). This is consistent with the antiaromatic nature of a partially in-plane four-electron transition state of the [1,2]-migration, as compared to the allowed six-electron transition state of the [2,3]-sigmatropic rearangement.[57,110,121] Clearly, the [2,3]-sigmatropic migration, which is known for other (bisheteroatom)carbenes,[122-124,181] should be highly favoured over the [1,2]-migration. Thus the observed experimental product ratios[105] (eq. 20) cannot be explained in terms of a competition between these two rearrangements.

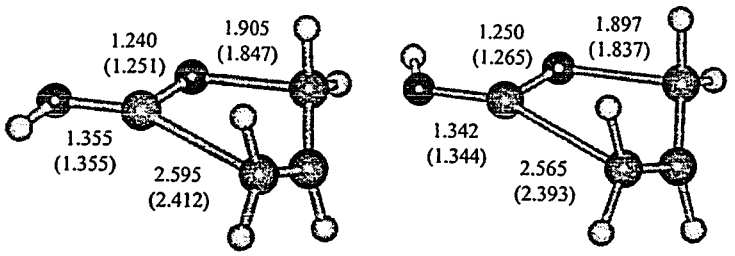

TS3(a) **TS3(b)**

Figure 20. TS geometries for the [2,3]-sigmatropic shift at the B3LYP/6-31+G(d) level with bond lengths (Å). MP2(FC)/6-31+G(d) bond lengths (Å) in parentheses.

Homolysis of dioxycarbenes to give radicals by means of a β-scission from T_1 (Scheme 50c) requires that this state be well populated. The experimental results[105] indicate that most of the apparent rearrangement products (**112**) come from a radical path, requiring a small S_0-T_1 gap if the radicals came from the triplet carbene. The potential energy surfaces were initially mapped out at the HF/3-21G level with the (0°, 180°), (90°, 180°), (180°, 180°) and (270°, 180°) starting geometries, from which, with θ_1 frozen, θ_2 was rotated through to 0° in 10° steps as the geometry was optimized at every point for the S_0 surface. The vertical triplet surfaces (T_{1v}) were calculated at the S_0 geometries. Qualitatively, the HF/3-21G results mirror those for dihydroxycarbene (**2**) in that minima on the S_0 surface represent maxima on the triplet surface and *vice versa*.[17,18,202] At this level of theory, the θ_1 = 90° and the θ_1 = 270° S_0 and T_{1v} surfaces enter overlapping regions which move apart at the higher levels until the θ_1 = 90° and the θ_1 = 270° surfaces have S_0-T_{1v} gaps of -25.53 and -25.94 kcal mol^{-1} respectively (B3LYP) (Table 2, Figure 21), and -25.25 and -26.12 kcal mol^{-1} respectively (MP2) (Table 2), in excellent agreement with previous results for dihydroxycarbene[17,119] and dimethoxycarbene.[16] The

(90°, 90°) and (270°, 90°) singlet conformers are more or less maxima that lie 40.99 kcal mol^{-1} and 38.52 kcal mol^{-1} (B3LYP)(Table 2, Figure 21) respectively and, 44.80 and 41.96 kcal mol^{-1} (MP2)(Table 2) respectively, above the lowest energy singlet conformer. It seems unreasonable then to suggest that the triplet state could be the radical source. A similar mechanism for fragmentation from the open shell singlet can also be ruled out since a singlet state derived from a given electronic configuration possessing two half-filled orbitals is always of higher energy than the triplet state of the same configuration, due to the exchange correlation which stabilizes the triplet relative to the singlet state.[203,204] Moss *et al.* have calculated that the HOMO → LUMO ($\sigma^2 \rightarrow \sigma^1p^1$) excitation to give the open-shell singlet for *cis,trans*- and *trans,trans*-dimethoxycarbene costs 109 and 104 kcal mol^{-1} respectively at the CIS/INDO/S//6-31G(d) level of theory.[16] This calculated excitation corresponded to an experimentally observed absorption at 255 nm (112 kcal mol^{-1}).[16]

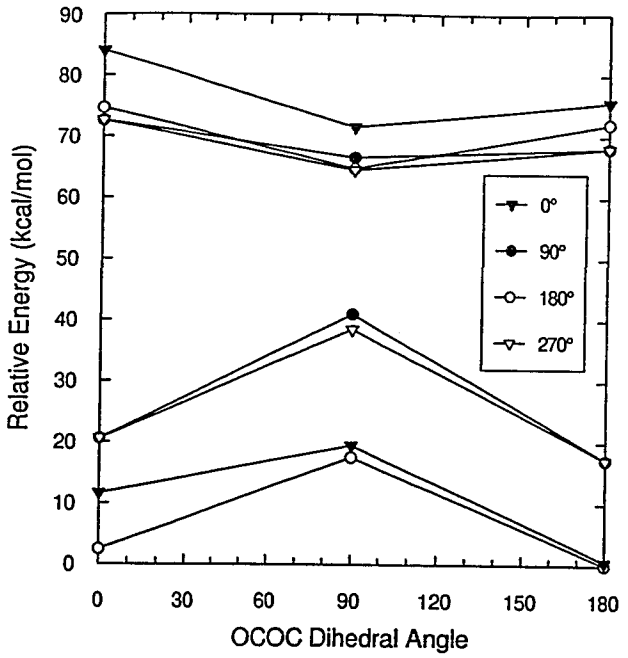

Figure 21. Energy diagram showing the singlet (S_0) and vertical triplet (T_{1v}) curves at the B3LYP/6-31+G(d) level, with θ_1 (HOCO dihedral angle) frozen at 0°, 90°, 180° and 270° and rotating about θ_2 (OCOC dihedral angle).

The possibility of homolysis from the singlet ground state of allyloxy(hydroxy)carbene can now be considered (Scheme 50, path (d)). It is a simple matter to calculate the dissociation energy of the carbene to radicals by calculating each of the radicals individually.[205] Large differences were observed for the B3LYP and MP2 results. The radicals (*trans*-**113** + **114**) were found to be 68.69 kcal mol^{-1} (73.75 kcal mol^{-1} without ZPE) above the lowest energy conformer of the carboxylic acid (*cis*-**113**) at the B3LYP level and 84.78 kcal mol^{-1} (89.59 kcal mol^{-1} without ZPE) at the MP2 level (Table 3, Figure 17). The B3LYP results are in better agreement with the experimentally derived[206,207] $\Delta H°_f$ of 75 ± 1 kcal mol^{-1}, consistent with previous workers who have found that DFT gives more reliable heats of formation for a variety of radicals than MP2

calculations.[205] The sum of the energies of the radicals, *trans*-**113** + **114**, was found to lie 11.41 kcal mol^{-1} above *cis,trans*-AHC using DFT and 22.82 kcal mol^{-1} above *cis,trans*-AHC using MP2 (Table 3, Figure 17). The fully optimized *trans,cis*-AHC conformer lies 2.39 kcal mol^{-1} above the *trans,trans*-AHC conformer, while the barrier for rotation to *trans,cis*-AHC through **TS4** (182.5°, 92.0° and 182.0°, 92.3°) is 14.30 and 15.70 kcal mol^{-1} at the DFT and MP2 levels respectively (Table 3, Figure 17). It can be seen from Table 3 that the [2,3]-sigmatropic rearrangement (**TS3(a)** and **TS3(b)**) has an activation energy that is either higher than or about equal to that of the homolysis. At 110 °C (the temperature for the thermolysis presented in eq. 20) radical formation from the singlet *trans,cis*-conformer (Scheme 50, path (d)) should be the dominant pathway due to entropic effects which would favour the dissociation pathway over the highly ordered [2,3]-sigmatropic rearrangement. This expectation is in keeping with the known temperature effects on Wittig rearrangements.[183,208,209] The observed regiochemistry (eq. 20) may arise from solvent cage effects similar to those used to explain the high retention of stereochemistry also found for [1,2]-Wittig rearrangements.[182]

It was pointed out in Section 1.5.1.1 of the introduction that Borden found a transition state in the homolysis of w-dihydroxycarbene (**2**).[110] However, due to the level of approximation it was not possible to conclude if such a barrier was real. Homolysis of s- or u-dihydroxycarbene (**2**) was not examined. Of course, if there is a transition state in the homolysis of oxycarbenes, this could change the interpretation of the allyloxy(hydroxy)carbene (**111**) results presented above. Furthermore, fragmentations of simple molecules do not normally have transition states, or in other words simple radicals

do not normally have barriers to coupling. This suggested the importance of further study, which could lead to a better understanding of the mechanism of homolysis of oxy- and dioxycarbenes from their singlet ground state.

2.1.2. Hydroxycarbene as a Model for the Homolysis of Oxy- and Dioxycarbenes

In this study the dissociation of hydroxycarbene (HCOH) was used as a model for the dissociation of the more complex oxy and dioxycarbenes, which appear to undergo homolysis from a singlet ground state (Section 1.5.1.1).[210] Scheme 51 shows the dissociation of the stable *cis* and *trans* isomers. Since the homolysis of formaldehyde (H_2CO) yields the same radicals, it was included in this work as a test for the methods used. The systems were modeled using Complete Active Space and Multireference Configuration Interaction methods. The potential energy surfaces were analyzed and the theory of atoms in molecules (AIM)[211] was used in the discussion of the electronic structure of the systems (Appendix II).

Scheme 51

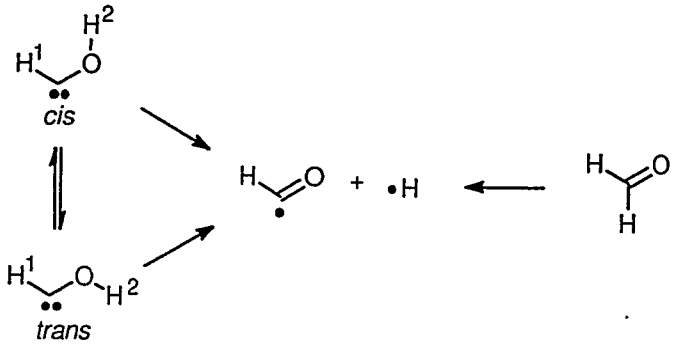

Calculations of the wave functions and optimizations for HCOH and its isomers were carried out using the General Atomic and Molecular Electronic Structure System of programs (GAMESS, version 6 MAY 1998).[212] Dunning's correlation-consistent, polarized-valence, double-zeta (cc-pVDZ) basis set was found to be appropriate for the study.[213] Geometries were optimized using the quasi-Newton-Raphson search with the quadratic approximation algorithm at the Complete Active Space Self-Consistent-Field (CASSCF) level of theory using several choices of active space. It was determined that in order to describe the dissociation processes correctly, the active space should include at least 8 electrons and 8 active in-plane orbitals to give an 8,8 active space (CAS(8,8)). This active space was augmented with the two lowest energy out-of-plane π-orbitals to give a 10,10 active space (CAS(10,10)) which was also utilized in the study. The modelling of the homolysis of *cis* and *trans*-HCOH at the CAS(10,10) level, using only the O-H bond length as a constraint, indicated that the dissociation proceeded in plane. Frequency calculations at the CAS(10,10) level indicated only one imaginary frequency for the transition states. As a consequence, both active spaces were employed to study the dissociation from the ground state (S_0), using the symmetry plane and the dissociating bond distance as constraints for the optimizations. The first singlet excited state (S_1) was calculated for the vertical excitation at the state-averaged CASSCF level of theory with averaging of the S_0 and S_1 states using the CAS(10,10) ground state (S_1) geometries. In these calculations, equal weights were given to each of the states.

Single-point Multireference Configuration Interaction (MRCI) calculations were performed using the 8,8 active space (MRCI(8,8)) at the corresponding CASSCF

optimized geometries. These MRCI(8,8) calculations included all single and double excitations from the CASSCF active space and provided the wave functions for the analysis of the electron density of the HCOH isomers. Calculations of the atomic properties, defined by the theory of atoms in molecules, were performed using the AIMPAC system of programs.[214] The formyl radical was also examined. The ground state wave function of this doublet was calculated at the SD-CI/cc-pVDZ level of theory, including all possible excitations from core and valence orbitals in the CI expansion, using the GAUSSIAN94, Revision E.2, system of programs.[194] This wave function was used to integrate the spin densities over the atomic basins in the radical.[215]

Figure 22 shows the potential energy curves for the dissociation of *cis*- and *trans*-HCOH at the CAS(8,8) and the CAS(10,10) levels. In order to evaluate the performance of these levels of theory, the analogous H_2CO dissociation is also included. In addition, Table 4 displays the energies for the equilibrium geometries, the approximate barrier heights, and the dissociation energies. A number of important points should be noted from these results. As expected, all three isomers dissociate to the same limit. At the equilibrium geometry the *trans* isomer is the lowest energy conformer of HCOH, in agreement with conclusions of previous workers.[17,108,111,216-220]

Table 4. Energies for important points on the dissociation curves for each isomer in kcal mol^{-1} at all levels. All energies are given relative to the radicals for dissociation of *cis*-HCOH at 7.0 Å whose total energy (hartrees) is given in parentheses for each active space.

Level	Isomer	Eq. Geom.	T. S. Barrier	R_{X-H} = 7.0 Å
CAS(10,10)/cc-pVDZ	*cis*-HCOH	-22.37	5.09	(-113.894618)
	trans-HCOH	-27.26	14.92	0.00
	H_2CO	-84.97	No T.S.	0.00
CAS(8,8)/cc-pVDZ	*cis*-HCOH	-35.74	3.24	(-113.822002)
	trans-HCOH	-40.52	11.25	0.00
	H_2CO	-85.04	No T.S.	0.00
MRCI(8,8)/cc-pVDZ// CAS(8,8)/cc-pVDZ	*cis*-HCOH	-44.79	No T.S.	(-113.900490)
	trans-HCOH	-49.37	6.03	0.00
	H_2CO	-85.91	No T.S.	0.00

For both CAS levels of theory, the calculated dissociation energies of formaldehyde are in good agreement with the experimental value of 87.1 kcal mol^{-1}, calculated from the heats of formation of the radicals and formaldehyde.[206,207] Previous SD-CI calculations using a DZ basis set with polarization functions gave a dissociation energy of 88.5 kcal mol^{-1}, which was lowered to 80.2 kcal mol^{-1} after an experimental zero point vibrational energy (ZPE) correction was added.[111] A more recent study, in which the radicals were calculated as doublets at the MP4(SDTQ)/6-311G**//MP2/6-31G* level, with a ZPE correction of 8.7 kcal mol^{-1} and annihilation of spin contamination, found that the radicals were 80.1 kcal mol^{-1} above formaldehyde.[217] Note that the dissociation energies in Table 4 were not corrected for the ZPE. The CAS(10,10) results are in better agreement with the energy difference of 54.2 ± 2 kcal mol^{-1} found between HCOH and

formaldehyde by cyclotron double resonance spectroscopy.[221] The CAS(10,10) value for the HCOH and formaldehyde energy difference is also in good agreement with previous theoretical work.[108,111,216-220,222] Consistent with other theoretical calculations,[111] H_2CO does not have a transition state for the homolysis at either level of theory. However, for both active spaces the *cis*- and *trans*-HCOH homolysis curves do have maxima, with the one for *trans*-HCOH being the most pronounced.

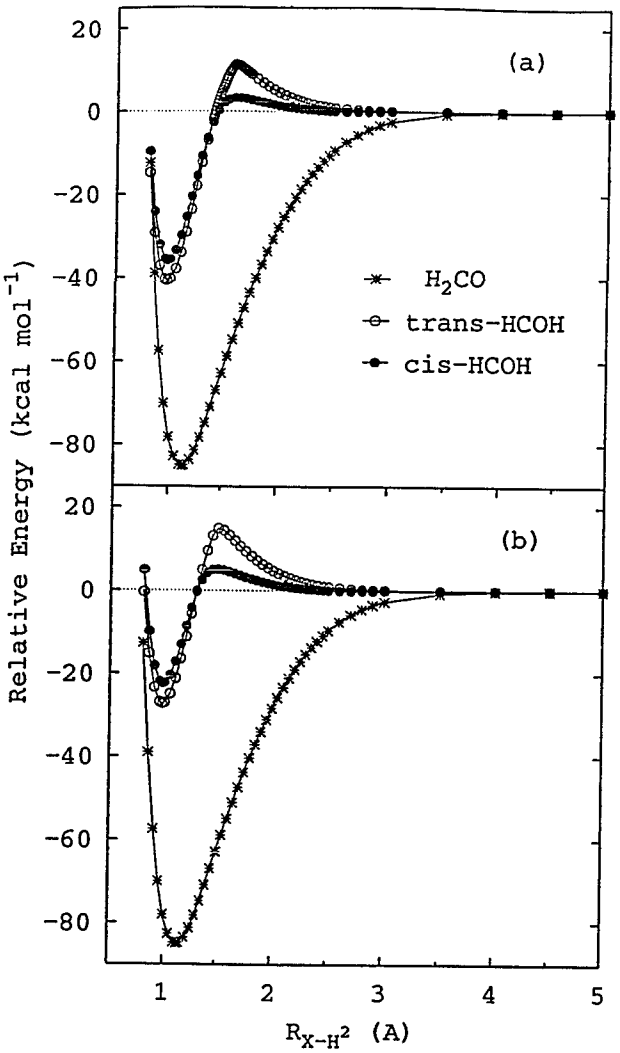

Figure 22. Potential energy curves for the homolysis of *cis*-HCOH, *trans*-HCOH and H_2CO: (a) at the CAS(8,8) level of theory; (b) at the CAS(10,10) level of theory.

One of the main objectives of this work was to determine if there is a transition state for the homolysis of oxy- and dioxycarbenes, and to understand the underlying physical nature of this process. Since both active spaces show similar dissociation curves, the (8,8) active space was selected to include dynamic electron correlation by means of MRCI calculations, which would not be possible with the larger 10,10 active

space due to computational limitations. Figure 23 shows the MRCI(8,8) potential energy curves for *cis*-HCOH, *trans*-HCOH and H_2CO as a function of the reaction coordinate. The energy of the carbenes relative to both formaldehyde and the radicals is less than that from the CAS results. Most remarkably, the maximum in the *trans*-HCOH potential energy surface remains, whereas it disappears for the *cis*-HCOH surface. Borden *et al.* have reported that the dissociation of singlet carbenes might involve a transition state.[110] However, their observation resulted from use of single-determinant wave functions, and they were unable to exclude the possibility that such behaviour was due to an inadequacy in the method of calculation used.

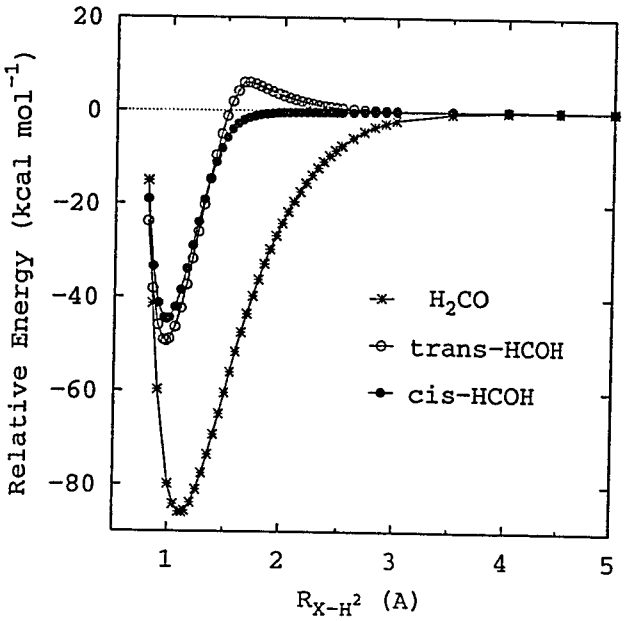

Figure 23. Potential energy curves for the homolysis of *cis*-HCOH, *trans*-HCOH and H_2CO at the MRCI(8,8) level of theory.

If there is a transition state for the homolysis of *trans*-hydroxycarbene the question arises as to what the source of this additional barrier could be. A valence-bond configuration mixing (VBCM) analysis of this system could be helpful here.[223,224] In this model, the valence-bond electronic states of the reactants and products are defined and their energies are plotted against the reaction coordinate to give a state correlation diagram. Here the reactant and product configurations will be defined as the carbene (n^2) and radical ($n^1\sigma^1$) configurations respectively (Figure 24). The equilbrium geometry of the carbene electronic configuration is shown in the lower left-hand corner of the state correlation diagram. If the O-H bond is stretched without changing the electronic configuration, the energy will rise and the carbene configuration can be followed until the dissociated geometry is reached in the upper right-hand corner. This would result in a formyl radical in which the unpaired electron is centered on oxygen. However, a simple Lewis structure analysis of the formyl radical indicates that the spin density should be highly localized on the carbon atom. At the SD-CI/cc-pVDZ level of theory, the populations are 0.5545, 0.2731 and 0.1724 α-electrons for C, O and H, respectively. These values are obtained by integration of the spin density over the atomic basins. Previous workers have shown that the spin density is spread over the entire molecule,[225,226] but the integrated values above also indicate that this is a carbon centred radical. This result is in agreement with the potential energy curves in Figure 22 and Figure 23 which show that the reverse reaction, the approach of the H atom to the HCO radical, would give formaldehyde as the preferred product. Therefore, the product radical configuration is best represented by the valence bond structure in the lower right-hand

corner of the state correlation diagram. If this configuration is followed back along the reaction coordinate a so called high energy "3-electron" O-H bond results. Of course, this does not actually happen. Instead, starting from the ground state carbene equilibrium configuration, the homolysis proceeds by following this electronic configuration until it meets the descending radical configuration. At this point on the reaction coordinate, the two configurations mix (interact) and the intended crossing does not occur. In other words, the two states do not cross and there is an avoided crossing on the potential energy surface, allowing the system to stay on a ground state surface, first defined by the carbene n^2 configuration and then by the product radical $n^1\sigma^1$ configuration.

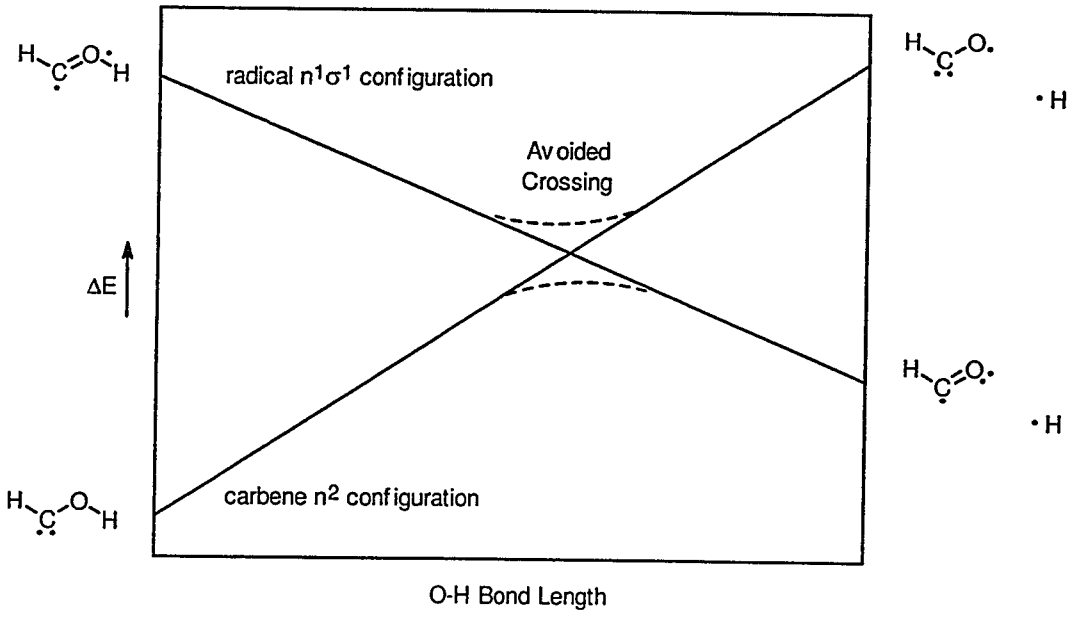

Figure 24. State correlation diagram for the valence-bond configuration mixing analysis of the homolysis of hydroxycarbene.

It is also useful to consider the interaction between the carbene n^2 configuration and the radcal $n^1\sigma^1$ configuration. The VBCM model can help provide some information

as to how the ground state moves from the carbene electronic configuration (n^2) to the radical ($n^1\sigma^1$) configuration. It is clear, especially upon examination of the reactant and product configuration on the left-hand side of the state correlation diagram (Figure 24) that the product electron configuration ($n^1\sigma^1$) is simply an $n\rightarrow\sigma^*$ excitation from the reactant configuration (n^2). This suggests that the homolysis involves a single electron transfer (SET) from the carbenic lone pair to σ^* of the O-H bond (Scheme 52) which would occur when the two electronic configurations begin to mix in the region of the avoided crossing. This picture suggests that as the O-H bond is stretched and the energy of σ^* decreases, there is a SET from the high energy carbenic lone pair (n^2) into this orbital. Taking this idea to its limit, it could be suggested that the hydrogen actually leaves with an electron from the carbenic lone pair, instead of from its own O-H bond, which becomes a lone pair on oxygen instead.

Scheme 52

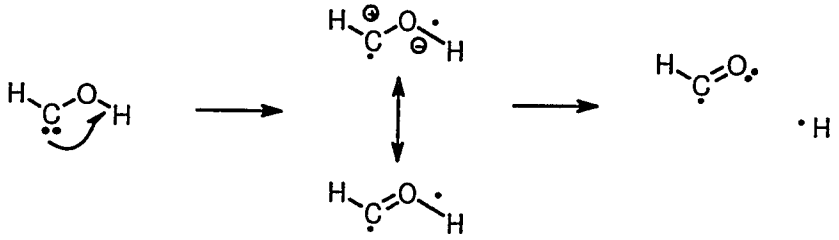

The advantage of VBCM theory is that it clearly states what causes a transition state.[24] A transition state is formed because reactants have to open their valence shells, stretch or break bonds, and thus climb up an energy hill until they meet a descending electronic state onto which they can cross. However, the analysis of *cis*-hydroxycarbene,

which was predicted not to have a transition state at the MRCI level of theory, would give the same state correlation diagram, predicting a transition state for homolysis from this conformer as well. This system also represents a failure of one of the rules of the VBCM model which suggests that stabilization of any key configuration with respect to the reactant configuration is likely to lead to a stabilization of the transition state and a corresponding rate enhancement.[223] Remember that for the hydroxycarbene system the *trans* conformer has a transition state. Destabilizing the carbene configuration in the form of the higher energy *cis* conformer should increase the transition state barrier (or at least increase the barrier to radical coupling), but instead the transition state disappears (Figure 23). Therefore, while this VBCM analysis does provide important insight into the formation of a transition state it cannot adequately explain the results obtained for both conformers.

In order to investigate further the nature of the transition state observed for *trans*-HCOH, state-averaged CAS(10,10) calculations involving the S_0 and the vertical S_1 state were carried out for the dissociation of both *cis*- and *trans*-HCOH. Note that this work was not an attempt to study the first excited singlet state of hydroxycarbene, whose geometry is thought to be gauche.[218] The analysis of the vertical S_1 state is included only to analyze its effect on the ground state in the vicinity of the avoided crossing of states of the same symmetry. Figure 25 shows the avoided crossing in the region of the transition state. On the carbene side of the potential energy curve, the excited state involves an important contribution of an excitation from the lone pair of the carbon atom to the σ^* orbital of the breaking O-H bond ($n \rightarrow \sigma^*$) to give a $n^1\sigma^1$ configuration. Beyond the

avoided crossing of states, this configuration becomes the main contribution corresponding to the ground state of the radicals. In effect, this suggests that the hydrogen atom leaves with an electron from the carbene lone pair (n^2) and not from the O-H sigma bond, a point that will be made clearer from the analysis of the electronic properties in the following sections. This result can be contrasted with some previous studies which have predicted that S_1 for hydroxycarbene, methoxymethylcarbene (**23**) and dimethoxycarbene **1** would comprise an important contribution of the $n^1\pi^1$ configuration resulting from an excitation from the carbon lone pair to π^*.[16,73,218] While the $n^1\pi^1$ configuration may be important, these results for hydroxycarbene, methoxymethylcarbene **23** and dimethoxycarbene **1** could be a consequence of the use of single reference correlated wave functions in those studies. On the other hand, the results presented here represent state-averaged calculations designed to study the homolysis, not S_1 at the equilbrium hydroxycarbene geometry. As was the case for the pure-state CAS calculations, there is a maximum in the potential energy curves of both HCOH conformers, but it is expected that at the MRCI level the one for the *cis* conformer will disappear. Due to computational limitations, the MRCI(10,10) state-averaged calculations could not be performed. Although both conformers have maxima, some qualitative conclusions can be drawn. As can be seen from Figure 25, the avoided crossing of states should occur first for the dissociation of the *cis* conformer. This is in part due to the steeper increase in the energy of the ground state for this conformer in comparison to *trans*-HCOH. As a result, the *trans* conformer maintains its carbene-like configuration (n^2) further along the reaction coordinate.

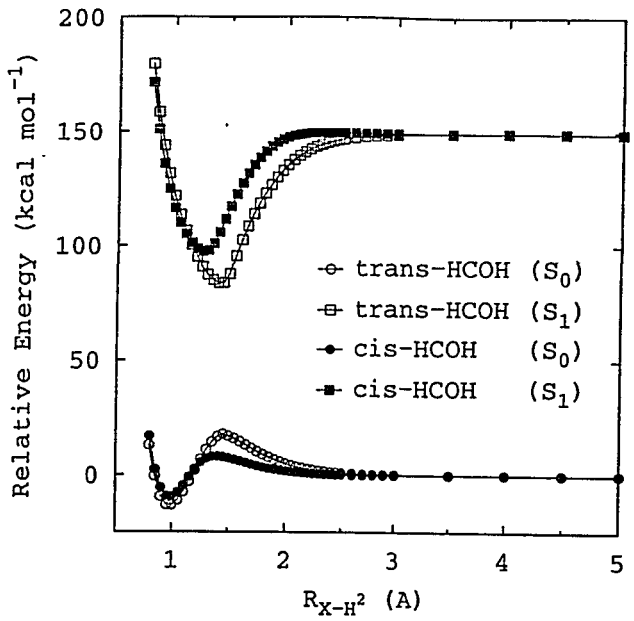

Figure 25. The S_0 and S_1 potential energy surfaces of *cis*- and *trans*-HCOH at the state-averaged CAS(10,10) level.

The changes in the electronic structure of HCOH can be analyzed in terms of the properties of the atoms defined by the theory of atoms in molecules, as well as in terms of the local properties of the electron density ($\rho(\mathbf{r})$) (Appendix II). The following analysis for each HCOH conformer was performed using MRCI(8,8) wave functions for a number of $R_{O\text{-}H}$ values. The atomic charges (q_Ω) are displayed in Figure 26, including those for the homolysis of the C-H bond of formaldehyde for comparison. In the case of the leaving hydrogen atom the final charge corresponds to the free atom. The evolution of the atomic charges during the homolysis of the HCOH conformers indicates that early in the dissociation the leaving hydrogen atom withdraws electron density from oxygen. However, it is carbon that loses electron density to hydrogen and oxygen in the region of

the avoided crossing of states due to the transition from the n^2 to the $n^1\sigma^1$ configuration. As a result, the net change in the atomic charge of oxygen is small as the carbene is transformed to radicals. These results are consistent with the formation of a carbon centred radical as indicated by the SD-CI/cc-pVDZ spin density results presented above. The decreasing positive charge on the forming H radical of both hydroxycarbene conformers is also in agreement with experimental results by Merkley and Warkentin.[107] Using benzyloxy(4-substituted benzyloxy)carbenes ($PhCH_2OCOCH_2Ar$) (**39**) they were able to show that homolytic fragmentation favoured formation of the benzyl radical with an electron withdrawing group in the para position (Section 1.5.1.1). A Hammett plot of the data gave a good correlation with σ^- substituent constants ($r = 0.994$, $\rho_{(PhH,\ 110\ °C)} = 0.7$) suggesting that the fragmentation involves charge separation in the sense that electron density increases on the group that is becoming a benzyl radical.

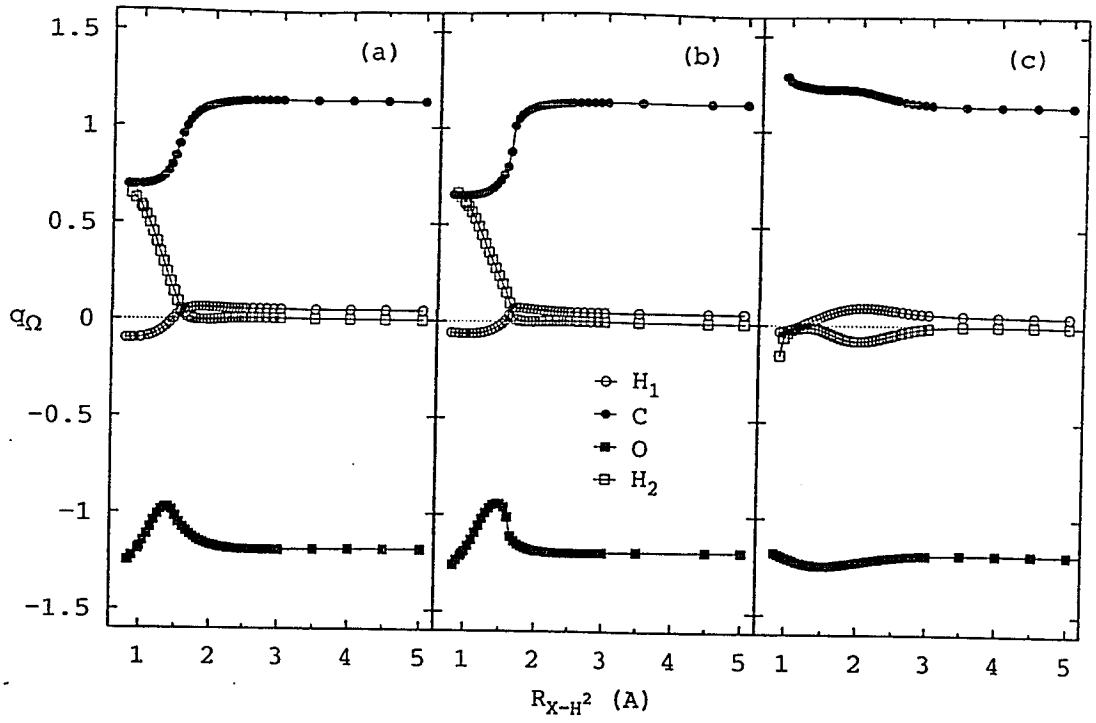

Figure 26. MRCI(8,8) atomic charges for: (a) *cis*-HCOH; (b) *trans*-HCOH ; (c) H_2CO.

It is also useful to compare the relative values of the atomic charges in the conformers. In the *trans* conformer, the atoms retain more carbene character as they approach the avoided crossing of states, and there is a build-up of the atomic charge on oxygen that occurs further along the reaction coordinate relative to *cis*-HCOH. This indicates that the carbon atom is less able to donate electron density to oxygen in the *trans* system when the carbene begins to dissociate. This behaviour can be contrasted with the observed trends for the atomic charges in formaldehyde where there is no similar dramatic change in the values during dissociation (Figure 26(c)). It is necessary to stress the relationship between this behaviour of the atomic charges of the three isomers to that of the corresponding potential energy surfaces. Dissociation of formaldehyde does not involve a transition state and the atomic charges display a monotonic behaviour. Due to

the persistence of its n^2 electronic state, *trans*-HCOH is the carbene conformer that shows the greatest changes in the atomic charges and is the only isomer that has a transition state for homolysis.

The local properties of the electron density ($\rho(\mathbf{r})$) provide information complementary to the atomic properties (Appendix II). The behaviour of the local properties of the electron density is well illustrated by the electron density itself, evaluated at the bond critical points, and by the Laplacian of the electron density ($\nabla^2\rho(\mathbf{r})$) in several regions of a molecule. Figure 27 displays the values of $\rho(\mathbf{r})$ at each of the three bond critical points for each conformer. As expected, the electron density at the O-H bond critical point decreases to approximately zero at long distances. This behaviour is consistent with the breaking of the O-H bond. It is also interesting that, whereas at the H-C bond critical point $\rho(\mathbf{r})$ remains almost unchanged, the value at the C-O bond critical point increases with the formation of the radicals due to an increase in the double bond character. This is in contrast to formaldehyde in which the electron density at the C-O bond critical point changes by only 0.013 atomic units.

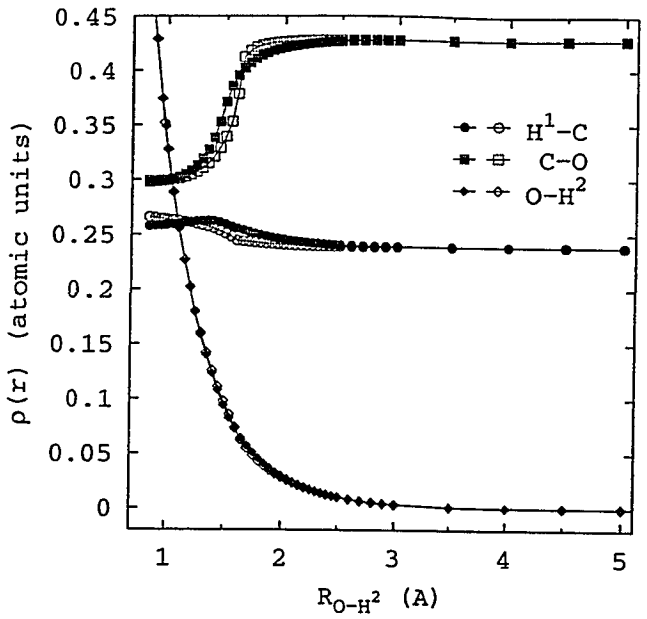

Figure 27. Electron density for the three bond critical points in *cis*-HCOH (solid symbols) and *trans*-HCOH (open symbols) versus the reaction coordinate using the MRCI(8,8) wave functions.

The Laplacian of the electron density also provides important information about the changes in the electronic structure of the conformers of HCOH during dissociation. These changes can be followed by the local charge concentrations indicated by the existence and location of local minima exhibited by this property. Figure 28 shows contours of $\nabla^2\rho(\mathbf{r})$ for some selected molecular geometries in each case. At short O-H bond distances there are regions of negative values of the $\nabla^2\rho(\mathbf{r})$ that correspond to two electron pairs; one each for the carbon and oxygen atoms. The occurrence of only one critical point corresponding to a minimum in the Laplacian of the electron density in the non-bonded region of the oxygen atom deserves some attention. In methanol for example, two critical points are found above and below the C-O-H plane.[227,228] However, in hydroxycarbene one of these oxygen lone pairs donates electron density to the virtual

p-orbital of the carbon atom to form a partial π bond, resulting in the observation of only one oxygen lone pair in the H-C-O-H plane.

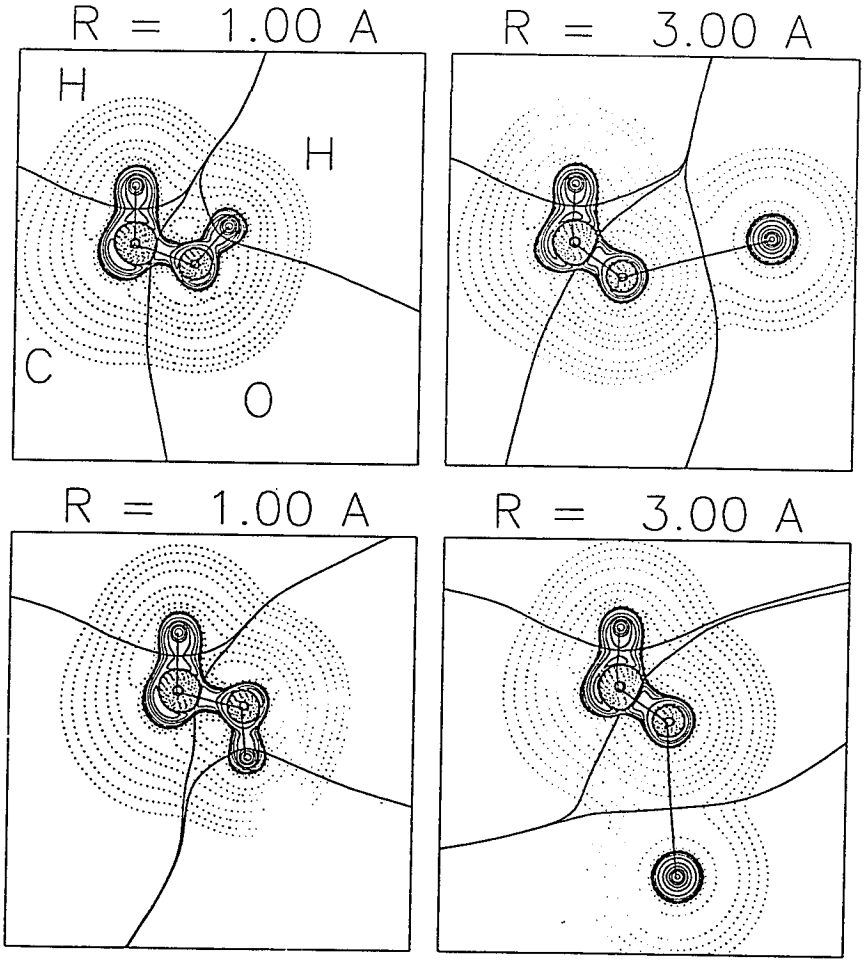

Figure 28. Contours of the Laplacian of the electron density, with superimposed interatomic surfaces, for some selected molecular geometries from the MRCI(8,8) wave functions. Dashed and solid lines correspond to positive and negative values of $\nabla^2\rho(r)$, respectively.

Figure 29 shows how the value of $\nabla^2\rho(\mathbf{r})$ at the carbon lone pair critical point becomes less negative during dissociation. The most important changes take place for O-H separations in the vicinity of the avoided crossing of the two lowest singlet electronic

states. This trend can be attributed to the transition from the carbene to the formyl radical and supports the contention that it is the carbon atom that donates an electron to hydrogen. It was also found that the oxygen lone pair that develops with the homolysis of the O-H bond begins to appear immediately following the avoided crossing for *trans*-HCOH. However, the lone pair does not start to develop for the *cis* conformer until the H-O bond length has reached ~ 2.7 Å. This suggests that the *cis* conformer undergoes a smoother change to radicals as compared with *trans*-HCOH.

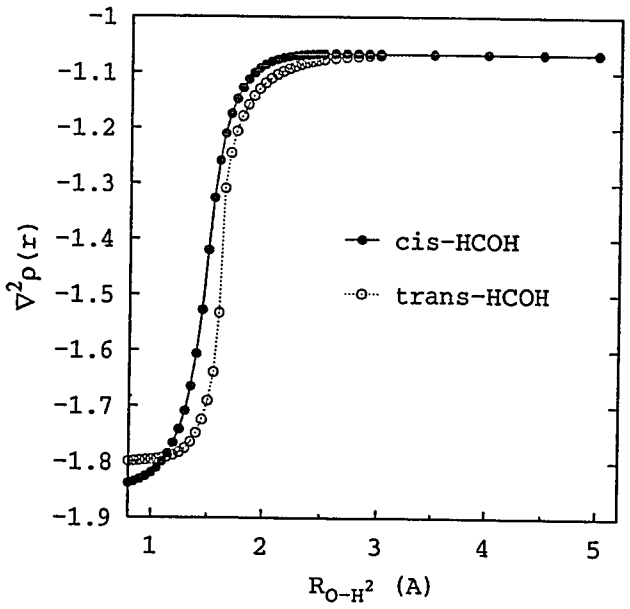

Figure 29. Laplacian of the electron density at the critical point corresponding to the carbon lone pair as it becomes a radical centre for both HCOH isomers, calculated using the MRCI(8,8) wave functions.

To this point, the examination of the electronic properties has indicated that the avoided crossing involves a substantial reordering of the electronic structure of both HCOH conformers, suggesting that a transition state might be expected. However, there

has been no indication why only one conformer has such a transition state. Careful analysis of the dipole moment in terms of its charge transfer and polarization contributions seems to provide an explanation for the differences observed in the potential energy curves of these conformers. Examination of Figure 30 and Figure 31 indicates that the main differences between the dipole moments of *cis*- and *trans*-HCOH occur on the carbene side of the potential energy curve. At these short distances, μ_p and μ_{ct} are nearly anti-parallel for trans-HCOH and almost cancel each other out. As the magnitude of the polarization contribution $|\mu_p|$ is slightly greater than that of the charge transfer $|\mu_{ct}|$, the former determines the direction of μ. This greater polarization of the charge distribution can be associated with the lone pairs on the carbon and oxygen atoms. In the case of *cis*-HCOH, the ratio $|\mu_p|/|\mu_{ct}|$ is similar to the one for the *trans* conformer. However in this case the vectors are oriented in a different manner, with a less effective cancellation between contributions, resulting in a greater dipole moment for *cis*-HCOH whose direction clearly differs from that of the *trans* conformer. This is a consequence of the relative positions of the lone pairs for each conformer. On the other hand, after the avoided crossing of states, μ_{ct} and μ_p are oriented in an anti-parallel manner in both cases, with the dominant contribution coming from the charge transfer. This greater contribution of μ_{ct} to μ is in part due to the increase of the charge transfer from carbon to oxygen, as indicated by the atomic charges in Figure 26. The dominance of the charge transfer component of μ in the formyl radical is similar to what has been previously reported for carbonyl compounds.[229]

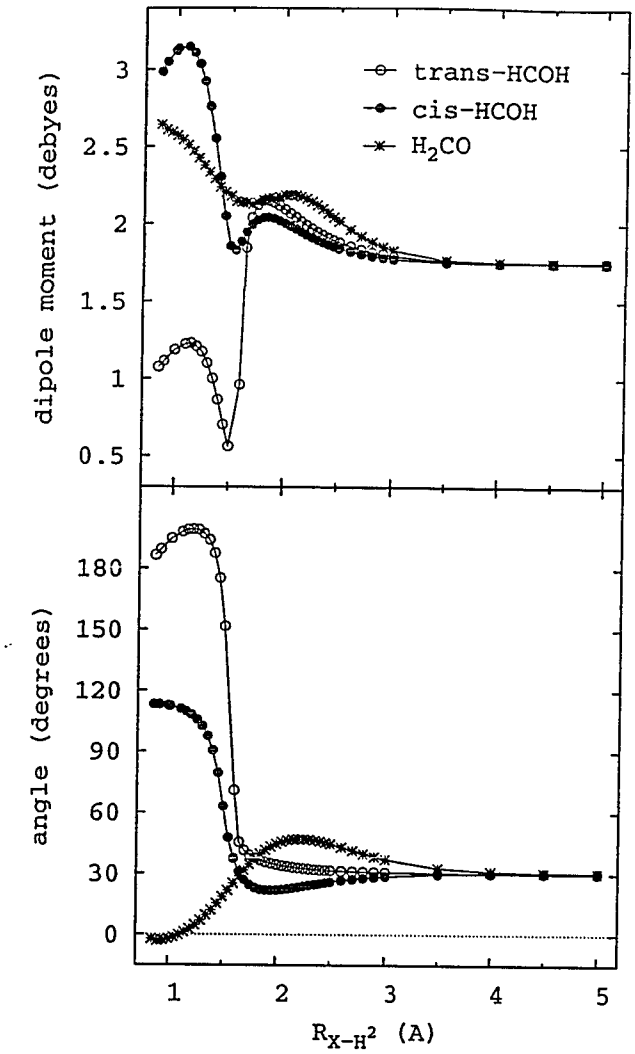

Figure 30. Magnitude and angle, relative to the C-O bond, of the dipole moment for *cis*-HCOH, *trans*-HCOH, and H_2CO. A positive angle corresponds to a clockwise rotation about the z-axis.

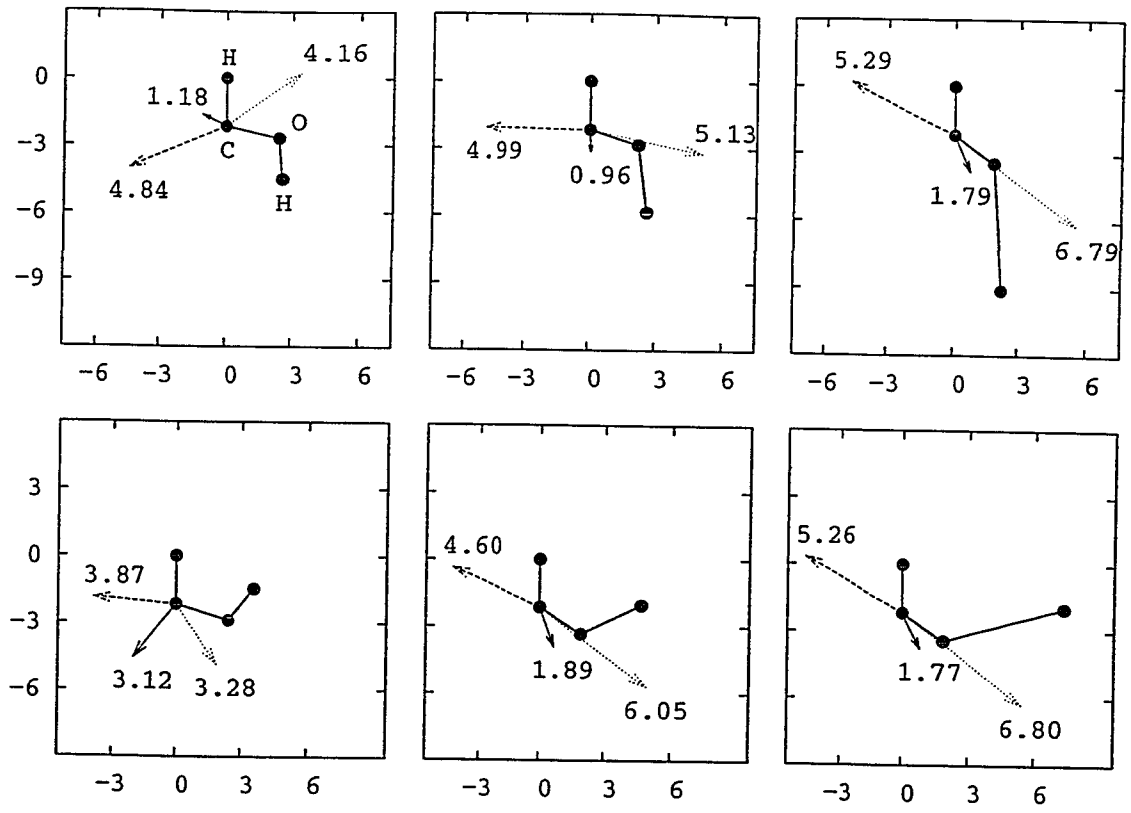

Figure 31. Dipole moment (μ) (solid arrows), its corresponding charge transfer (μ_{ct}) (dotted arrows), and polarization (μ_p) (dashed arrows) components for some selected geometries of *trans*-HCOH in the top row and *cis*-HCOH in the bottom row. Arrows point in the direction of the negative end of the dipole. Magnitudes are shown in atomic units.

It is apparent from Figure 30 and Figure 31 that the *trans* conformer has to undergo greater changes in its dipole moment during dissociation. After the avoided crossing of states, both isomers have very similar dipole moments and proceed to the same limit. Before the avoided crossing of states the magnitude of the dipole moment decreases for both conformers. In the case of *trans*-HCOH, $|\mu|$ is greater than that of the radical and initially moves away from the final value of the formyl radical. On the other

hand, *cis*-HCOH starts with a $|\mu|$ smaller than that of the radical and approaches the final value earlier during the homolysis. Hence, the electronic structures of the crossing electronic states do not properly match for *trans*-HCOH and the isomer is forced to undergo greater adjustments in its charge distribution during the avoided crossing. This is in contrast to the dipole moment of formaldehyde, which decreases smoothly to the common dissociation limit of all three isomers. The energetic cost of these adjustments in the electronic structure, as well as the greater buildup in charge concentrations demonstrated above, result in the occurrence of a transition state for *trans*-HCOH.

Figure 32 and Figure 33 show the evolution of the internal coordinates as a function of the reaction coordinate at the CAS(8,8) level. Similar behaviour was found for the 10,10 active space. As can be seen, the most important changes take place in the vicinity of the avoided crossing. In the case of *trans*-HCOH, these changes occur later and in a narrower interval around the transition state. This is in keeping with a delayed avoided crossing for the *trans* with respect to the *cis* conformer. The decreasing C-O bond distance presented in Figure 10 indicates increasing double bond character, and parallels the increasing electron density at the C-O bond critical point previously discussed (Figure 27). It is interesting to note that the H-C bond distances and the H-C-O bond angles reflect the behaviour observed for the dipole moments (Figure 30), in the sense that the geometry of the *cis*-HCOH carbene approaches that of the radical in the region of the avoided crossing. On the other hand the *trans* conformer does not display this convergent behaviour as a consequence of the differences in the electronic structure of the two states involved in the avoided crossing.

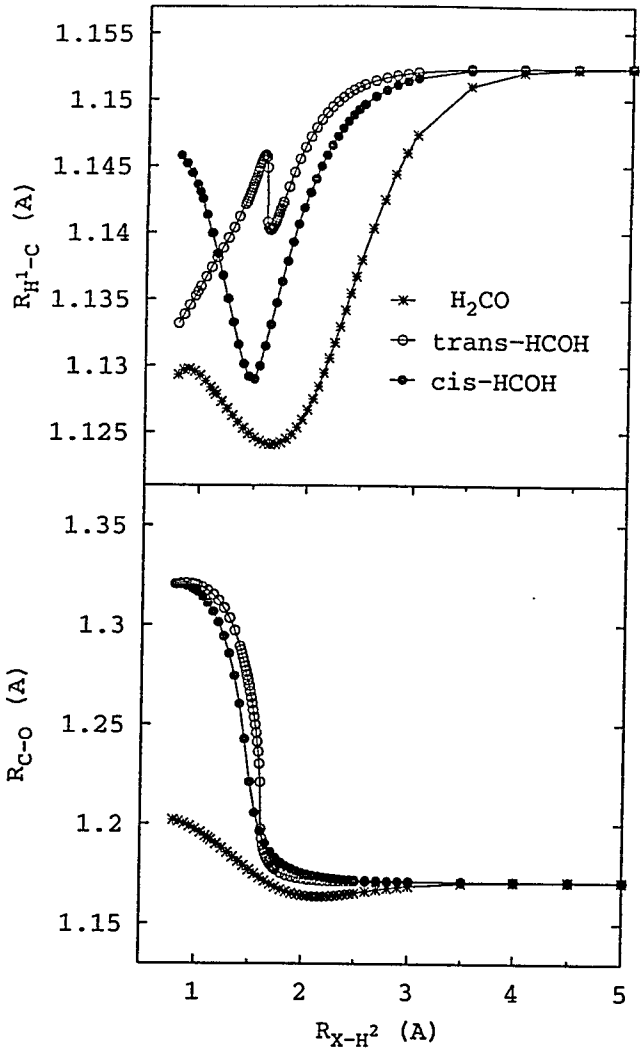

Figure 32. H-C and C-O bond distances versus the reaction coordinate for *cis*-HCOH, *trans*-HCOH and H_2CO at the CAS(8,8) level of theory.

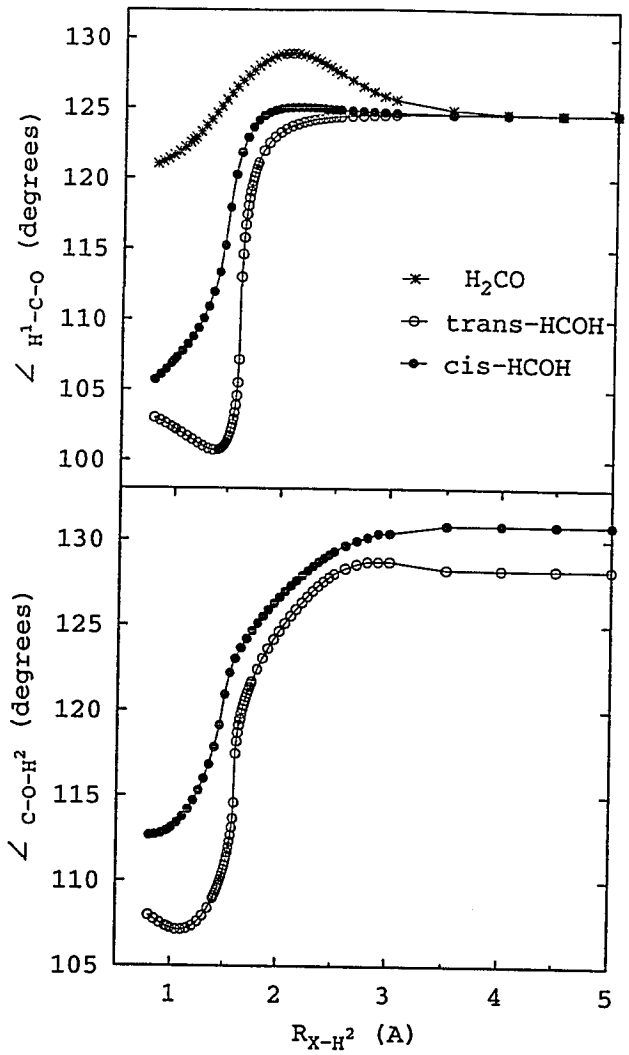

Figure 33. Relevant bond angles in the dissociation of *cis*- and *trans*-HCOH and of H_2CO, versus the reaction coordinate at the CAS(8,8) level of theory.

Homolytic fragmentations of simple molecules generally proceed without a transition state. The homolysis of oxy and dioxycarbenes seems to be an exception to this statement. The comparisons made for the changes in the molecular geometry of the conformers of HCOH during dissociation, along with the behaviour of the electronic structures, provide an explanation as to why there is a transition state for the *trans* and

not for the *cis* conformer. It appears that the necessary changes in electron configuration for the conversion of the carbenes to radicals involve a substantial reorganization of the electron density as described, for example, by its Laplacian and by the analysis of the atomic charges. The analysis of the dipole moment summarizes the changes taking place in the electron density during the homolysis and emphasizes the differences in the electronic structure of the reactant carbene and radical product configurations. In the case of *trans*-HCOH the dipole moments are very different just before and after the avoided crossing of states, resulting in electronic and geometric adjustments, which raise the energy of the homolysis and lead to a transition state. The effect of these electronic and geometric differences is summarized in Figure 34 which shows the correlation diagram for the electronic configurations involved in the homolysis of *cis*- and *trans*-HCOH. The blown-up portion of this figure shows the cross section of the avoided crossing representing a secondary reaction co-ordinate for the homolysis, not described by the O-H bond length. The electronic configurations can be thought of as two valleys. Due to the differences in the electronic structures of these configurations in *trans*-HCOH, and the resulting differences in the geometries (Figure 32 and Figure 33) these valleys are offset from each other. This results in poorer mixing of the reactant and product configurations and leads to an additional barrier for the homolysis of *trans*-HCOH. The transition state observed here for *trans*-HCOH, and probably for w-dihydroxycarbene, studied by Borden,[110] appears to be caused by a mismatch in the electronic structures of the states involved, rather than by an inadequacy of the level of calculation used.

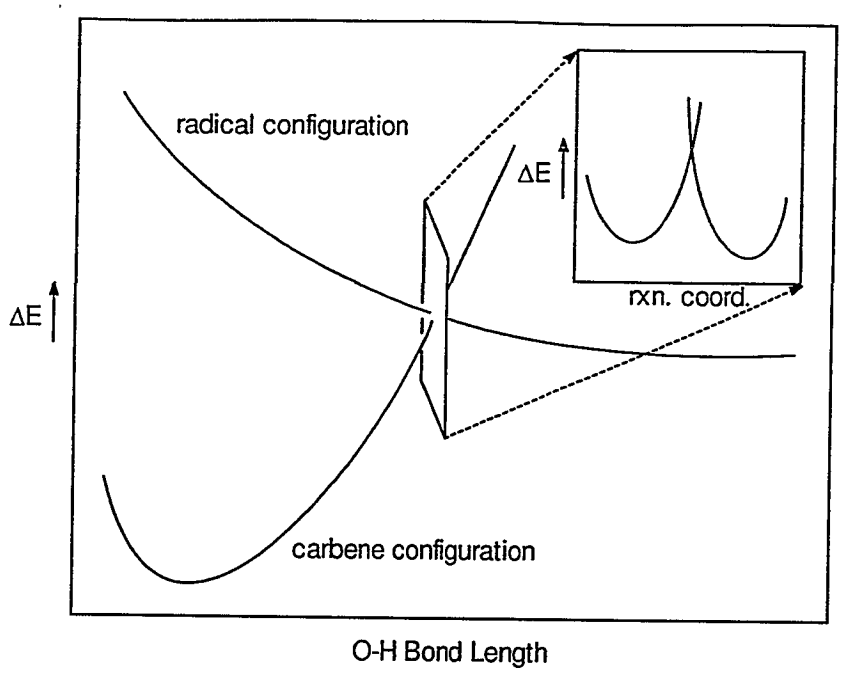

Figure 34. Electronic configuration correlation diagram showing a cross section of the avoided crossing.

Some mention should be made of the possible generality of this reaction. It is clear that homolysis of oxy and dioxycarbenes has been observed a number of times, usually under what would be considered harsh conditions. However, low temperature homolysis of oxycarbenes may also be possible. Consider the fragmentation of a singlet carbene to a carbonyl and an alkyl radical (Figure 35). The valence shell of a carbene carbon has six electrons (a sextet) instead of the preferred octet. The product carbonyl radical, like any carbon centered radical, has seven electrons (a septet) in its valence shell.

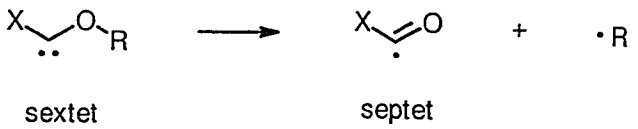

Figure 35. The change in the carbene centre's valence shell from a sextet to a septet upon fragmentation to radicals.

As a result of this difference in the valence shells of carbenes and radicals, a carbene should receive more stabilization from a X type electron donor such as oxygen than the radical (Figure 35). Therefore, replacing an oxygen substituent by hydrogen or an alkyl group should destabilize the carbene relative to the radicals, resulting in a lower dissociation energy. In Section 2.1.1 the homolysis of allyloxyhydroxycarbene (**111**) was shown to have a dissociation energy of 18.55 kcal mol^{-1} at the B3LYP/6-31+G(d) level *without* ZPE (Table 3) (Scheme 53(a)). Replacing the hydroxy group with hydrogen results in a dissociation energy of only 2.36 kcal mol^{-1} for allyloxycarbene (**41**) (Scheme 53(b)).

Scheme 53

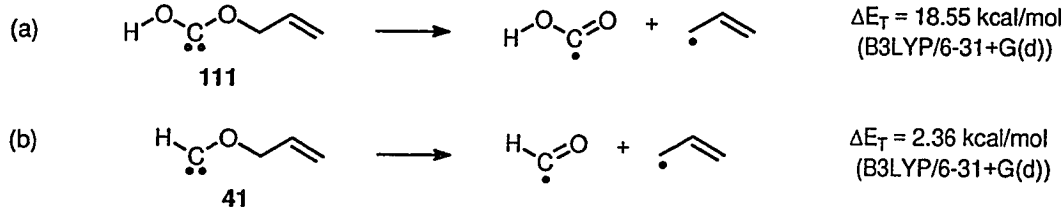

Calculation of the heat of formation for the isodesmic reaction represented by Scheme 54(a) indicates that a phenyl group stabilizes an allyl radical (**114**) by about 7.00

kcal mol^{-1}. Combining this result with the dissociation energy for allyloxycarbene (**41**) results in an estimated dissociation energy of -4.64 kcal mol^{-1} for cinnamyloxycarbene (**115**) (Scheme 54(b)). In other words for this system the fragmentation is about thermoneutral or possibly even exothermic. Interestingly, this would suggest that the cis carbene should not exist since there would be no barrier to homolysis. In any case, it is clear that these fragmentations may be facile reactions for a variety of carbenes.

Scheme 54

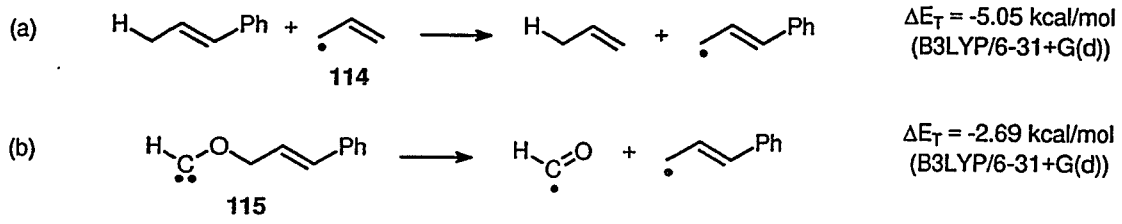

2.2. Reaction of Dioxycarbenes with Carbon Disulfide

2.2.1. Experimental Study of the Reaction of Dioxycarbenes with Carbon Disulfide

The results presented in Chapter 1, Section 1.5.2.3.3 highlight the intense interest that has been generated by the reaction of dioxycarbenes with carbonyl compounds. Initial studies using thiocarbonyl compounds have also been undertaken (Section 1.5.2.3.4). It is clear from this work that nucleophilic carbenes tend to react by stepwise mechanisms involving ionic intermediates. A number of examples were also presented in which carbon disulfide (CS_2) was shown to be an effective trap for diaminocarbenes[161] (**87**) and imidazol-2-ylidenes[162-164] (**88**). The zwitterionic dithioquaternary salts produced

by nucleophilic attack of the carbenes on carbon disulfide often constituted the final product and were themselves found to be good nucleophiles. These results indicate that carbon disulfide should be a good trap for dimethoxycarbene (**1**).

Dimethoxyoxadiazoline (**116**) (0.1 M) was thermolyzed at 110 °C for 24 hours in the presence of a 20 fold excess of carbon disulfide. The reactions were carried out in sealed thermolysis tubes with benzene solvent. Analysis by GCMS indicated one major product resulting from reaction of **1** and carbon disulfide. Careful purification by centrifugal chromatography, using triethylamine as co-elutant, led to the isolation of the primary product in the crude reaction mixture. This product was identified as **117** by ^{1}H NMR, ^{13}C NMR, gradient HMBC, and MS.

Two other products resulting from trapping of **1** with carbon disulfide were also observed in the GCMS. The first, a very minor product with a parent ion of m/z 236 has proven to be quite elusive and remains unidentified. The second, has been identified from the GCMS to be dimethyl thionocarbonate.

With this information a mechanism for the formation of **117** was proposed (Scheme 55). The mechanism suggests initial nucleophilic attack by dimethoxycarbene **1** at the CS_2 carbon to yield a zwitterion (**118**) or dithio-α-lactone (**119**) intermediate. The equilbrium likely lies far on the zwitterion side, as attested by the stable dithioquaternary salts isolated from the reactions of cyclodiaminocarbenes with CS_2.[161,162,164] With a build-up of the zwitterionic intermediate, intermolecular methyl transfers would become possible. Intermolecular methyl transfer is more likely then intramolecular methyl transfer since the five membered transition state required for intramolecular methyl

transfer is unfavourable according to Baldwin's rules.[230,231] Methyl transfer is followed by a second attack by **1** on the dimethyl dithiooxalate (**120**) and [1,2]-thiomethyl migration of **121**. Attack by an additional dimethoxycarbene (**1**) at the thiocarbonyl group of **122** will give the thiirane, **123**. The final product (**117**) could result from sulfur atom transfer from **123** to an additional dimethoxycarbene (**1**) equivalent. A variety of carbenes are known to effect desulfurization of thiiranes.[232,233] Although, dimethoxycarbene (**1**) is known to do this reaction, electrophilic carbenes are known to be more efficient.[232] Although sulfur atom abstraction by **1** does explain the dimethyl thionocarbonate observed in the GCMS it is just as likely that the thiirane **123** loses elemental sulfur. This is an efficient process for thiiranes with radical stabilizing groups.[233] The 35% yield of **117** was calculated to take into account three equivalents of carbene (**1**).

Scheme 55

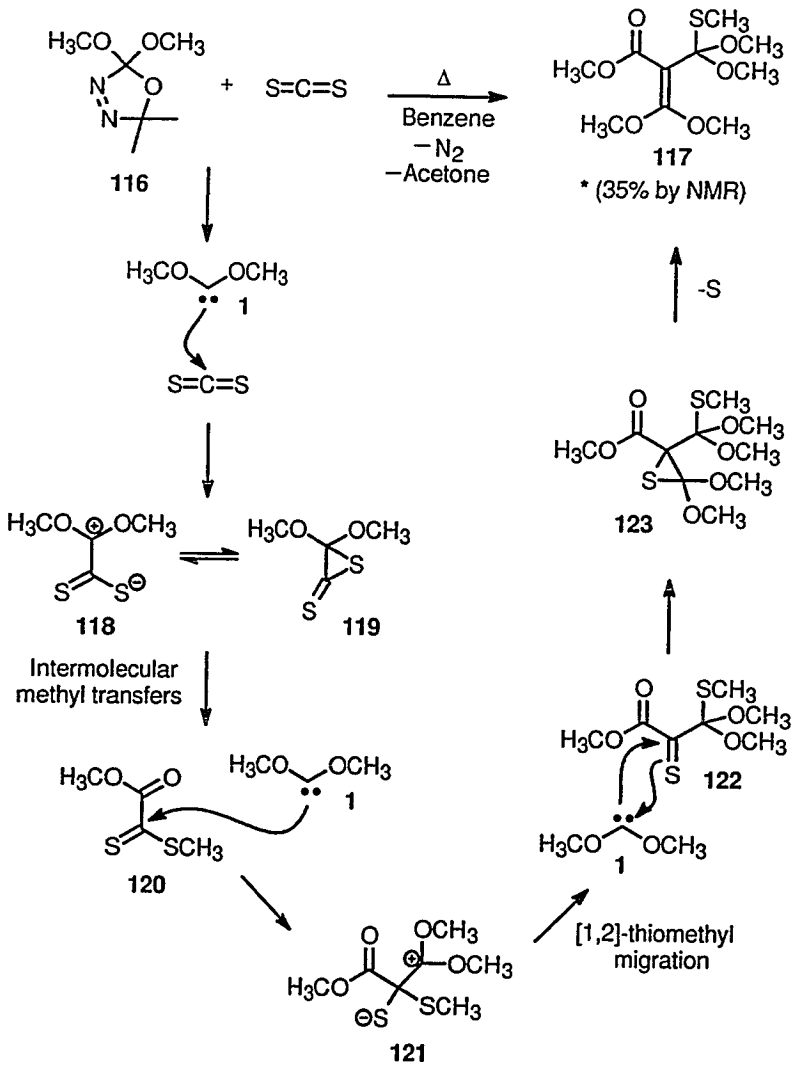

In order to differentiate between inter- and intramolecular methyl transfers for the zwitterion (**118**), a trapping experiment was carried out using trideuteriated dimethoxyoxadiazoline‡ (**124**). Since three dimethoxycarbene (**1**) units are incorporated into the final product (**117**), only D9-product would be expected if the reaction proceeds with intramolecular methyl transfer. However, if the intermolecular methyl transfer

‡ The trideuteriated dimethoxyoxadiazoline (**124**) is easly accessible by the acetoxy-exchange of 2-acetoxy-2-methoxyoxadiazoline with trideuteriated methanol and was supplied by David L. Pole.

mechanism is in operation, D6, D9 and D12-products would be expected in a ratio of 1:2:1 respectively, ignoring kinetic isotope effects. Unfortunately it has never been possible to observe the parent ion (m/z = 266) in the GCMS analysis of the labeled or unlabeled system. For this reason it is necessary to use the m/z = 192 peak which corresponds to loss of a $C(OCH_3)_2$ group that is not involved in the methyl transfers. In a deuteriated sample this ion should show a D3:D6:D9 ratio equivalent to the D6:D9:D12 ratio of 1:2:1 for the intermolecular reaction. The GCMS analysis indicated one peak containing the D3, D6 and D9 isomers. By integrating over different portions of this peak in was possible to identify the three labeled products, indicating that each had slightly different retention times. The different retention times indicate that D3, D6, and D9 isomers are formed during the thermolysis, and not from isomerization of a single D9 molecular ion. By integrating over this peak and comparing the relative intensities of the daughter ions the GCMS analysis showed that the D3:D6:D9 product ratios were 1:1.8:0.8 indicating that methyl transfer was in fact intermolecular.

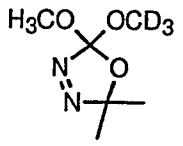

124

2,2-Diphenoxy-Δ^3-1,3,4-oxadiazoline[234] (**125**) was also thermolyzed in the presence of CS_2. Diphenyl thionocarbonate (**126**) was the only CS_2 derived product observed (Scheme 56). It could be formed by initial attack by the nucleophilic diphenoxycarbene (**127**) at the CS_2 carbon to yield a zwitterion (**128**). Since this zwitterion (**128**) has no substituents that can be easily exchanged by nucleophilic

substitution, it has littly else to do but collapse to its dithio-α-lactone isomer (**129**). Eventually this dithio-α-lactone (**129**) could lose CS to give the diphenyl thionocarbonate **126**. This result supports the suggestion that there could be a buildup of the zwitterionic intermediate in the first step of the formation of **117**.

Scheme 56

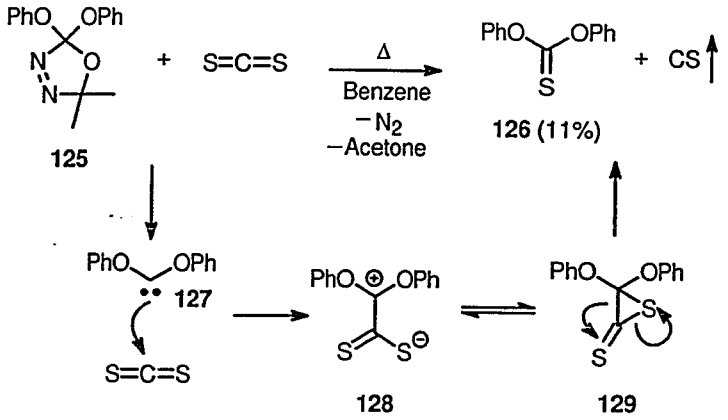

2.2.2. Theoretical Study of the Reactions of Dioxycarbenes with Carbon Disulfude

Theoretical work done in support of these experimental results provided some important insights. The dihydroxycarbene/CS_2 system was used as a model for the dimethoxycarbene (**1**) and diphenoxycarbene (**127**) systems described above. The focus of this research was to examine the behaviour of dihydroxycarbene **2** with CS_2 and to determine if the mechanism proposed in Scheme 56 for the formation of the thionocarbonate (**126**) was reasonable.

Three mechanisms (Scheme 57) for the formation of the diphenyl thionocarbonate (**126**) (Scheme 56) were investigated, allowing for the study of a number of interesting

aspects of the general reactivity of dioxycarbenes with carbon disulfide. This study employed the GAUSSIAN94, Revision E.2, system of programs,[194] using dihydroxycarbene (DHC) (**2**) as a model for dimethoxycarbene (**1**) and diphenoxycarbene (**127**). Räsänen *et al.* have found that for dihydroxycarbene (**2**) the w-conformer is the lowest energy conformer at high levels of theory[17] and this study was confined to the reactivity of this conformer. Electron correlation was included with the Møller-Plesset method with the correlation energy truncated at the second order (MP2). MP2 calculations were run with the frozen core approximation and zero point energies were corrected using a scaling factor of 0.97.[196,197] All calculations were restricted and no symmetry constraints were imposed. The energies are given relative to the sum of the fully optimized free w-dihydroxycarbene (**2**) and carbon disulfide reactants. The text refers to the ΔE_T + ZPE level unless stated otherwise (Table 5). Structural data for the fully optimized stationary points appear in Appendix I.

Scheme 57

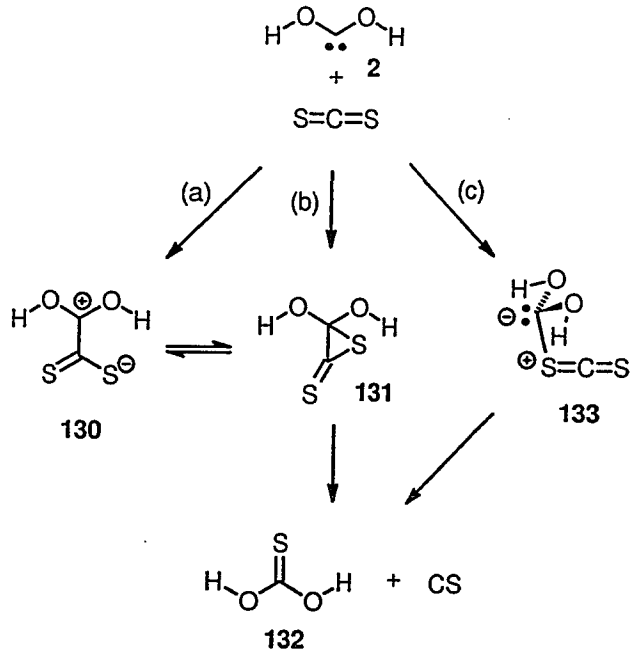

Scheme 57(a) and (b) differ only in the initial attack on carbon disulfide. Path (a) involves initial nucleophilic attack by dihydroxycarbene (**2**) at the sp carbon to give the zwitterionic intermediate (**130**) followed by ring closure to the 3,3-dihydroxy dithio-α-lactone **131.** This dithio-α-lactone may subsequently lose carbon monosulfide to give thionocarbonic acid (**132**). Attack at the CS_2 carbon was investigated by optimizing the zwitterion (**130**), which was found to be planar, and stretching the C-C bond. In this way a planar transition state (**TS5**) was located for nucleophilic attack of w-DHC at the sp carbon of CS_2. Note, however that this transition state does not have C_{2V} symmetry. The O-C-C and S-C-C angles differ by 8.0° and 2.9° respectively. It appears that **TS5** is a rather loose transition state and bends to take advantage of a sulfur/hydrogen interaction. Attempts to obtain a transition state of higher symmetry were unsuccessful. The barrier

for the nucleophilic attack was 4.97 kcal mol^{-1} at the MP2 level of theory while the zwitterion (**130**) itself was found to lie 26.36 kcal mol^{-1} below the sum of the reactants, dihydroxycarbene + CS_2 (Table 5). A similar reaction path was studied by Bock and Redington for the decomposition of oxalic acid (Section 1.5.2.3.4).[160] They located a zwitterion (**85**) corresponding to **130** for the reaction of dihydroxycarbene (**2**) with carbon dioxide which was 10.2 kcal mol^{-1} more stable than the free dihydroxycarbene and CO_2 at the MP2/6-31G*(5d)//HF/6-31G level of theory. Although a direct comparison cannot be made, the CS_2 analogue, **130**, appears to be considerably more stable than **85**. They also located a planar transition state (**86**) for the fragmentation of zwitterion **85** to dihydroxycarbene **2** and carbon dioxide which corresponded to **TS5**. This transition state (**86**) was only 11.0 kcal mol^{-1} higher in energy than the zwitterion and 0.7 kcal mol^{-1} above the free carbene **2** and carbon dioxide at the MP2/6-31G*(5d)//HF/6-31G level of theory.

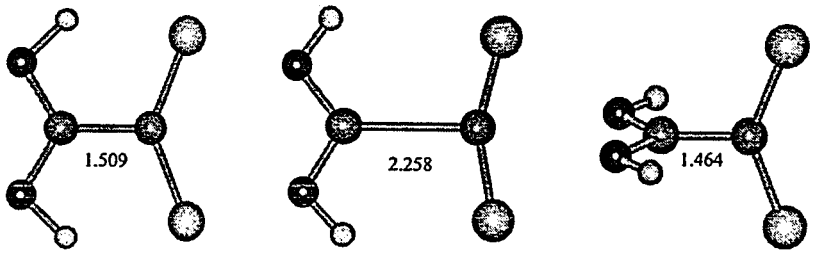

Figure 36. Geometries for the zwitterion **130**, the transition state **TS5** for nucleophilic attack at the CS_2 carbon by **2**, and the transition state **TS6** for rotation about the zwitterionic C-C bond. C-C bond lengths (Å) are included.

Table 5. Energies, relative to free w-dihydroxycarbene (**2**) + carbon disulfide, in kcal mol^{-1} for the stationary points at the MP2(FC)/6-31+G(d) level.

Isomer	ΔE_T	ΔE_T + ZPE
Zwitterion (**130**)	-22.10	-26.36
TS5	10.38	4.97
Dithio-α-lactone (**131**)	-8.29	-12.57
TS6	-8.06	-11.60
TS8	30.42	24.59
Thiocarbonyl ylide (**133**)	24.09	18.94
TS9	24.10	18.77
TS10	30.53	25.00
$(HO)_2CS$ (**132**) + CS	10.38	4.43

[a] For free w-DHC (**2**) + CS_2 in hartrees; ΔE_T = -1022.450324, ΔE_T + ZPE = -1022.401993.

The transition states discussed above for the reaction of the heterocumulenes, CS_2 and CO_2, with dihydroxycarbene **2** are quite different than those located in the past for nucleophilic carbene attack on non-cumulated carbonyl compounds.[156-159] In the few examples that have been studied, nucleophilic addition of carbenes to carbonyl compounds has been found to occur through a concerted cycloaddition (Section 1.5.2.3.3). These results suggest a second mode of attack on CS_2, represented by Scheme 57, path (b), which was also considered. This pathway involves the possible concerted attack of **2** on one of the C=S double bonds of CS_2 to form the dithio-α-lactone (**131**). For this analysis a new approach was required. Using mixed internal and Cartesian coordinates[235], the dithio-α-lactone (**131**) was optimized with a "dummy atom"[235] (X) fixed 0.5 Å below the midpoint of the thiirane C2-S1 bonds as in Figure 37. The dithio-α-lactone (**131**) was found to be 12.57 kcal mol^{-1} more stable than the free carbene (**2**) and CS_2. The X-C3 distance was then increased while optimizing all dithio-α-lactone

parameters. A transition state for concerted attack of dihydroxycarbene on a C=S double bond could not be located. Instead, the dithio-α-lactone (**131**) structure opened to a twisted zwitterionic structure which rotated about the C-C bond to give the planar zwitterion (**130**).

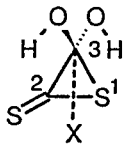

Figure 37. Representation of the dithio-α-lactone (**131**) showing the position of the dummy atom (X) for the study of cycloaddition represented in path (b), Scheme 57.

Analysis of the C-C bond rotational barrier for the zwitterionic intermediate (**130**) led to the location of a transition state (**TS6**) for C-C bond rotation that was 14.76 kcal mol^{-1} above the energy of the planar zwitterionic geometry (**130**). Thus, the twisted zwitterion transition state (**TS6**) was only 0.97 kcal mol^{-1} higher in energy than the dithio-α-lactone (**131**). Unfortunately, it was not possible to locate a transition state (**TS7**) for the ring opening of the dithio-α-lactone to the twisted zwitterions. However, the barrier for this process is undoubtedly very small.

It seems that the planar zwitterion (**130**) represents an energy well for the free carbene (2) and CS_2, resulting in a planar transition state (**TS5**) for attack at carbon. Although direct nucleophilic attack at the sp carbon, path (a), Scheme 57, is preferred over the concerted cycloaddition (Scheme 57, path (b)) the dithio-α-lactone (**131**) is accessible by C-C bond rotation of the zwitterion (**130**) and ring closure. Once **131** is

formed, it could potentially lose carbon monosulfide by a concerted cycloreversion or a stepwise mechanism. To investigate this cycloreversion, the dithio-α-lactone (**131**) was optimized using mixed internal and Cartesian coordinates[235] with a "dummy atom"[235] (X) fixed 0.5 Å below the midpoint of the thiirane C3-S1 bonds as shown in Figure 38. In this case a transition state (**TS8**) was located for a concerted cycloreversion of the dithio-α-lactone (**131**) with a barrier of 37.57 kcal mol^{-1} above **131**. The final products, thionocarbonic acid (**132**) and CS have a total energy of 4.43 kcal mol^{-1} above the reactants, dihydroxycarbene (2) and CS_2.

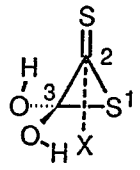

Figure 38. Representation of the dithio-α-lactone (**131**) showing the position of the dummy atom (X) used to study the loss of carbon monosulfide, path (b), Scheme **57**.

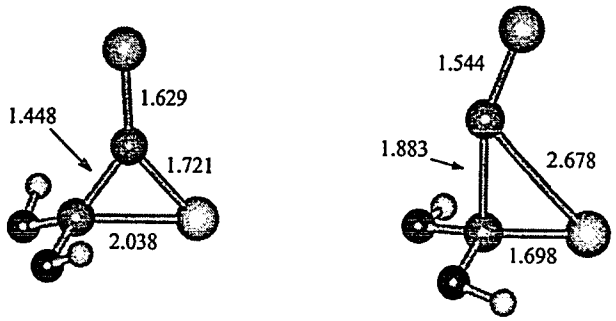

131 **TS8**

Figure 39. Geometries for the α-dithiolactone (**131**) and the loss of CS (**TS8**) with important bond lengths (Å).

Path (c), Scheme 57, represents an alternative pathway to thionocarbonic acid (**132**) involving electrophilic attack of the dihydroxycarbene (**2**) at the sulfur of carbon disulfide. In this initial study electron correlation was included using the MP2 method, which has been found to be sufficient for the location of carbonyl ylides in the past.[157,236] However, these ylides can have significant diradical character[157,237-239] and higher levels of electron correlation may be required to obtain accurate energies.[157] It was possible to locate an apparent intermediate **133** on this reaction path, resulting from electrophilic attack of **2** on sulfur, although it lies 18.94 kcal mol^{-1} above the reactants. However, examination of the transition state (**TS9**) energies for the formation of this ylide indicates that it represents a minimum on the enthalpy surface only, and that with the inclusion of the ZPE **133** has no barrier to fragmentation back to reactants, **2** and CS_2. Of course these are gas phase results and in solution structure **133** may be stabilized enough to be a real intermediate. It is interesting to note the SCSC backbone of this "intermediate" does not represent a plane of symmetry and has a dihedral angle of 5.9°. Lowering the geometric cutoffs did not result in a planar structure. In fact, imposing symmetry resulted in a structure which was higher in energy than the twisted thiocarbonyl ylide (**133**). This thiocarbonyl ylide (**133**) is also very different than other carbonyl or thiocarbonyl ylides located in the past which prefer planar geometries.[30,237,238,240,241] In this case the OCO plane is virtually perpendicular to the SCS plane. Furthermore, the former carbene carbon is sp^3 hybridized. It was not possible to locate any structure corresponding to the more traditional planar carbonyl or thiocarbonyl ylides. Planar ylides are normally stabilized by electron withdrawing groups at one end and electron donating groups at the

other, a form of stabilization referred to as push-pull stabilization.[237] In the absence of electron withdrawing groups, electron donating groups offer very little stabilization to ylides[236,237] and may even destabilize them.[157] The ylide (**133**) located here is also a member of a relatively new class of *cumulated* ylides.[239]

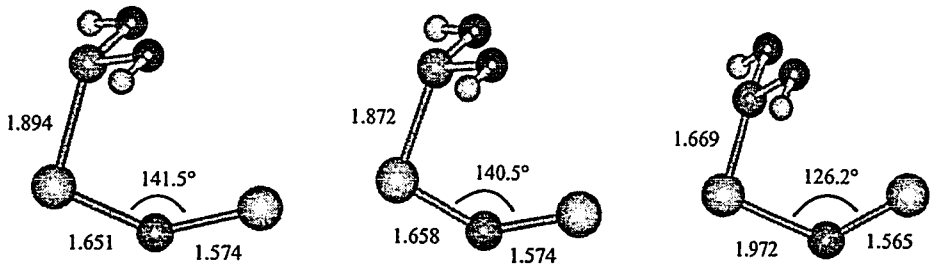

TS9 **133** **TS10**

Figure 40. Geometries for the ylide **133** and the related transition states, **TS9** and **TS10**, with important bond lengths (Å) and angles.

Stretching the C=S bond allowed for the location of the fragmentation transition state (**TS10**), which was 6.06 kcal mol^{-1} above the thiocarbonyl ylide **133** but 25.00 kcal mol^{-1} above the w-hydroxycarbene (**2**) and CS_2.

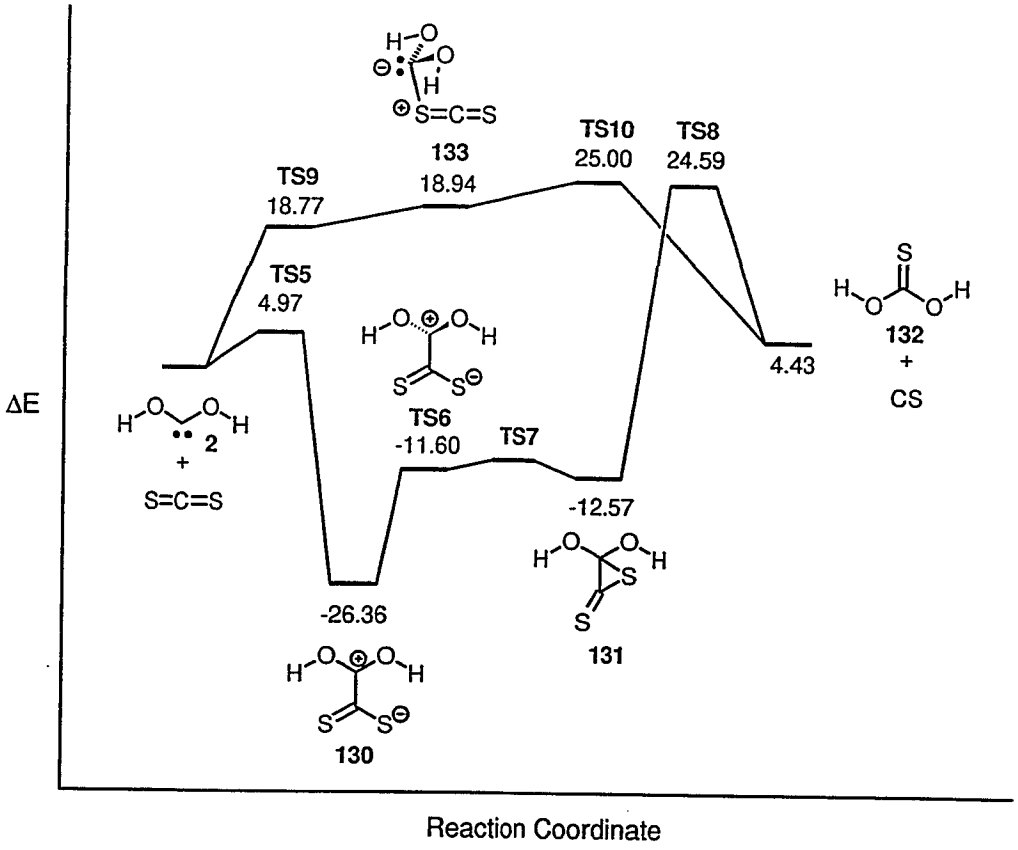

Figure 41. Schematic representation of the reaction coordinate (kcal mol^{-1}) for the reaction of dihydroxycarbene (**2**) with CS_2 at the MP2(FC)/6-31+G(d) + ZPE level.

Clearly an important element mediating the chemistry of nucleophilic carbenes with carbon disulfide, in the absence of other traps, is the presence of exchangable groups on the carbene. These groups provide the zwitterionic intermediates with a path to neutral products. It is also apparent that the thiocarbonyl intermediates formed in the reaction of CS_2 with dimethoxycarbene (**1**) are very susceptible to additional nucleophilic attacks by dimethoxycarbene, leading to some very interesting chemistry. The theoretical results strongly suggest a planar attack for the formation of the zwitterionic intermediate. This intermediate also represents a rather stable structure, which is highly favoured over

the dithio-α-lactone, in agreement with previous experimental results that show that dithioquaternary salts formed in the reaction of cycloaminocarbenes with CS_2 can be isolated.[161,162,164] Of the two mechanisms considered here for the formation of the O,O-thiocarbonates and CS, it is not clear if path (a) or (c), Scheme 57, would be preferred. The results of trapping dimethoxycarbene with CS_2 indicate that there is a buildup of the zwitterionic intermediate **118** (Scheme 55). Given that restriction, both path (a) and (c), Scheme 57, have equal energy requirements from the zwitterion.

Chapter 3

Summary and Conclusions

The goal of the first half of this research was to provide computational support for the unexpected observation of a homolytic fragmentation mechanism for the rearrangement of allyloxymethoxycarbenes. The work presented here provides strong support for a homolysis mechanism from the singlet ground state and led to a unique study in which the Theory of Atoms in Molecules was used to isolate the factors influencing the homolysis. This research presented an opportunity to explore the nature of transition states themselves and provided important insights into the homolysis mechanism. The dioxycarbene trapping studies performed with CS_2 hint at the rich chemistry possible with thiocarbonyl compounds, while the theoretical work performed in support of these results also indicates the rather unique nature of the dioxycarbene/CS_2 interactions.

3.1. Homolytic Fragmentations of Oxycarbenes

3.1.1. **Homolysis of Allyloxyhydroxycarbene. A Density Functional and Ab Initio Study**

In this study four mechanisms for the formation of esters from allyloxymethoxycarbenes (**36**) were investigated computationally (Section 2.1.1, Scheme 50). The concerted [1,2]-migration was shown to have a relatively high activation energy

(Table 3) due to the antiaromatic component (Figure 19) of the transition state (Figure 18, **TS2**). The [2,3]-sigmatropic rearrangement was also modelled and Rautenstrauch type transition states (Figure 20, **TS3**) were located. Owing to the aromatic character of the transition state a very low activation energy was observed, about half that of the [1,2]-allyl migration. Consistent with the experimental results, which implicated radicals in the formation of esters, the theoretical results suggest that the experimentally observed product ratios cannot be explained in terms of competing concerted [1,2]-migrations and [2,3]-sigmatropic rearrangements. In agreement with previous workers the singlet-triplet gap for allyloxyhydroxycarbene was also found to be prohibitively large (Table 2). This result indicated that the triplet state could not be populated in competition with the [2,3]-sigmatopic rearrangement or even the [1,2]-migration and a β-scission to radicals from the triplet state was ruled out. However the dissociation energy for the formation of the hydroxycarbonyl and allyl radicals from allyloxyhydroxycarbene was found to be very low, on the same order or possibly even lower in energy than the concerted [2,3]-sigmatropic rearrangement (Table 3).

Given the known entropic effect on [2,3]-Wittig rearrangements of allyl substituted ethers,[183,208,209] it seems likely that the homolysis from the singlet ground state should dominate the thermochemistry of allyl substituted dioxycarbenes.

3.1.2. Hydroxycarbene as a Model for the Homolysis of Oxy and Dioxycarbene

The homolysis of oxycarbenes was studied in detail using hydroxycarbene as a model for oxycarbenes (Section 2.1.2). Using high level complete active space and

multireference configuration interaction methods a transition state was located for the fragmentation of *trans*-hydroxycarbene (Table 4), in agreement with Borden's CISD results[110] for w-dihydroxycarbene. The transition state for the homolysis of these oxycarbenes could be rationalized by a valence-bond configuration mixing model which suggested the existence of an avoided crossing for this fragmentation (Figure 24). However this first order analysis could not explain the absence of a transition state for the homolysis *cis*-HCOH. State-averaged CAS calculations provided support for the prediction of an avoided crossing in the homolysis of *trans*- and *cis*-HCOH between a carbene n^2 electronic configuration and a radical $n^1\sigma^1$ electronic configuration. Analysis of the dipole moments at each step along the reaction coordinate (Figure 30) for *cis*-HCOH indicated a good match in the electronic structures of the carbene and radical configurations in the region of the avoided crossing. This match allows for efficient mixing of the electronic configurations. For the homolysis of *trans*-HCOH the evolution of the dipole moment over the reaction coordinate indicates a mismatch in the electronic structure of the carbene and radical configurations in the region of the avoided crossing. This mismatch of the electronic configurations was traced to the differences in the dipole moments of the *cis* and *trans*-HCOH conformers at their equilibrium geometries. These differences in the carbene and radical electronic configurations of *trans*-HCOH impose the requirement for major electronic and geometric adjustments in the region of the avoided crossing (Figure 34). The poor mixing of the electronic configurations results in a delay as the ground state moves from one configuration to the next and explains the buildup of the atomic charges along the reaction coordinate. The buildup of atomic

charges, combined with the necessary adjustments in the geometric and electronic structure raise the energy of the system, resulting in a transition state for *trans*-HCOH.

Theoretical results were also presented which suggest that oxycarbenes with the proper substitutent groups could fragment at much lower temperatures than has been observed in the past for dioxycarbenes. In fact initial experiments by the Warkentin group indicate that cinnamyloxyphenylcarbene, generated by the diazirine method, fragments to radicals at room temperature.[242] However, attempts to study the rate of this homolysis using laser flash photolysis techniques were unsuccessful, in that no radicals were detected on the LFP time scale. Replacing the phenyl group by a methyl substituent may increase the fragmentation rate constant. Furthermore, Moss has been able to observe separate absorptions for *cis* and *trans*-methoxymethylcarbene.[73] This raises the interesting possibility of observing unique rate constants for the different conformations.

The detailed analysis of these simple oxycarbene systems presented here may also offer some insight into the more complex, stepwise Wittig rearrangements of deprotonated ethers. Recently, computational work has appeared in which avoided crossings, similar to those discussed here for oxycarbenes, have been observed in the homolysis of deprotonated ethers.[187] These studies have been greatly complicated by the counter ions. Research on the Wittig rearrangement may benefit from an analysis similar to the one conducted here and from comparison to the simple hydroxycarbene system presented in this work. The hydroxycarbene results also suggest the power of applying the theory of atoms in molecules (AIM) in conjuction with models such as the VBCM

model to complicated chemical transformations. A number of studies of reactivity could benefit from this rigorous approach.

3.2. Reactions of Dioxycarbenes with Carbon Disulfide

3.2.1. Experimental Study of the Reactions of Dioxycarbenes with Carbon Disulfide

The reaction of dimethoxycarbene (**1**) with CS_2 resulted in a complicated series of reactions, which suggested the participation of zwitterionic and dipolar intermediates. Using deuterium labeling experiments, it was shown that the initially formed zwitterionic intermediate (**118**) underwent intermolecular methyl transfers. The resulting thiocarbonyl group is apparently quite reactive and undergoes subsequent nucleophilic attack followed by a [1,2]-thiomethyl rearrangement to recover a thiocarbonyl group. A final dimethoxycarbene addition to the thiocarbonyl group followed by loss of sulfur from the thiirane ring, gives the final product (**117**). This is a surprisingly complicated series of reactions, considering the simplicity of the starting materials. The apparent reactivity of the thiocarbonyl intermediates, **120** and **122**, also suggest that thiocarbonyl groups deserve further study.

3.2.2. Theoretical Study of the Reactions of Dioxycarbenes with Carbon Disulfide

In this study dihydroxycarbene (**2**) was used to model the interactions of dioxycarbenes with carbon disulfide. A transition state (**TS5**) was located for direct nucleophilic attack by dihydroxycarbene at the CS_2 carbon to yield a zwitterionic

intermediate (**130**). This result is in agreement with results obtained by Bock and Redington for the interactions of dihydroxycarbene with CO_2.[160] Although the dithio-α-lactone (**131**) was accessible by ring closure of **130**, no evidence was found for a concerted cycloaddition of dihydroxycarbene (**2**) to a CS_2 double bond. The lack of a concerted cycloaddition emphasizes the differences between the cumulated thiocarbonyl, CS_2 system, and the non-cumulated carbonyl systems studied in the past.[156-159]

The presence of a dithio-α-lactone on the reaction coordinate may explain the observation of the thionocarbonate (**126**) observed in the reaction of diphenoxyoxadiazoline (**125**) with CS_2 (Section 2.2.1). A transition state was located for the fragmentation of the dithio-α-lactone **131** to thionocarbonic acid (**132**) and carbon monosulfide. This transition state (**TS8**) represented a rather asynchronous but concerted cycloreversion. Although the barrier for this fragmentation was high, it could be a viable pathway in the absence of other alternatives as in the case of the reaction of diphenoxycarbene (**127**) with carbon disulfide.

An initial investigation of the possibility of ylide formation between **2** and CS_2 was also undertaken. A potential thiocarbonyl ylide intermediate was located, resulting from elecrophilic attack of dihydroxycarbene (**2**) at a CS_2 sulfur atom centre. This thiocarbonyl ylide (**133**) represented a high energy intermediate on the reaction coordinate which had a minimal barrier to fragmentation back to the carbene (**2**) and CS_2. There was also a low barrier from this intermediate (**133**) to thionocarbonic acid (**132**) and carbon monosulfide. It was not possible to distinguish between Paths (a) and (c) of Scheme 57 for the formation of thionocarbonates.

Chapter 4

Experimental

General Methods. NMR spectra were recorded on a Bruker DXR-500 or AC-200 spectrometer. Chemical shifts for ^{1}H NMR spectra were measured using C_6H_6 (δ = 7.15) or $CHCl_3$ (δ = 7.24) as internal references, while ^{13}C NMR spectra were referenced to the chloroform-*d* triplet (δ = 77.0) or benzene-d_6 triplet (128.0). Mass spectra were recorded on a Hewlett Packard MSD GCMS. FTIR spectra were obtained with a Bio-Rad, FTS-40 instrument. Benzene and THF were distilled from sodium/benzophenone ketyl, carbon disulfide was distilled from anhydrous calcium chloride, and hexanes were distilled, removing the first and last fractions.

4.1. Preparation of 2,2-Dioxy-Δ^3-*1,3,4*-Oxadiazolines

2,2-Dimethoxy-Δ^3-1,3,4-oxadiazoline (116). Compound **116** was prepared by the oxidation of the (methoxycarbonyl)hydrazone of acetone with lead tetraacetate[83] or iodobenzene diacetate[243] in methanol solvent according to previously published methods, or by the acetoxy exchange method.[84]

2-Diphenoxy-Δ^3-1,3,4-oxadiazoline (125). Compound **125** was produced by acetoxy exchange of 2-acetoxy-2-phenoxy-Δ^3-1,3,4-oxadiaxoline **134.** The

acetoxy(phenoxy)oxadiaxoline **134** was prepared by adding lead tetraacetate ($Pb(OAc)_4$) (12.69 g, 28.62 mmol, 1.0 M) and methylene chloride (10 mL) to a 100 mL two-neck flask under nitrogen. This mixture was stirred and cooled in an ice bath. Using a dropping funnel (phenoxycarbonyl)hydrazone of acetone (**135**) (5.0 g, 26.00 mmol, 0.9 M) was added slowly over 20 minutes in methylene chloride (20 mL). During this addition the solution turned from yellow to brown. The solution was stirred for an additional 2h during which time the ice bath was allowed to melt. A small amount of brown precipitate was observed. Water (~10 mL) and CH_2Cl_2 (~10 mL) were added to the reaction mixture which was then was filtered through a Celite pad. The filtrate was washed with sodium bicarbonate (5% w/v) until the bubbling stopped and extracted with CH_2Cl_2. The extract was dried over anhydrous $MgSO_4$, filtered and concentrated. This produced 4.48 g of a mixture containing 58% of **134** and 42% of an acyclic side product ($PhOCON{=}NC(CH_3)_2OAc$) **136**. ^1H NMR of **134** and **136** (200 MHz, $CDCl_3$) δ: 1.347 (s, 3H, CCH_3 (**134**)), 1.661 (s, 3H, CCH_3 (**134**)), 1.710 (s, 6H, $C(CH_3)_2$ (**136**)), 2.097 (s, 3H, $OCOCH_3$ (**134**)), 2.017 (s, 3H, $OCOCH_3$ (**136**)), 7.278 (m, HArO (**134** and **136**)). A typical procedure for the synthesis of **125** involved charging a 50 mL round bottom flask with a mixture of **134** (57%) and **136** (43%) (1.05 g which equals 0.60 g, 2.39 mmol, 0.3 M of **134**), phenol (0.412 g, 4.378 mmol, 0.5 M), a catalytic amount of trifluoroacetic acid (0.06 mL, 0.74 mmol) and CH_2Cl_2 (8.5 mL). The solution was stirred for 24 h at room temperature. Aqueous NaOH (10 mL, 10% w/v) was then added to the solution and left to stir for 3 h. The solution was extracted with CH_2Cl_2 and water. The extract was then filtered, dried ($MgSO_4$) and concentrated to give **125** (51%) as a light yellow oil

which was pure by ^{1}H NMR. ^{1}H NMR **125** (200 MHz, $CDCl_3$) δ: 1.227 (s, 6H, $C(CH_3)_2$), 7.224 (m, 10H, OPh); ^{13}C NMR (50.323 MHz, C_6D_6) δ: 23.6 ($C(\underline{C}H_3)_2$), 121.5 (Ar), 122.2 (Ar), 125.0 (Ar), 129.1 (Ar), 136.1 ($\underline{C}(CH_3)_2$), 151.7 ($\underline{C}(OPh)_2$); IR (CCl_4) cm^{-1}: 3071m, 3047m, 2996m, 2941w, 1939w, 1785s, 1594s, 1492s, 1459m, 1384w, 1370w; MS (EI) m/z: 284 (M^+, not observed), 215 (11%), 191 (M- OPh, 100%), 135 (37%), 119 (78%), 105 (46%), 77 (Ph, 43%).

(Phenoxycarbonyl)hydrazone of acetone **(135).** Phenyl hydrazinocarboxylate **137** (5.74 g, 37.7 mmol) and $NaSO_4$ (~6 g) was stirred in acetone (150 mL) for 12 h. The crude reaction mixture was filtered and concentrated to give pure **135** (6.87 g, 35.7 mmol, 95%). ^{1}H NMR (200 MHz, $CDCl_3$) δ: 1.903 (s, 3H, CH_3), 2.103 (s, 3H, CH_3), 7.188 (m, 3H, *o*- and *p*-HAr), 7.379 (m, 2H, *m*-HAr), 7.773 (s, 1H, H-N); MS (EI) m/z: MS (EI) m/z: 192 (M^+, 2%), 98 (M-HOPh, 30%), 94 (HOPh, 100%), 66 (22%), 65 (20%), 56 ($N=C(CH_3)_2$, 13%); MS (CI, NH_3) m/z: 210 $(M+NH_3)^+$, 193 $(M+H)^+$.

Phenyl hydrazinocarboxylate **(137).** Compound **137** was prepared according to previously published methods.[244] ^{1}H NMR **137** (200 MHz, $CDCl_3$) δ: 3.878 (s, 2H, NH_2), 6.403 (s, 1H, NH), 7.261 (m, 5H, ArH).

4.2. Reactions with Carbon Disulfide

Typical procedure for the thermolysis of 2,2-dimethoxy-Δ^3-1,3,4-oxadiazoline (116) in the presence of carbon disulfide (CS_2). A thermolysis tube (50 mL) was charged

with a solution of CS_2 (3.811 g, 50.05 mmol, 2.0 M) and 2,2-dimethoxy-Δ^3-1,3,4-oxydiazoline (0.409 g, 2.55 mmol, 0.1 M) in dry benzene (25mL). Following three freeze-pump-thaw cycles the thermolysis tube was sealed and placed in a thermolysis bath at 110 ± 0.1 °C for 24h at which point it was cooled and opened. GCMS of the crude reaction mixture indicated the presence of dimethyl thionocarbonate, the product **117**, and a very minor amount of an unknown. GCMS (dimethyl thionocarbonate) (ei) m/z (rel. intensity): 106 (M^+, 52), 75 (M^+-CH_3O, 35), 61 (54), 59 (39), 47 (85), 45 (100), 29 (44); GCMS (unknown) (ei) m/z (rel. intensity): 236 (27), 177 (100), 121 (46), 117 (25), 105 (57), 103 (25), 59 (94), 58 (22), 45 (19), 29 (20). Following evaporation of the solvent, **117**, a yellow oil was isolated by centrifugal chromatography using a 1mm silica gel plate. Solutions of ethyl acetate (0-20%), and hexanes, with 1% triethylamine, were used as the eluting solvents. ^{1}H NMR **117** (500 MHz, C_6D_6) δ: 2.026 (s, 3H, SCH_3), 3.162 (s, 3H, OCH_3), 3.384 (s, 6H, thioorthoformate-OCH_3), 3.521 (s, 3H, $COOCH_3$), 3.580 (s, 3H, OCH_3); ^{13}C NMR (125 MHz, C_6D_6) δ: 13.5 (SCH_3), 51.1(OCH_3), 51.6 (thioorthoformate-OCH_3), 55.4 (OCH_3), 61.3 (OCH_3), 125.8 ($\underline{C}(OCH_3)_2(SCH_3)$), 167.5 (C=O), 174.2 ($\underline{C}(OCH_3)_2$); Gradient HMBC (500 MHz, C_6D_6) was consistent with these assignments. IR (Neat) cm^{-1}: 2991w, 2905m, 2838w, 1743m (C=C), 1700s (C=O), 1549s, 1494m, 1433m, 1292s, 1274s, 1194s, 1092s, 1068s, 997w, 952w, 854w, 777w; MS (EI) m/z: 266 (M^+, 4%), 251 (M-CH_3, 9%), 237 (3), 192 (M-$C(OCH_3)_2$, 2), 177 (4), 161 (M-$C(OCH_3)_3$, 8), 121 ($C(OCH_3)_2(SCH_3)$, 100), 105 ($C(OCH_3)_2$, 58), 75 ($O{=}CSCH_3$, 24), 58 ($O{=}COCH_3$, 27), 45 (3); MS (CI, NH_3) m/z: 267 (M+H).

Thermolysis of 2-methoxy-2-trideuteromethoxy-Δ^3-1,3,4-oxadiazoline (124) in the presence of carbon disulfide. A thermolysis tube (20 mL) was charged with a solution of CS_2 (0.941 g, 12.4 mmol, 2.0 M) and 2-methoxy-2-trideuteromethoxy-Δ^3-1,3,4-oxadiazoline **(6)** (0.108 g, 0.662 mmol, 0.11 M) in dry benzene. Following three freeze-pump-thaw cycles the thermolysis tube was sealed and placed in a thermolysis bath at 110 ± 0.1 °C for 24h at which point it was cooled and opened. Analysis of the crude reaction mixture by GCMS indicated that the D6, D9 and D12 analoges of **117** were formed. GCMS (ei) m/z (abund.) 195 (M^+, 1798), 198 (M^+, 3276), 201 (M^+, 1452).

Thermolysis of 2,2-diphenoxy-Δ^3-1,3,4-oxadiazoline (10) in the presence of carbon disulfide. A medium walled NMR tube was charged with a solution of CS_2 (38.07 mg, 0.5 mmol, 1.0 M) and 2,2-diphenoxy-Δ^3-1,3,4-oxadiazoline (**10**) (14.20 mg, 0.05 mmol, 0.1 M) in 0.5 ml of benzene-D6. Following three freeze-pump-thaw cycles the NMR tube was sealed and placed in a thermolysis bath at 100 ± 0.1 °C for 24h. Diphenyl thionocarbonate was the only CS_2-derived product observed by GCMS analysis and was identified by comparison to its literature spectrum.[245] GCMS (ei) m/z 230 (M^+), 214, 202, 169, 141, 137, 109, 94, 77, 65, 51, 39.

References

1. March, J. Carbocations, Carbanions, Free Radicals, Carbenes, and Nitrenes; In *Advanced Organic Chemistry: Reactions, Mechanisms, and Structure*; John Wiley & Sons, Inc.: Toronto, 1992; pp 165-204.

2. *Carbene(oide) Carbine, Methoden der Organischen Chemie (Houben-Weyl), 4th ed. (E19b, parts 1and 2)*; Regitz, M. Ed.; G. Thieme Verlag: Stuttgart, 1989; pp. 1-1021 and 1022-1901.

3. *Advances in Carbene Chemistry*; Brinker, U. H. Ed.; JAI Press Inc.: London, 1994; Vol. 1.

4. *Advances in Carbene Chemistry*; Brinker, U. H. Ed.; JAI Press Inc.: London, 1998; Vol. 2.

5. Gaspar, P. P.; Hammond, G. S. Spin States in Carbene Chemistry; In *Carbenes*; Moss, R. A., Jones, M., Jr., Eds; John Wiley & Sons: Toronto, 1975; pp 207-362.

6. Trozzolo, A. M.; Wasserman, E. Structure of Arylcarbenes; In *Carbenes*; Moss, R. A., Jones, M. Jr., Eds. John Wiley & Sons: Toronto, 1975; pp 185-206.

7. Herzberg, G.; Johns, J. W. C. *J. Chem. Phys.* **1971**, *54*, 2276-2278.

8. Shavitt, I. *Tetrahedron.* **1985**, *41*, 1531-1542.

9. Leopold, D. G.; Murray, K. K.; Stevens Miller, A. E.; Lineberger, W. C. *J. Chem. Phys.* **1985**, *83*, 4849-4865.

10. Richards, C. A. Jr.; Kim, S.-J.; Yamaguchi, Y.; Schaefer, H. F. III. *J. Am. Chem. Soc.* **1995**, *117*, 10104-10107.

11. Matzinger, S.; Fülscher, M. P. *J. Phys. Chem.* **1995**, *99*, 10747-10751.

12. Tomioka, H. Persistent Triplet Carbenes; In *Advances in Carbene Chemistry*; Brinker, U. H., Ed. JAI Press Inc.: London, 1998; Vol. 2, pp 175-214.

13. Fleming, I. *Frontier Orbitals and Organic Chemical Reactions*; John Wiley and Sons: New York, 1976.

14. Murray, K. K.; Leopold, D. G.; Miller, T. M.; Lineberger, W. C. *J. Chem. Phys.* **1988**, *89*, 5442-5453.

15. Koda, S. *Chem. Phys.* **1982**, *66*, 383-390.

16. Moss, R. A.; Włostowski, M.; Shen, S.; Krogh-Jespersen, K.; Matro, A. *J. Am. Chem. Soc.* **1988**, *110*, 4443-4444.

17. Räsänen, M.; Raaska, T.; Kunttu, H.; Murto, J. *J. Mol. Struct. (Theochem)* **1990**, *208*, 79-90.

18. Feller, D.; Borden, W. T.; Davidson, E. R. *Chem. Phys. Lett.* **1980**, *71*, 22-26.

19. Wasserman, E.; Snyder, L. C.; Yager, W. A. *J. Chem. Phys.* **1964**, *41*, 1763-1772.

20. Wasserman, E.; Hutton, R. S. *Acc. Chem. Res.* **1977**, *10*, 27-32.

21. Farràs, J.; Olivella, S.; Solé, A.; Vilarrasa, J. *J. Comp. Chem.* **1986**, *7*, 428-442.

22. Baird, N. C.; Taylor, K. F. *J. Am. Chem. Soc.* **1978**, *100*, 1333-1339.

23. Stracener, L. L.; Halter, R. J.; McMahon, R. J.; Castro, C.; Karney, W. L. *J. Org. Chem.* **2000**, *65*, 199-204.

24. Lowry, T. H.; Richardson, K. S. *Mechanism and Theory in Organic Chemistry*; Harper and Row: New York, 1987.

25. Turro, N. J.; Cha, Y.; Gould, I. R. *J. Am. Chem. Soc.* **1987**, *109*, 2101-2107.

26. Kirmse, W. Carbenes and the O-H Bond; In *Advances In Carbene Chemistry*; Brinker, U. H., Ed.; JAI Press: London, 1994; Vol. 2, pp 1-57.

27. Skell, P. S.; Woodworth, R. C. *J. Am. Chem. Soc.* **1956**, *78*, 4496-4497.

28. Skell, P. S. *Tetrahedron* **1985**, *41*, 1427-1428.

29. Bernardi, F.; Bottoni, A.; Canepa, C.; Olivucci, M.; Robb, M. A.; Tonachini, G. *J. Org. Chem.* **1997**, *62*, 2018-2024.

30. Kirmse, W. Reactions with Carbon-Hydrogen Bonds; In *Carbene Chemistry*; Academic Press: New York, 1971; pp 209-266.

31. Richardson, D. B.; Simmons, M. C.; Dvoretzky, I. *J. Am. Chem. Soc.* **1961**, *83*, 1934-1937.

32. Closs, G. L. Structures of Carbenes and the Stereochemistry of Carbene Additions to Olefins; In *Topics in Stereochemistry*; Eliel, E. L., Allinger, N. L., Eds. Interscience Publishers, John Wiley & Sons: Toronto, 1968; pp 193-235.

33. Hoffmann, R. *J. Am. Chem. Soc.* **1968**, *90*, 1475-1485.

34. Skell, P. S.; Garner, A. Y. *J. Am. Chem. Soc.* **1953**, *78*, 5430-5433.

35. Doering, W. v. E.; Henderson, W. A., Jr. *J. Am. Chem. Soc.* **1958**, *80*, 5274-5277.

36. Moss, R. A. *Acc. Chem. Res.* **1980**, *13*, 58-64.

37. Moss, R. A. *Acc. Chem. Res.* **1989**, *22*, 15-21.

38. Rondan, N. G.; Houk, K. N.; Moss, R. A. *J. Am. Chem. Soc.* **1980**, *102*, 1770-1776.

39. Moss, R. A.; Perez, L. A.; Włostowska, J.; Guo, W.; Krogh-Jespersen, K. *J. Org. Chem.* **1982**, *47*, 4177-4180.

40. Warkentin, J. Diamino-, Amino(oxy)-, Dioxy-, Amino(thio)-, Oxy(thio)-, and Dithiocarbenes; In *Advances in Carbene Chemistry*; Brinker, U. H., Ed.; JAI Press Inc.: London, 1998; Vol. 2, pp 245-295.

41. Scheeren, J. W.; Staps, R. J. F. M.; Nivard, R. J. F. *Recl. Trav. Chim. Pays-Bas* **1973**, *92*, 11-19.

42. Olofson, R. A.; Walinsky, S. W.; Marino, J. P.; Jernow, J. L. *J. Am. Chem. Soc.* **1968**, *90*, 6554-6555.

43. Oele, P. C.; Louw, R. *Tetrahedron Lett.* **1972**, *48*, 4941-4944.

44. Hoffmann, R. W.; Reiffen, M. *Chem. Ber.* **1977**, *110*, 49-52.

45. Crawford, R. J.; Raap, R. *Proc. Chem. Soc.* **1963**, 370-370.

46. McDonald, R. M.; Krueger, R. A. *J. Org. Chem.* **1966**, *31*, 488-494.

47. Borden, W. T.; Hoo, L. H. *J. Am. Chem. Soc.* **1978**, *100*, 6274-6276.

48. Ayral-Kaloustian, S.; Agosta, W. C. *J.Org.Chem.* **1982**, *47*, 284-287.

49. Yamamoto, S.; Back, R. A. *J. Phys. Chem.* **1985**, *89*, 622-625.

50. Lapidus, G.; Barton, D.; Yankwich, P. E. *J. Phys. Chem.* **1964**, *68*, 1863-1865.

51. Rosenfeld, R. N.; Weiner, B. *J. Am. Chem. Soc.* **1983**, *105*, 3485-3488.

52. Weiner, B.; Rosenfeld, R. N. *J. Org. Chem.* **1983**, *48*, 5362-5364.

53. Pirrung, M. C.; Chang, V. K.; DeAmicis, C. V. *J. Am. Chem. Soc.* **1989**, *111*, 5824-5831.

54. Yates, P.; Loutfy, R. O. *Acc. Chem. Res.* **1975**, *8*, 209-216.

55. Lee-Ruff, E.; Xi, F.; Qie, J. H. *J. Org. Chem.* **1996**, *61*, 1547-1550.

56. Hoffmann, R. W. *Angew. Chem. Int. Ed. Engl.* **1971**, *10*, 529-537.

57. Hoffmann, R.; Woodward, R. B. *Angew. Chem. Int. Ed. Engl.* **1969**, *8*, 781-853.

58. Hoffmann, R. W.; Hauser, H. *Tetrahedron Lett.* **1964**, 563-572.

59. Lemal, D. M.; Gosselink, E. P.; Ault, A. *Tetrahedron Lett.* **1964**, 579-585.

60. Lemal, D. M.; Gosselink, E. P.; McGregor, S. D. *J. Am. Chem. Soc.* **1966**, *88*, 582-600.

61. Lemal, D. M.; Lovald, R. A.; Harrington, R. W. *Tetrahedron Lett.* **1965**, 2779-2785.

62. Hoffmann, R. W.; Hirsch, R.; Fleming, R.; Reetz, M. T. *Chem. Ber.* **1972**, *105*, 3532-3541.

63. Gassman, P. G.; Aue, D. H.; Patton, D. S. *J. Am. Chem. Soc.* **1968**, *90*, 7271-7276.

64. Lustgarten, R. K.; Richey, H. G. Jr. *J. Am. Chem. Soc.* **1974**, *96*, 6393-6402.

65. Hoffmann, R. W. *Acc. Chem. Res.* **1985**, *18*, 248-253.

66. Prinzbach, H.; Rivier, J.; Englert, G. *Helv. Chim. Acta* **1970**, *53*, 2219-2230.

67. Hoffmann, R. W.; Schneider, J. *Tetrahedron Lett.* **1967**, *44*, 4347-4350.

68. Moss, R. A.; Cox, D. P. *Tetrahedron Lett.* **1985**, *26*, 1931-1934.

69. Hoffmann, R. W.; Schneider, J. *Chem. Ber.* **1967**, *100*, 3698-3702.

70. Kopecky, K. R.; Molina, J.; Rico, R. *Can. J. Chem.* **1988**, *66*, 2234-2243.

71. Włostowska, J.; Moss, R. A.; Guo, W.; Chang, M. J. *J. Chem. Soc., Chem. Commun.* **1982**, 432-433.

72. Moss, R. A.; Fedorynski, M.; Kmiecik-Lawrynowicz, G.; Terpinski, J. *Tetrahedron Lett.* **1986**, *27*, 2707-2710.

73. Sheridan, R. S.; Moss, R. A.; Wilk, B. K.; Shen, S.; Włostowski, M.; Kesselmayer, M. A.; Subramanian, R.; Kmiecik-Lawrynowicz, G.; Krogh-Jespersen, K. *J. Am. Chem. Soc.* **1988**, *110*, 7563-7564.

74. Moss, R. A. *Pure and Appl. Chem.* **1995**, *67*, 741-747.

75. Moss, R. A.; Włostowski, M.; Terpinski, J.; Kmiecik-Lawrynowicz, G.; Krogh-Jespersen, K. *J. Am. Chem. Soc.* **1987**, *109*, 3811-3812.

76. Ge, C.-S.; Jefferson, E. A.; Moss, R. A. *Tetrahedron Lett.* **1993**, *34*, 7549-7552.

77. Moss, R. A.; Shen, S.; Hadel, L. M.; Kmiecik-Lawrynowicz, G.; Włostowska, J.; Krogh-Jespersen, K. *J. Am. Chem. Soc.* **1987**, *109*, 4341-4349.

78. Békhazi, M.; Warkentin, J. *J. Am. Chem. Soc.* **1981**, *103*, 2473-2474.

79. Békhazi, M.; Warkentin, J. *J. Am. Chem. Soc.* **1983**, *105*, 1289-1292.

80. Békhazi, M.; Risbood, P. A.; Warkentin, J. *J. Am. Chem. Soc.* **1983**, *105*, 5675-5679.

81. Békhazi, M.; Warkentin, J. *Can. J. Chem.* **1983**, *61*, 619-624.

82. Békhazi, M.; Smith, P. J.; Warkentin, J. *Can. J. Chem.* **1984**, *62*, 1646-1652.

83. El-Saidi, M.; Kassam, K.; Pole, D. L.; Tadey, T.; Warkentin, J. *J. Am. Chem. Soc.* **1992**, *114*, 8751-8752.

84. Kassam, K.; Pole, D. L.; El-Saidi, M.; Warkentin, J. *J. Am. Chem. Soc.* **1994**, *116*, 1161-1162.

85. Pole, D. L.; Warkentin, J. *Liebigs Ann. Chem.* **1995**, 1907-1914.

86. Chiba, T.; Okimoto, M. *J. Org. Chem.* **1992**, *57*, 1375-1379.

87. Wong, T.; Warkentin, J.; Terlouw, J. K. *Int. J. Mass Spectrom. Ion Processes* **1992**, *115*, 33-52.

88. Suh, D.; Pole, D. L.; Warkentin, J.; Terlouw, J. K. *Can. J. Chem.* **1996**, *74*, 544-558.

89. Burgers, P. C.; McGibbon, G. A.; Terlouw, J. K. *Chem. Phys. Letters* **1994**, *224*, 539-543.

90. Wiedmann, F. A.; Cai, J.; Wesdemiotis, C. *Rapid Commun. Mass Spectrom.* **1994**, *8*, 804-807.

91. Wesdemiotis, C.; McLafferty, F. W. *J. Am. Chem. Soc.* **1871**, *109*, 4760-4761.

92. Feng, R.; Wesdemiotis, C.; McLafferty, F. W. *J. Am. Chem. Soc.* **1987**, *109*, 6521-6522.

93. Bouma, W. J.; Burgers, P. C.; Holmes, J. L.; Radom, L. *J. Am. Chem. Soc.* **1986**, *108*, 1767-1775.

94. Wesdemiotis, C.; Leyh, B.; Fura, A.; McLafferty, F. W. *J. Am. Chem. Soc.* **1990**, *112*, 8655-8660.

95. Polce, M. J.; Wesdemiotis, C. *J. Am. Chem. Soc.* **1993**, *115*, 10849-10856.

96. Hemminger, J. C.; Rusbult, C. F.; Lee, E. K. C. *J. Am. Chem. Soc.* **1971**, *93*, 1867-1871.

97. Lee-Ruff, E.; Hopkinson, A. C.; Kazarians-Moghaddam, H. *Tetrahedron Lett.* **1983**, *24*, 2067-2070.

98. Foster, A. M.; Agosta, W. C. *J. Am. Chem. Soc.* **1973**, *95*, 608-609.

99. Smith, A. B. I.; Foster, A. M.; Agosta, W. C. *J. Am. Chem. Soc.* **1972**, *94*, 5100-5101.

100. Foster, A. M.; Agosta, W. C. *J. Am. Chem. Soc.* **1972**, *94*, 5777-5781.

101. Corey, E. J.; Winter, R. A. E. *J. Am. Chem. Soc.* **1963**, *85*, 2677-2678.

102. Corey, E. J.; Carey, F. A.; Winter, R. A. E. *J. Am. Chem. Soc.* **1965**, *87*, 934-935.

103. Corey, E. J. *Pure and Appl. Chem.* **1967**, *14*, 19-37.

104. Sauers, R. R. *Tetrahedron Lett.* **1994**, *35*, 7213-7216.

105. Venneri, P. C.; Warkentin, J. *J. Am. Chem. Soc.* **1998**, *120*, 11182-11183.

106. Merkley, N.; Warkentin, J. *Can. J. Chem.* **2000**, *78*, 356-361.

107. Merkley, N.; Warkentin, J. *Can. J. Chem.* **2000**, Accepted.

108. Altmann, J. A.; Csizmadia, I. G.; Yates, K.; Yates, P. *J. Chem. Phys.* **1977**, *66*, 298-302.

109. Altmann, J. A.; Csizmadia, I. G.; Robb, M. A.; Yates, K.; Yates, P. *J. Am. Chem. Soc.* **1978**, *100*, 1653-1657.

110. Feller, D.; Borden, W. T.; Davidson, E. R. *J. Comp. Chem.* **1980**, *1*, 158-166.

111. Goddard, J. D.; Schaefer, H. F., III *J. Chem. Phys.* **1979**, *70*, 5117-5134.

112. Kakumoto, T.; Saito, K.; Imamura, A. *J. Chem. Phys.* **2000**, *91*, 2366-2371.

113. Modarelli, D. A.; Morgan, S.; Platz, M. S. *J. Am. Chem. Soc.* **1992**, *114*, 7034-7041.

114. Nickon, A. *Acc. Chem. Res.* **1993**, *26*, 84-89.

115. Moss, R. A.; Ho, G.-J.; Liu, W. *J. Am. Chem. Soc.* **1992**, *114*, 959-963.

116. Moss, R. A.; Jang, E. G.; Fan, H.; Włostowski, M.; Krogh-Jespersen, K. *J. Phys. Org. Chem.* **1992**, *5*, 104-107.

117. Goddard, J. D.; Yamaguchi, Y.; Schaefer, H. F. III. *J. Chem. Phys.* **1992**, *96*, 1158-1166.

118. Francisco, J. S. *J. Chem. Phys.* **1992**, *96*, 1167-1175.

119. Redington, R. L.; Bock, C. W.; Aboab, B. *J. Mol. Struct.* **1990**, *224*, 89-112.

120. Francisco, J. S. *J. Chem. Soc., Faraday Trans.* **1992**, *88*, 3521-3525.

121. Iwamura, H.; Iwai, M.; Kihara, H. *Chem. Lett.* **1977**, 881-884.

122. Baldwin, J. E.; Walker, J. A. *J. Chem. Soc., Chem. Commun.* **1972**, 354-355.

123. Nakai, T.; Mikami, K. *Chem. Lett.* **1978**, *11*, 1243-1244.

124. Nakai, T.; Mikami, K. *Chem. Lett.* **1979**, 1081-1084.

125. Chan, K.-K.; Saucy, G. *J. Org. Chem.* **1977**, *42*, 3828-3832.

126. Büchi, G.; Cushman, M.; Wüest, H. *J. Am. Chem. Soc.* **1974**, *96*, 5563-5565.

127. Hammond, G. S. *J. Am. Chem. Soc.* **1955**, *77*, 334-338.

128. Couture, P.; Pole, D. L.; Warkentin, J. *J. Chem. Soc., Perkin Trans. 2* **1997**, 1565-1570.

129. Du, X.-M.; Fan, H.; Goodman, J. L.; Kesselmayer, M. A.; Krogh-Jespersen, K.; LaVilla, J. A.; Moss, R. A.; Shen, S.; Sheridan, R. S. *J. Am. Chem. Soc.* **1990**, *112*, 1920-1926.

130. Moss, R. A.; Shen, S.; Włostowski, M. *Tetrahedron Lett.* **1988**, *29*, 6417-6420.

131. LaVilla, J. A.; Goodman, J. L. *J. Am. Chem. Soc.* **1989**, *111*, 712-714.

132. LaVilla, J. A.; Goodman, J. L. *J. Am. Chem. Soc.* **1989**, *111*, 6877-6878.

133. LaVilla, J. A.; Goodman, J. L. *Tetrahedron Lett.* **1990**, *31* , 6287-6290.

134. Moss, R. A.; Ge, C.-S.; Włostowska, J.; Jang, E. G.; Jefferson, E. A.; Fan, H. *Tetrahedron Lett.* **1995**, *36*, 3083-3086.

135. Hoffmann, R. W.; Lilienblum, W.; Dittrich, B. *Chem. Ber.* **1974**, *107*, 3395-3407.

136. de Meijere, A.; Kozhushkov, S. I.; Yufit, D. S.; Boese, R.; Haumann, T.; Pole, D. L.; Sharma, P. K.; Warkentin, J. *Liebigs Ann. Chem.* **1996**, 601-612.

137. Moss, R. A.; Huselton, J. K. *J. Chem. Soc., Chem. Commun.* **1976**, 950-951.

138. Pole, D. L.; Sharma, P. K.; Warkentin, J. *Can. J. Chem.* **1996**, *74*, 1335-1340.

139. Ross, J. P.; Couture, P.; Warkentin, J. *Can. J. Chem.* **1997**, *75*, 1331-1335.

140. Dunn, J. A.; Pezacki, J. P.; McGlinchey, M. J.; Warkentin, J. *J. Org. Chem.* **1999**, *64*, 4344-4352.

141. Isaacs, L.; Diederich, F. *Helv. Chim. Acta* **1993**, *76*, 2454-2464.

142. Win, W. W.; Kao, M.; Eiermann, M.; McNamara, J. J.; Wudl, F.; Pole, D. L.; Kassam, K.; Warkentin, J. *J. Org. Chem.* **1994**, *59*, 5871-5876.

143. Diederich, F.; Isaacs, L.; Philp, D. *Chem. Soc. Rev.* **1994**, 243-255.

144. Moss, R. A.; Young, C. M.; Perez, L. A.; Krogh-Jespersen, K. *J. Am. Chem. Soc.* **1981**, *103*, 2413-2415.

145. Lilienblum, W.; Hoffmann, R. W. *Chem. Ber.* **1977**, *110*, 3405-3409.

146. Lu, X.; Warkentin, J. *Tetrahedron Lett.* **1999**, *40*, 1483-1486.

147. Lu, X.; Warkentin, J. *Can. J. Chem.* **2000**, Manuscript in Preparation.

148. Kassam, K.; Venneri, P. C.; Warkentin, J. *Can. J. Chem.* **1997**, *75*, 1256-1263.

149. Kassam, K.; Warkentin, J. *Can. J. Chem.* **1997**, *75*, 120-128.

150. Kassam, K.; Warkentin, J. *J. Org. Chem.* **1994**, *59*, 5071-5075.

151. Britten, J. F.; Kassam, K.; Warkentin, J. *Acta Crystallographica C.* **1997**, *C53*, 243-245.

152. Hoffmann, R. W.; Steinbach, K.; Lilienblum, W. *Chem. Ber.* **1976**, *109*, 1759-1768.

153. Pole, D. L.; Warkentin, J. *J. Org. Chem.* **1997**, *62*, 4065-4067.

154. Venneri, P. C.; Warkentin, J. *Can. J. Chem.* **2000**, Accepted.

155. Gerninghaus, C.; Kümmell, A.; Seitz, G. *Chem. Ber.* **1993**, *126*, 733-738.

156. León, S. *Chem. Phys. Letters* **1998**, *296*, 292-298.

157. Pliego, J. R. Jr.; De Almeida, W. B. *J. Chem. Phys.* **1997**, *106*, 3582-3586.

158. Ahmed, S. N.; McKee, M. L.; Shevlin, P. B. *J. Am. Chem. Soc.* **1985**, *107*, 1320-1324.

159. Pole, D. L. *Mechanistic Studies on the Reactions of Dialkoxycarbenes with Carbonyl Compounds.* Ph.D. thesis, **1996**, McMaster University, Hamilton, Ontario, Canada.

160. Bock, C. W.; Redington, R. L. *J. Chem. Phys.* **1986**, *85*, 5391-5400.

161. Kuhn, N.; Bohnen, H.; Henkel, G. *Z. Naturforsch., B: Chem. Sci.* **1994**, *49*, 1473-1480.

162. Winberg, H. E.; Coffman, D. D. *J. Am. Chem. Soc.* **1965**, *87*, 2776-2777.

163. Schössler, W.; Regitz, M. *Chem. Ber.* **1974**, *107*, 1931-1948.

164. Krasuski, W.; Nikolaus, D.; Regitz, M. *Liebigs Ann. Chem.* **1982**, 1451-1465.

165. Schönherr, H.-J.; Wanzlick, H.-W. *Chem.Ber.* **1970**, *103*, 1037-1046.

166. Schönherr, H.-J.; Wanzlick, H.-W. *Liebigs Ann. Chem.* **1970**, *731*, 176-179.

167. Hoffmann, R. W.; Steinbach, K.; Dittrich, B. *Chem.Ber.* **1973**, *106*, 2174-2184.

168. Duus, F. Thiocarbonyl Compounds; In *Comprehensive Organic Chemistry*; Barton, D. H. R., Ollis, W. D., Eds. Pergamon Press: Oxford, 1979; pp 373-487.

169. McGregor, W. M.; Sherrington, D. C. *Chem. Soc. Rev.* **1993**, 199-204.

170. Reiffen, M.; Hoffmann, R. W. *Chem. Ber.* **1977**, *110*, 37-48.

171. Regitz, M.; Hocker, J.; Schössler, W.; Weber, B.; Leidhegener, A. *Liebigs Ann. Chem.* **1971**, *748*, 1-19.

172. Regitz, M.; Hocker, J. *Synth.* **1970**, 301-302.

173. Hoffmann, R. W.; Hagenbruch, B.; Smith, D. M. *Chem. Ber.* **1977**, *110*, 23-36.

174. Takamizawa, A.; Harai, K.; Matsumoto, S. *Tetrahedron Lett.* **1968**, *37*, 4027-4030.

175. Er, H.-T.; Pole, D. L.; Warkentin, J. *Can. J. Chem.* **1996**, *74*, 1480-1489.

176. Rigby, J. H.; Cavezza, A.; Ahmed, G. *J. Am. Chem. Soc.* **1996**, *118*, 12848-12949.

177. Rigby, J. H.; Laurent, S. *J. Org. Chem.* **1999**, *64*, 1766-1767.

178. Rigby, J. H.; Cavezza, A.; Heeg, M. J. *Tetrahedron Lett.* **1999**, *40*, 2473-2476.

179. Rigby, J. H.; Danca, M. D. *Tetrahedron Lett.* **1999**, *40*, 6891-6894.

180. Colomvakos, J. D.; Egle, I.; Ma, J.; Pole, D. L.; Tidwell, T. T.; Warkentin, J. *J. Org. Chem.* **1996**, *61*, 9522-9527.

181. Hoffmann, R. W. *Angew. Chem. Int. Ed. Engl.* **1979**, *18*, 563-640.

182. Tomooka, K.; Yamamoto, H.; Nakai, T. *Liebigs Ann./Recueil* **1997**, 1275-1281.

183. Nakai, T.; Mikami, K. *Chem. Rev.* **1986**, *86*, 885-902.

184. Brückner, R. In *Comprehensive Organic Synthesis*; Trost, B. M., Fleming, I., Eds. Pergamon Press: London, 1991; pp 873-908.

185. Okajima, T.; Yoshimasa, F. *Nippon Kagaku Kaishi* **1999**, 97-103 (Chem. Abstr., 1999, 130, 282090f).

186. Sheldon, J. C.; Taylor, M. S.; Bowie, J. H.; Dua, S.; Chia, C. S. B.; Eichinger, P. C. H. *J. Chem. Soc., Perkin Trans. 2* **1999**, 333-340.

187. Antoniotti, P.; Tonachini, G. *J. Org. Chem.* **1998**, *63*, 9756-9762.

188. Okajima, T. *Nippon Kagaku Kaishi* **1997**, 529-531 (Chem. Abstr., 1997, 127, 161403q).

189. Okajima, T.; Fukazawa, Y. *Chem. Lett.* **1997**, 81-82.

190. Antoniotti, P.; Fukazawa, Y. *Trends Org. Chem.* **1995**, *5*, 189-201 (Chem Abstr., 1997, 126, 317108q).

191. Fischer, N.; Opitz, G. *Org. Synth.* **1973**, *5*, 877-879.

192. Antoniotti, P.; Tonachini, G. *J. Org. Chem.* **1993**, *58*, 3622-3632.

193. Kim, C. K.; Lee, I.; Lee, H. W.; Lee, B.-S. *Bull. Korean Chem. Soc.* **1991**, *12*, 678-681 (Chem. Abstr., 1992, 116, 105329f).

194. Frisch, M. J.; Trucks, G. W.; Schlegel, H. B.; Gill, P. M. W.; Johnson, B. G.; Robb, M. A.; Cheeseman, J. R.; Keith, T.; Petersson, G. A.; Montgomery, J. A.; Raghavachari, K.; Al-Laham, M. A.; Zakrzewski, V. G.; Ortiz, J. V.; Foresman, J. B.; Cioslowski, J.; Stefanov, B. B.; Nanayakkara, A.; Challacombe, M.; Peng, D. Y.; Ayala, P. Y.; Chen, W.; Wong, M. W.; Andres, J. L.; Replogle, E. S.; Gomperts, R.; Martin, R. L.; Fox, D. J.; Binkley, J. S.; Defrees, D. J.; Baker, J.; Stewart, J. P.; Head-Gorden, M.; Gonzalez, C.; Pople, J. A. *Gaussian 94, Revision E.2*; Gaussian, Inc.: Pittsburgh, PA, 1995.

195. Reid, D. L.; Hernández-Trujillo, J.; Warkentin, J. *J. Phys. Chem. A*, **2000**, *104*, 3398-3405.

196. Scott, A. P.; Radom, L. *J. Phys. Chem.* **1996**, *100*, 16502-16513.

197. Wong, M. W. *Chem. Phys. Lett.* **1996**, *256*, 391-399.

198. Singh, Y.; Prager, R. H. *Aust. J. Chem.* **1992**, *45*, 1811-1823.

199. Anh, N. T.; Maurel, F. *New J. Chem.* **1997**, *21*, 861-871.

200. Klopman, G. *Chemical Reactivity and Reaction Paths*; John Wiley & Sons: New York, 1974.

201. Keating, A. E.; Garcia-Garibay, M. A.; Houk, K. N. *J. Am. Chem. Soc.* **1997**, *119*, 10805-10809.

202. Feller, D.; Borden, W. T.; Davidson, E. R. *J. Chem. Phys.* **1979**, *71*, 4987-4992.

203. Turro, N. J. Electronic Orbitals, Configurations and States; In *Modern Molecular Photochemistry*; The Benjamin/Cummings Publishing Co., Inc: London, 1978; pp 17-37.

204. Szabo, A.; Ostlund, N. S. Many-Electron Wave Functions and Operators; In *Modern Quantum Chemistry, Introduction to Advanced Electronic Structure Theory*; McGraw-Hill Publishing Company: Toronto, 1982; pp 39-107.

205. Jursic, B. S. *Int. J. Quantum Chem.* **1997**, *62*, 291-296.

206. Benson, S. D. *Thermochemical Kinetics: Methods for the Estimation of Thermochemical Data and Rate Parameters*; John Wiley & Sons, Inc.: New York, 1976.

207. Benson, S. D.; O'Neal, H. E. *Kinetic Date on Gas Phase Unimolecular Reactions*; National Bureau of Standards, NSRDS-NBS 21: 1970.

208. Rautenstrauch, V. *Chem. Commun.* **1970**, 4-6.

209. Baldwin, J. E.; DeBernardis, J.; Patrick, J. E. *Tetrahedron Lett.* **1970**, 353-356.

210. Reid, D. L.; Warkentin, J. *J. Chem. Soc., Perkin Trans. 2*, **2000**, Accepted.

211. Bader, R. F. W. *Atoms in Molecules. A Quantum Theory*; Oxford University Press: Oxford, UK, 1990.

212. Schmidt, M. W.; Baldridge, K. K.; Boatz, J. A.; Elbert, S. T.; Gordon, M. S.; Jensen, J. H.; Koseki, S.; Matsunaga, N.; Nguyen, K. A.; Su, S. J.; Windus, T. L.; Dupuis, M.; Montgomery, J. A. *J. Comp. Chem.* **1993**, *14*, 1347-1363.

213. Dunning, T. H. Jr. *J. Chem. Phys.* **1989**, *90*, 1007-1023.

214. Biegler-König, F. W.; Bader, R. F. W.; Tang, T.-H. *J. Comp. Chem.* **1982**, *3*, 317-328.

215. Bader, R. F. W. *Atoms in Molecules. A Quantum Theory*; Oxford University Press: Oxford, UK, 1990. (Modification of Proaimv, Hernández-Trujillo, J., **1999**.)

216. Deng, L.; Ziegler, T.; Fan, L. *J. Chem. Phys.* **1993**, *99*, 3823-3835.

217. Kamiya, K.; Morokuma, K. *J. Chem. Phys.* **1991**, *94*, 7287-7298.

218. Goddard, J. D.; Yamaguchi, Y.; Schaefer, H. F., III *J. Chem. Phys.* **1981**, *75*, 3459-3465.

219. Frisch, M. J.; Krishnan, R.; Pople, J. A. *J. Phys. Chem.* **1981**, *85*, 1467-1468.

220. Harding, L. B.; Schlegel, H. B.; Krishnan, R.; Pople, J. A. *J. Phys. Chem.* **1980**, *84*, 3394-3401.

221. Pau, C.-F.; Hehre, W. J. *J. Phys. Chem.* **1982**, *86*, 1252-1253.

222. Lucchese, R. R.; Schaefer, H. F., III *J. Am. Chem. Soc.* **1978**, *100*, 298-299.

223. Pross, A.; Shaik, S. S. *Chem. Rev.* **1983**, *16*, 363-370.

224. Pross, A. *Acc. Chem. Res.* **1985**, *18*, 212-219.

225. Bruna, P. J.; Buenker, R. J.; Peyerimhoff, S. D. *J. Mol. Struct.* **1976**, *32*, 217-233.

226. Feller, D.; Davidson, E. R. *J. Chem. Phys.* **1983**, *80*, 1006-1017.

227. Bader, R. F. W.; Essén, H. *J. Chem. Phys.* **1984**, *80*, 1943-1960.

228. Esseffar, M.; El Mouhtadi, M.; López, V.; Yáñez, M. *J. Mol. Struct. (Theochem)* **1992**, *255*, 393-408.

229. Slee, T.; Larouche, A.; Bader, R. F. W. *J. Phys. Chem.* **1988**, *92*, 6219-6227.

230. Baldwin, J. E. *Chem. Commun.* **1976**, 734-736.

231. Tenud, L.; Farooq, S.; Seibl, J.; Eschenmoser, A. *Helv. Chim. Acta* **1970**, *53*, 2059-2069.

232. Pezacki, J. P.; Wood, P. D.; Gadosy, T. A.; Lusztyk, J.; Warkentin, J. *J. Am. Chem. Soc.* **1998**, *120*, 8681-8691.

233. Dittmer, D. C. Thiiranes and Thiirenes; In *Comprehensive Hetrolytic Chemistry. The Structure, Reactions, Synthesis and Uses of Heterocyclic Compounds*; Lwowski, W., Ed. Pergamon Press: Toronto, 1984; pp 131-184.

234. Lu, X.; Reid, D. L.; Warkentin, J. *Can. J. Chem.* **2000**, Manuscript in Preparation.

235. Frisch, M. J.; Frisch, A.; Foresman, J. B. *Gaussian 94 User's Reference*; Gaussian, Inc.: Pittsburgh, 1994.

236. Pliego, J. R. Jr.; De Almeida, W. B. *J. Braz. Chem. Soc.* **1988**, *9*, 181-186.

237. Houk, K. N.; Rondan, N. G.; Santiago, C.; Gallo, C. J.; Gandour, R. W.; Griffin, G. W. *J. Am. Chem. Soc.* **1980**, *102*, 1504-1512.

238. Arduengo, A. J.; Burgess, E. M. *J. Am. Chem. Soc.* **1976**, *98*, 5021-5023.

239. Aono, M.; Terao, Y.; Achiwa, K. *Heterocycles*, **1995**, *40*, 249-260.

240. Kellogg, R. M. *Tetrahedron*, **1976**, *32*, 2165-2184.

241. Imai, N.; Tokiwa, H.; Aono, M.; Terao, Y.; Akahori, Y.; Achiwa, K. *Het* **1986**, *24*, 2423-2427.

242. Reid, D. L.; Venneri, P. C.; Warkentin, J.; Johnston, L. J. *Unpublished Work*, **2000**.

243. Gregoire, B.; Carre, M.-C.; Caubere, P. *J. Org. Chem.* **1986**, *51*, 1419-1427.

244. Diels, O. *Chem. Ber.* **1914**, *47*, 2183-2195.

245. Stein, S.; Levitsky, A.; Fukev, O.; Mallard, G. National Institute of Standards and Techonology (Mass Spectral Search Program for the NIST/EPA/NIH Mass Spectral Library), Version 1.6d, **1997**, US Secretary of Commerce, USA.

246. Bader, R. F. W.; Beddall, P. M.; Cade, P. E. *Phys. and Inorg. Chem.* **1971**, *93*, 3095-3107.

247. Gillespie, R. J.; Robinson, E. A. *Angew. Chem. Int. Ed. Engl.* **1996**, *35*, 495-514.

Appendix I

Structural Data

I.1. Z-matrix for Table 6, Table 7 and Table 8.

O1
C2 O1 R1
O3 C2 R2 O1 A1
C4 O3 R3 C2 A2 O1 D1
C5 C4 R4 O3 A3 C2 D2
C6 C5 R5 C4 A4 O3 D3
H7 O1 R6 C2 A5 O3 D4
H8 C4 R7 C5 A6 C6 D5
H9 C4 R8 C5 A7 C6 D6
H10 C5 R9 C4 A8 H9 D7
H11 C6 R10 C5 A9 C4 D8
H12 C6 R11 C5 A10 C4 D9

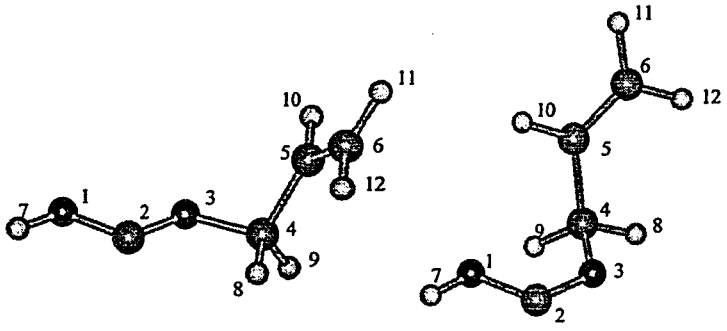

trans,trans-AHC

trans,cis-AHC

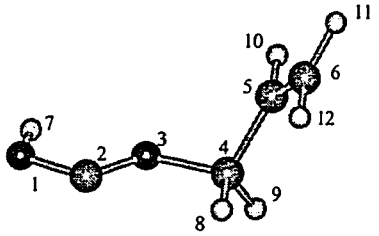

cis,trans-AHC

Figure 42. Optimized structures and atom numbering for *trans,trans*-AHC, *trans,cis*-AHC, and *cis,trans*-AHC at the B3LYP/6-31+G(d) level of theory.

Table 6. Structural data for *trans,trans*-AHC, *trans,cis*-AHC, and *cis,trans*-AHC with distances in Å and angles in degrees.

	trans,trans-AHC		*trans,cis*-AHC		*cis,trans*-AHC	
	B3LYP/ 6-31+G(d)	MP2(FC)/ 6-31+G(d)	B3LYP/ 6-31+G(d)	MP2(FC)/ 6-31+G(d)	B3LYP/ 6-31+G(d)	MP2(FC)/ 6-31+G(d)
Variable:						
R1	1.338	1.341	1.352	1.357	1.322	1.326
R2	1.317	1.321	1.306	1.313	1.331	1.338
R3	1.454	1.461	1.490	1.484	1.458	1.463
R4	1.499	1.493	1.496	1.492	1.499	1.493
R5	1.336	1.342	1.337	1.342	1.336	1.342
R6	0.970	0.975	0.970	0.975	0.989	0.991
R7	1.093	1.093	1.091	1.091	1.093	1.092
R8	1.096	1.093	1.092	1.092	1.095	1.093
R9	1.090	1.089	1.088	1.087	1.090	1.089
R10	1.087	1.086	1.087	1.086	1.087	1.086
R11	1.088	1.087	1.089	1.087	1.088	1.087
A1	105.1	104.8	109.8	109.1	107.5	107.1
A2	115.8	114.2	124.1	122.6	116.3	114.7
A3	109.9	109.2	111.6	111.1	110.1	109.4
A4	123.6	122.6	123.3	122.3	123.5	122.6
A5	106.6	105.8	106.5	105.7	111.8	110.7
A6	112.1	112.0	111.6	111.5	112.1	112.0
A7	111.3	112.1	112.2	112.7	111.5	112.3
A8	116.0	116.8	116.4	117.1	116.1	116.9
A9	121.6	121.5	121.6	121.5	121.6	121.5
A10	121.8	121.5	121.7	121.6	121.7	121.4
D1	179.4	178.5	-1.9	-1.4	179.	178.3
D2	244.9	251.9	83.9	79.5	246.2	253.5
D3	127.1	122.3	111.6	109.8	124.7	119.7
D4	179.8	179.6	179.2	179.2	-0.4	-0.5
D5	6.1	2.2	-3.1	-4.3	4.2	0.0
D6	-117.1	-122.2	-127.1	-128.6	-119.3	-124.5
D7	61.7	57.7	52.3	51.0	59.6	55.4
D8	178.0	179.0	178.9	179.3	178.1	179.2
D9	-1.9	-1.0	-0.9	-0.6	-1.8	-0.9

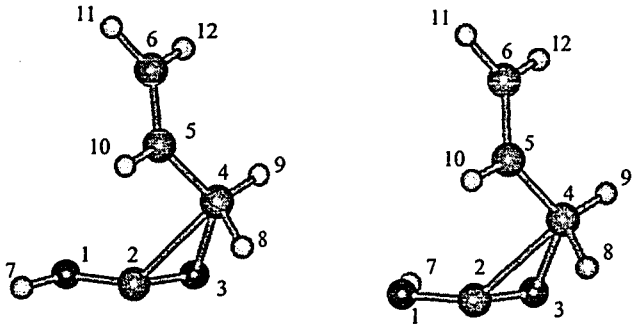

Figure 43. Optimized structures and atom numbering for **TS1(a)** and **TS1(b)** at the B3LYP/6-31+G(d) level of theory.

Table 7. Structural data for **TS1(a)** and **TS1(b)** with distances in Å and angles in degrees.

	1,2-migration (**TS1a**)		1,2-migration (**TS1b**)	
	B3LYP/ 6-31+G(d)	MP2(FC)/ 6-31+G(d)	B3LYP/ 6-31+G(d)	MP2(FC)/ 6-31+G(d)
Variable:				
R1	1.361	1.361	1.337	1.341
R2	1.270	1.291	1.281	1.303
R3	1.936	1.860	1.945	1.864
R4	1.462	1.475	1.461	1.473
R5	1.346	1.347	1.346	1.347
R6	0.973	0.977	0.991	0.995
R7	1.083	1.085	1.082	1.084
R8	1.088	1.092	1.088	1.092
R9	1.088	1.088	1.087	1.087
R10	1.086	1.086	1.086	1.085
R11	1.088	1.087	1.088	1.087
A1	112.0	111.0	114.7	113.7
A2	77.2	73.8	76.9	74.0
A3	124.6	126.3	123.5	124.8
A4	122.4	121.8	122.1	121.4
A5	107.4	106.8	108.4	107.7
A6	117.4	116.4	117.6	116.7
A7	114.3	111.6	114.5	111.9
A8	116.8	117.1	117.0	117.3
A9	121.5	121.4	121.5	121.3
A10	121.6	121.4	121.7	121.5
D1	128.3	126.2	133.2	127.5
D2	313.5	312.3	312.3	310.3
D3	272.1	274.2	269.9	271.8
D4	174.3	176.1	-1.0	0.2
D5	150.7	145.9	149.2	144.1
D6	11.7	13.3	9.7	10.9
D7	192.4	193.5	190.2	190.8
D8	182.9	182.3	183.1	182.4
D9	3.7	3.3	3.6	3.0

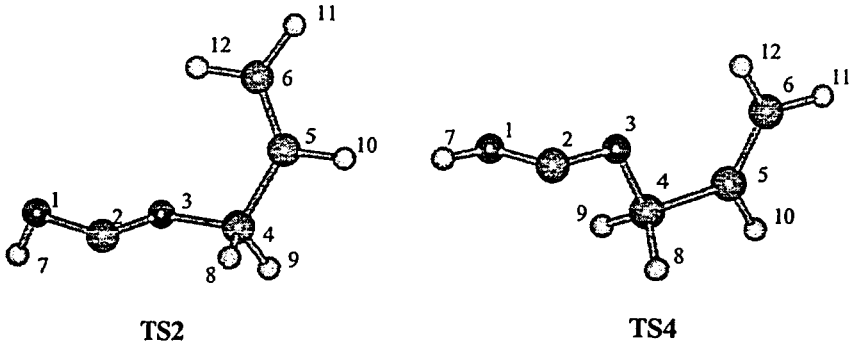

Figure 44. Optimized structures and atom numbering for **TS2** and **TS4** at the B3LYP/6-31+G(d) level of theory.

Table 8. Structural data for **TS2** and **TS4** with distances in Å and angles in degrees.

	TS2		**TS4**	
	B3LYP/ 6-31+G(d)	MP2(FC)/ 6-31+G(d)	B3LYP/ 6-31+G(d)	MP2(FC)/ 6-31+G(d)
Variable:				
R1	1.367	1.374	1.333	1.332
R2	1.315	1.317	1.347	1.357
R3	1.448	1.455	1.439	1.445
R4	1.500	1.496	1.499	1.496
R5	1.335	1.340	1.334	1.339
R6	0.973	0.977	0.974	0.979
R7	1.096	1.095	1.101	1.099
R8	1.096	1.094	1.099	1.098
R9	1.091	1.090	1.091	1.090
R10	1.086	1.085	1.086	1.085
R11	1.086	1.085	1.086	1.085
A1	106.3	105.9	106.2	105.9
A2	115.9	114.5	119.1	115.2
A3	111.4	110.3	110.1	109.0
A4	126.2	125.2	125.8	124.9
A5	112.8	111.6	106.9	106.3
A6	111.8	112.1	110.5	110.8
A7	110.9	111.4	110.4	110.7
A8	113.6	114.5	113.7	114.5
A9	120.9	120.5	121.0	120.7
A10	121.9	121.9	121.4	121.3
D1	176.4	176.0	272.0	272.3
D2	240.7	244.5	188.0	188.5
D3	4.1	3.1	1.0	1.7
D4	89.0	88.6	182.5	182.0
D5	-116.8	-117.1	-119.1	-118.0
D6	-238.2	-240.0	-238.3	-238.2
D7	-58.4	-60.5	-58.3	-58.2
D8	179.6	179.3	180.1	180.1
D9	-0.5	-0.8	0.2	0.1

I.2. Z-matrix for Table 9.

```
O1
C2  O1  R1
O3  C2  R2  O1  A1
C4  O3  R3  C2  A2  O1  D1
C5  C4  R4  O3  A3  C2  D2
C6  C2  RR5 C5  AA4 C4  DD3
H7  O1  R6  C2  A5  O3  D4
H8  C4  R7  C5  A6  C6  D5
H9  C4  R8  C5  A7  C6  D6
H10 C5  R9  C4  A8  H9  D7
H11 C6  R10 C5  A9  C4  D8
H12 C6  R11 C5  A10 C4  D9
```

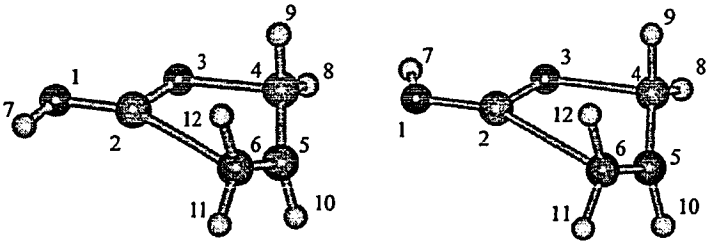

Figure 45. Optimized structures and atom numbering for **TS3(a)** and **TS3(b)** at the B3LYP/6-31+G(d) level of theory.

Table 9. Structural data for **TS3(a)** and **TS3(b)**.

	TS3(a)		TS3(b)	
	B3LYP/ 6-31+G(d)	MP2(FC)/ 6-31+G(d)	B3LYP/ 6-31+G(d)	MP2(FC)/ 6-31+G(d)
Variable:				
R1	1.355	1.355	1.342	1.344
R2	1.240	1.251	1.250	1.262
R3	1.905	1.847	1.897	1.837
R4	1.412	1.408	1.413	1.410
RR5	2.595	2.412	2.565	2.393
R6	0.970	0.975	0.986	0.989
R7	1.086	1.087	1.086	1.087
R8	1.086	1.087	1.085	1.087
R9	1.088	1.087	1.088	1.087
R10	1.087	1.087	1.087	1.087
R11	1.085	1.085	1.084	1.085
A1	112.7	112.0	115.0	114.5
A2	111.1	109.1	111.0	109.3
A3	102.9	102.6	102.9	102.6
AA4	29.3	30.8	29.5	30.9
A5	106.9	106.3	110.4	109.9
A6	120.5	120.5	120.4	120.4
A7	119.6	118.9	119.5	118.7
A8	118.8	119.1	118.8	119.1
A9	121.9	121.9	122.0	122.0
A10	121.4	120.7	121.5	120.8
D1	177.3	177.1	177.4	177.3
D2	393.1	393.7	393.1	393.8
DD3	-132.9	-132.9	-133.2	-133.0
D4	179.7	179.7	0.2	0.3
D5	-170.2	-168.8	-169.7	-168.6
D6	36.5	40.4	37.5	41.3
D7	-166.8	-167.8	-166.6	-167.5
D8	163.3	162.0	162.3	160.9
D9	-25.6	-32.8	-26.2	-33.0

I.3. Z-matrix for Table 10.

O1
C2 O1 R1
O3 C2 R2 O1 A1
C4 C2 R3 O3 A2 O1 D1
C5 C4 R4 C2 A3 O1 D2
C6 C5 R5 C4 A4 C2 D3
H7 O1 R6 C2 A5 O3 D4
H8 C4 R7 C5 A6 C6 D5
H9 C4 R8 C5 A7 C6 D6
H10 C5 R9 C4 A8 H9 D7
H11 C6 R10 C5 A9 C4 D8
H12 C6 R11 C5 A10 C4 D9

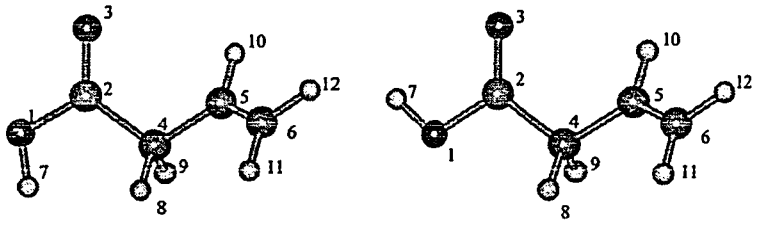

Figure 46. Optimized structures and atom numbering for *trans*-**112** and *cis*-**112** at the B3LYP/6-31+G(d) level of theory.

Table 10. Structural data for *trans*-4 *and cis*-4 with distances in Å and angles in degrees.

	trans-4		*cis*-4	
	B3LYP/ 6-31+G(d)	MP2(FC)/ 6-31+G(d)	B3LYP/ 6-31+G(d)	MP2(FC)/ 6-31+G(d)
Variable:				
R1	1.365	1.371	1.359	1.364
R2	1.205	1.214	1.212	1.221
R3	1.529	1.522	1.517	1.510
R4	1.504	1.499	1.505	1.500
R5	1.335	1.341	1.335	1.341
R6	0.972	0.976	0.976	0.982
R7	1.099	1.098	1.095	1.095
R8	1.103	1.101	1.102	1.100
R9	1.088	1.088	1.088	1.088
R10	1.087	1.085	1.087	1.085
R11	1.089	1.087	1.089	1.087
A1	119.8	119.8	122.4	2.7
A2	125.1	124.9	126.2	6.1
A3	113.2	112.3	113.3	112.3
A4	124.1	123.3	124.0	123.2
A5	111.1	110.3	107.1	106.4
A6	110.5	110.2	111.9	111.6
A7	110.1	110.6	110.3	110.9
A8	115.7	116.5	115.9	116.6
A9	121.4	121.3	121.4	121.3
A10	122.1	121.8	122.0	121.8
D1	178.2	178.0	178.0	178.1
D2	188.8	190.1	198.9	199.0
D3	130.6	125.4	132.8	126.9
D4	180.6	180.9	0.6	0.8
D5	7.0	2.8	8.8	4.2
D6	-110.2	-115.0	-109.0	-114.3
D7	69.7	65.2	70.6	65.6
D8	179.1	179.6	178.9	179.4
D9	-1.1	-0.6	-1.1	-0.7

I.4. Z-matrix for Table 11.

O1
C2 O1 R1
O3 C2 R2 O1 A1
C4 O1 R3 C2 A2 O3 D1

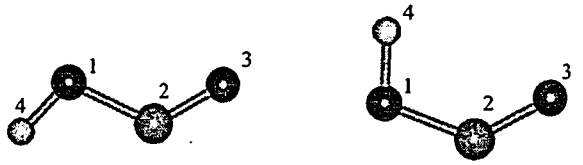

trans-**5** *cis*-**5**

Figure 47. Optimized structures and atom numbering for *trans*-**113** and *cis*-**113** at the B3LYP/6-31+G(d) level of theory.

Table 11. Structural data for *trans*-**113** *and cis*-**113** with distances in Å and angles in degrees.

	trans-**113**		*cis*-**113**	
	B3LYP/ 6-31+G(d)	MP2(FC)/ 6-31+G(d)	B3LYP/ 6-31+G(d)	MP2(FC)/ 6-31+G(d)
Variable:				
R1	1.346	1.352	1.330	1.339
R2	1.186	1.195	1.192	1.200
R3	0.973	0.977	0.985	0.986
A1	126.7	126.8	130.4	130.4
A2	109.0	108.1	110.0	108.9
D1	180.0	180.0	0.0	0.0

I.5. Z-matrix for Table 12.

C1
C2 C1 R1
C3 C2 R2 C1 A1
H4 C1 R3 C2 A2 C3 D1
H5 C1 R4 C2 A3 C3 D2
H6 C2 R5 C1 A4 H5 D3
H7 C3 R6 C2 A5 C1 D4
H8 C3 R7 C2 A6 C1 D5

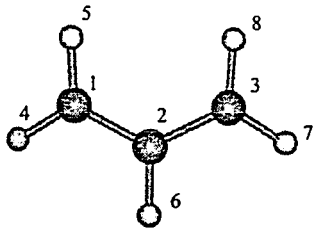

114

Figure 48. Optimized structure and atom numbering for the allyl radical (**114**) at the B3LYP/6-31+G(d) level of theory.

Table 12. Structural data for **114** with distances in Å and angles in degrees.

	Allyl radical **114**	
	B3LYP/6-31+G(d)	MP2(FC)/6-31+G(d)
Variable:		
R1	1.389	1.381
R2	1.389	1.381
R3	1.086	1.083
R4	1.088	1.085
R5	1.091	1.089
R6	1.086	1.083
R7	1.088	1.085
A1	125.0	124.4
A2	121.6	121.6
A3	121.1	121.0
A4	117.5	117.8
A5	121.6	121.6
A6	121.1	121.0
D1	180.0	180.0
D2	0.0	0.0
D3	180.0	180.0
D4	180.0	180.0
D5	0.0	0.0

I.6. Z-matrix for Table 13.

```
H1
C2  H1  R1
O3  C2  R2   H1  A1
C4  O3  R3   C2  A2  H1  D1
C5  C4  R4   O3  A3  C2  D2
C6  C5  R5   C4  A4  O3  D3
H7  C4  R6   C5  A5  C6  D4
H8  C4  R7   C5  A6  C6  D5
H9  C6  R8   C5  A7  C4  D6
H10 C6  R9   C5  A8  C4  D7
H11 C5  R10  C6  A9  C9  D8
```

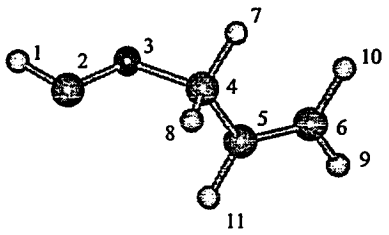

41

Figure 49. Optimized structure and atom numbering for the allyloxycarbene (**41**) at the B3LYP/6-31+G(d) level of theory.

Table 13. Structural data for the allyloxycarbene (**41**) with distances in Å and angles in degrees a the B3LYP/6-31+G(d) level of theory.

Allyloxycarbene (**41**)					
Variable:		Variable:		Variable:	
R1	1.117	A1	102.1	D1	180.6
R2	1.302	A2	116.9	D2	112.3
R3	1.471	A3	109.6	D3	119.5
R4	1.496	A4	123.8	D4	2.7
R5	1.336	A5	111.9	D5	-122.6
R6	1.093	A6	112.6	D6	177.9
R7	1.095	A7	121.6	D7	-1.6
R8	1.087	A8	121.8	D8	-0.7
R9	1.089	A9	120.4		
R10	1.090				

I.7. Z-Matrix for Table 14.

H1
C2 H1 R1
O3 C2 R2 H1 A1

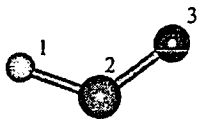

Figure 50. Optimized structure and atom numbering for the formal radical (from Scheme 53) at the B3LYP/6-31+G(d) level of theory.

Table 14. Structural data for the formyl radical (from Scheme 53) with distances in Å and angles in degrees at the B3LYP/6-31+G(d) level of theory.

	MP2(FC)/6-31+G(d)
Variables:	
R1	1.126
R2	1.183
A1	123.7

I.8. Z-matrix for Table 15.

C1
C2 C1 R1
C3 C2 R2 C1 A1
H4 C1 R3 C2 A2 C3 D1
H5 C1 R4 C2 A3 C3 D2
H6 C2 R5 C1 A4 H5 D3
H7 C3 R6 C2 A5 C1 D4
H8 C3 R7 C2 A6 C1 D5
H9 C3 R8 C2 A7 C1 D6

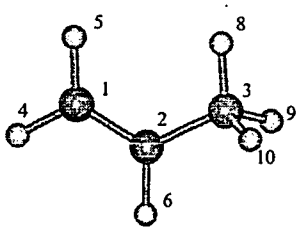

Figure 51. Optimized structure and atom numbering for propene (from Scheme 54) at the B3LYP/6-31+G(d) level of theory.

Table 15. Structural data for the propene (from Scheme 54) with distances in Å and angles in degrees a the B3LYP/6-31+G(d) level of theory.

Propene					
Variable:		Variable:		Variable:	
R1	1.337	A1	125.3	D1	180.0
R2	1.503	A2	121.7	D2	0.0
R3	1.087	A3	121.7	D3	180.0
R4	1.089	A4	118.8	D4	239.3
R5	1.092	A5	111.1	D5	0.0
R6	1.099	A6	111.5	D6	120.7
R7	1.096	A7	111.1		
R8	1.099				

I.9. Z-matrix for Table 16.

(This z-matrix is presented for clarity, but was not used for the optimization)

```
C1
C2  C1  R1
C3  C2  R2  C1  A1
C4  C3  R3  C2  A2  C1  D1
C5  C4  R4  C3  A3  C2  D2
C6  C5  R5  C4  A4  C3  D3
C7  C6  R6  C5  A5  C4  D4
C8  C7  R7  C6  A6  C5  D5
C9  C8  R8  C7  A7  C6  D6
H10 C1  R9  C2  A8  C3  D7
H11 C1  R10 C2  A9  C3  D8
H12 C2  R11 C3  A10 C4  D9
H13 C3  R12 C4  A11 C5  D10
H14 C5  R13 C6  A12 C7  D11
H15 C6  R14 C7  A13 C8  D12
H16 C7  R15 C8  A14 C9  D13
H17 C8  R16 C7  A15 C6  D14
H18 C9  R17 C8  A16 C7  D15
H19 C1  R18 C2  A17 C3  D16
```

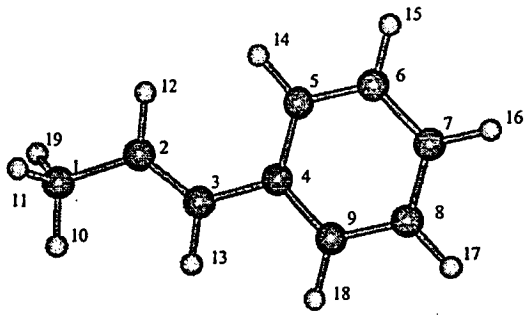

Figure 52. Optimized structure and atom numbering for the *trans*-1-phenylpropene at the B3LYP/6-31+G(d) level of theory.

Table 16. Structural data for *trans*-1-phenylpropene with distances in Å and angles in degrees at the B3LYP/6-31+G(d) level of theory.

trans-1-Phenylpropene					
Variable:		Variable:		Variable:	
R1	1.502	A1	124.468	D1	180.0
R2	1.344	A2	127.837	D2	0.0
R3	1.473	A3	123.543	D3	180.0
R4	1.409	A4	121.012	D4	0.0
R5	1.394	A5	120.498	D5	0.0
R6	1.400	A6	119.291	D6	0.0
R7	1.397	A7	120.089	D7	0.0
R8	1.396	A8	111.587	D8	120.7
R9	1.096	A9	111.184	D9	0.0
R10	1.099	A10	119.827	D10	180.0
R11	1.091	A11	114.481	D11	180.0
R12	1.092	A12	119.047	D12	180.0
R13	1.086	A13	119.959	D13	180.0
R14	1.087	A14	120.413	D14	180.0
R15	1.087	A15	120.192	D15	180.0
R16	1.087	A16	119.532	D16	-120.7
R17	1.088	A17	111.184		
R18	1.099				

I.10. Z-matrix for the Table 17.

(This z-matrix is presented for clarity, but was not used for the optmization)

```
C1
C2  C1  R1
C3  C2  R2  C1  A1
C4  C3  R3  C2  A2  C1  D1
C5  C4  R4  C3  A3  C2  D2
C6  C5  R5  C4  A4  C3  D3
C7  C6  R6  C5  A5  C4  D4
C8  C7  R7  C6  A6  C5  D5
C9  C8  R8  C7  A7  C6  D6
H10 C1  R9  C2  A8  C3  D7
H11 C1  R10 C2  A9  C3  D8
H12 C2  R11 C3  A10 C4  D9
H13 C3  R12 C4  A11 C5  D10
H14 C5  R13 C6  A12 C7  D11
H15 C6  R14 C7  A13 C8  D12
H16 C7  R15 C8  A14 C9  D13
H17 C8  R16 C7  A15 C6  D14
H18 C9  R17 C8  A16 C7  D15
```

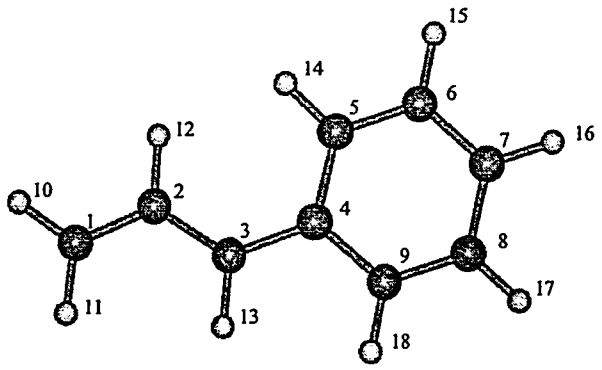

Figure 53. Optimized structure and atom numbering for the cinnamyl radical at the B3LYP/6-31+G(d) level of theory.

Table 17. Structural data for the cinnamyl radical with distances in Å and angles in degrees.

Cinnamyl Radical					
Variable:		Variable:		Variable:	
R1	1.372	A1	124.2	D1	180.0
R2	1.410	A2	127.3	D2	0.0
R3	1.439	A3	123.7	D3	180.0
R4	1.420	A4	121.0	D4	0.0
R5	1.391	A5	120.7	D5	0.0
R6	1.402	A6	119.3	D6	0.0
R7	1.401	A7	120.2	D7	180.0
R8	1.391	A8	121.5	D8	0.0
R9	1.085	A9	121.4	D9	0.0
R10	1.088	A10	118.4	Di0	180.0
R11	1.089	A11	116.0	D11	180.0
R12	1.090	A12	119.0	D12	180.0
R13	1.086	A13	119.9	D13	180.0
R14	1.087	A14	120.4	D14	180.0
R15	1.087	A15	120.1	D15	180.0
R16	1.087	A16	119.7		
R17	1.088				

I.11. Z-matrix for Table 18.

S1
C2 S1 R1
X3 C2 R2 S1 A1
S4 C2 R3 X3 A1 S1 D1

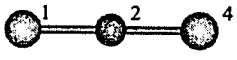

CS_2

Figure 54. Optimized structure and atom numbering for CS_2 at the MP2(FC)/6-31+G(d) level of theory.

Table 18. Structural data for CS_2 with distances in Å and angles in degrees.

	MP2(FC)/6-31+G(d)
Variable:	
R1	1.563
R3	1.563
A1	90.0
Constant:	
R2	1.0
D1	180.0

I.12. Z-matrix for Table 19.

H1
O2 H1 R1
C3 O2 R2 H1 A1
O4 C3 R3 O2 A2 H1 D1
H5 O4 R4 C3 A3 O2 D2

2

Figure 55. Optimized structure and atom numbering for w-dihydroxycarbene (**2**) at the MP2(FC)/6-31+G(d) level of theory.

Table 19. Structural data for dihydroxycarbene (**2**) with distances in Å and angles in degrees.

	MP2(FC)/6-31+G(d)
Variable:	
R1	0.975
R2	1.333
R3	1.333
R4	0.975
A1	106.3
A2	104.6
A3	106.3
D1	180.0
D2	180.0

I.13. Z-matrix for Table 20.

H1
O2 H1 R1
C3 O2 R2 H1 A1
O4 C3 R3 O2 A2 H1 D1
H5 O4 R4 C3 A3 O2 D2
C6 C3 R5 O2 A4 H1 D3
S7 C6 R6 C3 A5 O2 D4
S8 C6 R7 C3 A6 O2 D5

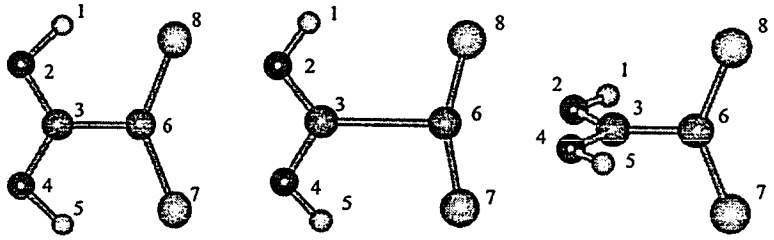

Figure 56. Optimized structures and atom numbering for the zwitterion (**130**), the transition state, **TS5**, and the transition state, **TS6**, at the MP2(FC)/6-31+G(d) level of theory.

Table 20. Structural data for the zwitterion (**130**), the transition state, **TS5**, and the transition state, **TS6**, with distances in Å and angles in degrees.

	Zwitterion (**130**)	**TS5**	**TS6**
	MP2(FC)/6-31+G(d)	MP2(FC)/6-31+G(d)	MP2(FC)/6-31+G(d)
Variable:			
R1	1.029	0.983	0.983
R2	1.285	1.314	1.303
R3	1.285	1.308	1.303
R4	1.029	0.989	0.983
R5	1.509	2.258	1.464
R6	1.678	1.591	1.671
R7	1.678	1.597	1.671
A1	102.3	105.9	108.8
A2	118.2	110.3	112.0
A3	102.3	104.9	108.8
A4	120.9	128.9	124.0
A5	113.3	103.9	111.2
A6	113.3	101.0	111.2
D1	180.0	180.0	180.0
D2	180.0	108.0	180.0
D3	0.0	0.0	0.0
D4	0.0	0.0	90.0
D5	180.0	180.0	270.0

I.14. Mixed coordinates for Table 21.

C2 0 xc2 -ysc zc2
S1 0 xs1 ysc zs1
X 0 xx yx zx
C3 X R1 S1 A1 C2 D1
S4 C3 R2 C2 A2 S1 D2
O5 C2 R3 S1 A3 X D3
O6 C2 R4 S1 A4 X D4
H7 O5 R5 C2 A5 S1 D5
H8 O6 R6 C2 A6 S1 D6

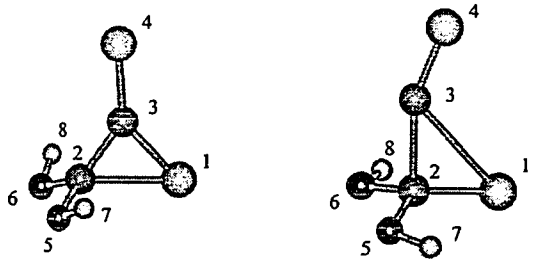

119 **TS8**

Figure 57. Optimized structures and atom numbering for **119** and **TS8** at the MP2(FC)/6-31+G(d) level of theory.

Table 21. Structural data for **131** and **TS8** with distances in Å and angles in degrees.

	lactone	CS loss TS
	MP2(FC)/6-31+G(d)	MP2(FC)/6-31+G(d)
Variable:		
Ysc	1.019	0.849
R1	1.716	2.600
R2	1.629	1.544
R3	1.349	1.362
R4	1.349	1.362
R5	0.978	0.977
R6	0.978	0.977
A1	71.0	83.7
A2	138.9	119.2
A3	117.9	122.0
A4	117.9	122.0
A5	109.1	106.8
A6	109.1	106.8
D2	180.0	-180.0
D3	-66.3	-71.0
D4	-293.7	-289.0
D5	-51.2	-15.4
D6	51.2	15.4
Constant:		
D1	0.0	0.0
Xx	-0.5	-0.5
Yx	0.0	0.0
Zx	0.0	0.0
Xs	0.0	0.0
Zs	0.0	0.0
Xc	0.0	0.0
Zc	0.0	0.0

I.15. Z-matrix for Table 22.

S1
C2 S1 R1
X3 C2 R2 S1 A1
S4 C2 R3 X3 A1 S1 D1
C5 S4 R4 C2 A2 X3 D2
O6 C5 R5 S4 A3 C2 D3
O7 C5 R6 S4 A4 C2 D4
H8 O6 R7 C5 A5 S4 D5
H9 O7 R8 C5 A6 S4 D6

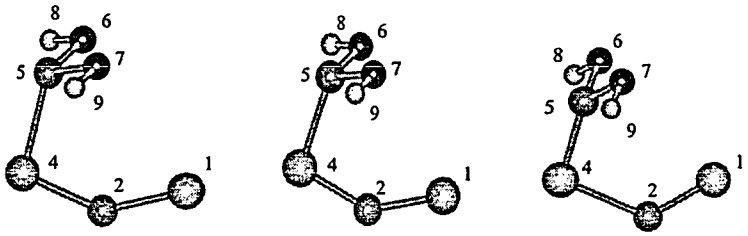

Figure 58. Optimized structures and atom numbering for **TS9**, **133** and **TS10** at the MP2(FC)/6-31+G(d) level of theory.

Table 22. Structural data for **TS9, 133** and **TS10** with distances in Å and angles in degrees.

	Ylide (133)	TS9	TS10
	MP2(FC)/6-31+G(d)	MP2(FC)/6-31+G(d)	MP2(FC)/6-31+G(d)
Variable:			
R1	1.574	1.574	1.565
R3	1.658	1.651	1.972
R4	1.872	1.894	1.669
R5	1.367	1.364	1.363
R6	1.363	1.360	1.359
R7	0.977	0.977	0.978
R8	0.978	0.978	0.978
A1	70.3	70.7	63.1
A2	99.1	99.0	97.6
A3	113.3	112.9	122.9
A4	113.4	113.0	121.9
A5	108.2	108.2	107.9
A6	108.4	108.4	108.1
D2	5.9	6.0	10.6
D3	67.1	67.5	77.7
D4	-50.6	-49.8	-63.8
D5	59.3	60.1	30.1
D6	-59.2	-59.9	-35.0
Constant:			
R2	1.0	1.0	1.0
D1	180.0	180.0	180.0

I.16. Z-matrix for Table 23.

H1
O2 H1 R1
C3 O2 R2 H1 A1
O4 C3 R3 O2 A2 H1 D1
H5 O4 R4 C3 A3 O2 D2
S6 C3 R5 O2 A4 H1 D3

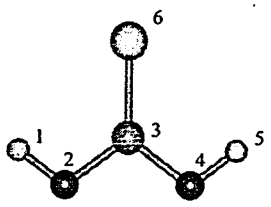

132

Figure 59. Optimized structure and atom numbering for **132** at the MP2(FC)/6-31+G(d) level of theory.

Table 23. Structural data for **132** with distances in Å and angles in degrees.

	MP2(FC)/6-31+G(d)
Variable:	
R1	0.9783
R2	1.3409
R3	1.3409
R4	0.9783
R5	1.6365
A1	107.3121
A2	107.1893
A3	107.3105
A4	126.4112
D1	180.0
D2	180.0
D3	0.0

I.17. Z-matrix for Table 24.

C1
S2 C1 R1

CS

Figure 60. Optimized structure and atom numbering for CS at the MP2(FC)/6-31+G(d) level of theory.

Table 24. Structural data for CS with distances in Å and angles in degrees.

Variable	MP2(FC)/6-31+G(d)
R1	1.543

Appendix II.

Atoms in Molecules

The theory of atoms in molecules provides a rigorous definition of an atom in a molecule and offers the means to obtain its properties.[211] Within this theory, an atom in a molecule is defined as an open subset in real space that generally contains an atomic nucleus and whose boundary is a zero-flux surface of electron density gradient. Such a boundary can be considered as the union of interatomic surfaces that define the interactions between pairs of atoms in the molecule. For each interatomic surface there is a pair of gradient paths that go to each of the associated atomic nuclei. These gradient paths start from a common point on the interatomic surface, which corresponds to a critical point of the electron density and is called a bond critical point. It is over the volume defined by the atomic basin that the observables are integrated to yield the corresponding atomic properties. Examples of such atomic properties are the charge, the first moment of the electron density and the energy.

The analysis of the dipole moment (μ) of the molecule, in terms of the atomic charges and atomic first moments, has proven to be useful in understanding the polarization of a given charge distribution.[211,246] If $\{\mathbf{R}_\alpha\}$ denotes the set of nuclear coordinates referred to an arbitrary origin and $\{\mathbf{M}_\alpha\}$ the atomic moments of a given molecule, the dipole moment can be written as $\mu = \sum_\alpha q_\alpha \mathbf{R}_\alpha + \sum_\alpha \mathbf{M}_\alpha = \mu_{ct} + \mu_p$. In this expression μ_{ct} and μ_p are called the charge transfer and polarization contributions,

respectively. For a neutral molecule, μ and its contributors μ_{ct} and μ_p are origin independent. This allows the partition of the dipole moment into contributions readily interpretable in physical terms. That is, μ_{ct} results from the transfer of charge among the atoms in the molecule and represents the contribution to the dipole moment of a set of spherical charge densities. On the other hand, μ_p accounts for the non-sphericity of the atoms in the molecule, as the atomic moments indicate the direction of polarization of the electron density in each of the atoms.

The Laplacian of the electron density ($\nabla^2\rho(\mathbf{r})$) is also an important property for it contains information about the electron structure that is not directly available from the electron density.[211,227] For example, it has been shown that $\nabla^2\rho(\mathbf{r})$ displays the shell structure of free atoms as well as of atoms in a molecule and that negative values of $\nabla^2\rho(\mathbf{r})$ refer to points in space where the electron density is locally concentrated or depleted. It has been suggested that the critical points defined by the minima in the Laplacian of the electron density can be used to identify, for example, a lone pair in a molecule and also provide a physical basis for the VSEPR model.[247]